UNIVERSITY OF LIVERPOOL

A potential role for *Streptococcus gordonii* in haem acquisition by *Porphyromonas gingivalis*

Thesis submitted in accordance with the requirements of the University of Liverpool for the degree of Master of Philosophy

by

Jason Brown (BSc Hons)

June 2017

Acknowledgements

The experimental work presented in this thesis was completed in the School of Dentistry, University of Liverpool, between October 2015 and September 2016.

During my time at Liverpool Dental School, I had the extreme privilege to be mentored by Dr John Smalley, who provided continual support and guidance throughout my MPhil studies. I have gained invaluable research experience under his supervision, and truly could not have asked for better mentor. Also, the wealth of knowledge offered by my second supervisor, Dr Ed Yates, was instrumental in helping me compile the protein data. I must also offer my gratitude to Dr Rosalind Jenkins who performed the mass spectrometry analysis, and to Professor Teresa Olzcak, whose kind donations of the *Porphyromonas gingivalis* haemophore made a large proportion of this work possible.

I would like to thank everyone else from the Dental School who offered help during my studies, and in particular, Karen Garcia for her friendship during her short time in the lab. Also, thanks must go to my now PhD supervisors, Dr John Butcher and Dr Shauna Culshaw who have both been incredibly patient whilst I found time in-between experiments to write up my MPhil thesis. On a personal note, I wholeheartedly thank my family and especially my parents for their support, financial and otherwise, and Jazz for her continued patience and encouragement.

Abstract

Periodontitis (PD) is an inflammatory disease arising from the dental plaque bacterial insult upon the soft periodontal tissues, resulting in damage to the tooth supporting structures. Severe forms of the disease are the main cause of tooth loss in adults, which impacts on oral health and quality of life. As control of the growth of dental plaque is only partially successful in reducing the severity of PD, a better understanding of the biochemical interactions that exist between key pathogenic inhabitants within plaque may potentially lead to the development of novel therapeutic agents that could further aid in moderating PD.

Porphyromonas gingivalis, a black-pigmenting species requiring haem for growth and virulence, is identified as one of the main protagonists in the onset and maintenance of PD. *P. gingivalis* co-aggregates with other auxiliary pathogens in dental plaque, including *Streptococcus gordonii*, a member of the viridans streptococci. This study primarily investigated a potential role for *S. gordonii* in one of the central mechanisms utilised by *P. gingivalis* to acquire haem from haemoglobin (Hb) i.e., via methaemoglobin (metHb) production. It was shown herein that hydrogen peroxide production by *S. gordonii* was responsible for mediating the formation of metHb; the Fe(III)haem-containing Hb species utilised by *P. gingivalis* for haem extraction. The haem from metHb generated by *S. gordonii*, was more easily extracted from the protein by the HmuY haemophore of *P. gingivalis*, than from metHb formed by auto-oxidation. Using circular dichroism spectroscopy, it was revealed that the increased rate of HmuY-Fe(III)haem complex formation likely arose as a result of subtle changes to the Hb structure following exposure to *S. gordonii*-generated hydrogen peroxide.

Diabetes mellitus, which is characterised by hyperglycaemia and increased levels of glycated Hb, has long been considered a risk factor of PD. The numbers of Red complex microorganisms such as *P. gingivalis* and viridans streptococci are also increased in the subgingival plaque of diabetic individuals. Here, it was demonstrated that the HmuY haemophore of *P. gingivalis* extracted haem more readily from Hb glycated *in vitro* than from un-glycated Hb. Mass spectroscopy of

the glycated Hb indicated that the protein contained multiple glycated lysine amino acids, including Lys-90(α) and Lys-95(β) located on the same F8 helix-loops as the proximal histidines which are involved in haem-globin binding.

The experimental data obtained in this study has provided evidence for two potential mechanisms through which haem availability to *P. gingivalis* might be enhanced. The first involves formation of metHb via streptococcal production of hydrogen peroxide. The second mechanism points to Hb glycation, a process which enhances haem extraction by HmuY. These effects may contribute to haem acquisition by *P. gingivalis* and might account for the increased numbers in dental plaque of diabetics.

Preface

Chapter 1 introduces the background and aims of the thesis, with an overview of periodontitis and highlights the importance of haem availability to *P. gingivalis* pathogenicity.

Chapter 2 provides a detailed appraisal of the methods and materials used in the study.

Chapter 3 primarily characterises the Hb species extracted from zones of α-haemolysis by *S. gordonii*, and that produced following exposure of oxyhaemoglobin (oxyHb) to *S. gordonii* cell suspensions.

Chapter 4 expands on observations presented in chapter 3, and examines the ability of the HmuY haemophore of *P. gingivalis* to pick-up haem from the Hb species produced by *S. gordonii*.

Chapter 5 investigates the susceptibility of glycated Hb to haem extraction by the HmuY haemophore.

Chapter 6 summarises the findings presented in the study in a general discussion.

Contents

List of Figures

List of Tables

Abbreviations

A	Absorbance
AGEs	Advanced glycation end products
BHI	Brain Heart Infusion
deoxyHb	Deoxyhaemoglobin
dH_2O	Deionised water
ε	Millimolar extinction coefficient (mM^{-1} cm^{-1})
Fe(II) haem	Iron(II) protoporphyrin IX
Fe(III) haem	Iron(III) protoporphyrin IX
Fe(IV) Hb	Ferryl haemoglobin
g	Acceleration due to gravity
GCF	Gingival crevicular fluid
G	Glucose
GOX	Glucose oxidase
Hb	Haemoglobin
His	Histidine
5-HMF	5-hydroxymethylfurfural
H_2O_2	Hydrogen peroxide
InpA	Interpain A (of *P. intermedia*)

kDa	Kilodaltons
Kgp	Lysine-specific gingipain of *P. gingivalis*
K_d	Dissociation constant
λ_{max}	Maximum wavelength
metHb	Methaemoglobin
mol/L	Moles per litre
$Na_2S_2O_4$	Sodium dithionite
oxyHb	Oxyhaemoglobin
O_2^-	Superoxide anion
OH^-	Hydroxyl ion
$OH_2^\bullet$	Hydroxyl radical
PBA	Phenylboronic acid
Phe	Phenylalanine amino acid residue
RgpA/RgpB	Arginine-specific gingipains (of *P. gingivalis)*
rpm	Revolutions per minute
Tris	Trisaminomethane $(HOCH_2)_3CNH_2$
Trp	Tryptophan
Tyr	Tyrosine
v/v	Volume per unit volume
w/v	Weight per unit volume

Chapter 1 General Introduction

P. gingivalis is a Gram negative oral anaerobe which accumulates a cell surface black pigmentation (consisting of ferrihaem) when grown on blood-containing solid media. *P. gingivalis* is considered the "keystone pathogen" in the development of periodontitis (Hajishengallis, 2015), a disease that arises from an inflammatory response to oral bacteria affecting ≥50% of the adult population (Petersen et al., 2005; Chapple, 2014). The following section discusses the microbiology and the aetiology of periodontitis, and the importance of haem acquisition systems in the virulence of *P. gingivalis*.

1.1 The oral microcosm in periodontitis

1.1.1 The role of bacterial dental plaque in the aetiology of periodontitis

Periodontitis (PD) is associated with inflammation of the gums and supporting tissues of the teeth, resulting in loss of collagen fibre attachment between the tooth and alveolar bone (Loesche & Grossman, 2001). PD arises from an inflammatory response to bacteria in dental plaque, which is defined as a complex community of microflora embedded within a self-produced extracellular matrix rich in proteins, polysaccharides, lipids and nucleic acids (Flemming & Wingender, 2010). There is evidence for over 700 species or phylotypes of microorganisms located in the oral cavity, including bacteria, viruses and yeast (Aas et al., 2005). A symbiotic relationship exists between the host and the plaque community, where 'commensal' bacteria such as oral streptococci compete with pathogens for the ecological niche which in turn prevents infection and maintains tissue homeostasis (Socransky & Haffajee, 1991; Hajishengallis, 2014). A shift in symbiosis, to a dysbiotic state, increases the propensity for infection (Hajishengallis, 2015).

Oral microorganisms inhabit supragingival dental plaque; located coronal to the gingival margin, and subgingival dental plaque; apical to the gingival margin (Chandki et al., 2011). Microbial composition differs in supragingival and subgingival plaque (Ximenez-Fyvie et al., 2000). The pioneering species, Gram positive bacteria belonging largely to the streptococci genus, drive early colonisation of supragingival dental plaque through attachment to salivary pellicle on the tooth enamel surface

and the gingival epithelium (Pratt-Terpstra et al., 1989; Thurnheer et al, 2014). A shift to Gram negative microflora in subgingival dental plaque may arise if plaque is left undisturbed, a process driven by subtle alterations in the local micro-environment through host inflammatory responses and/or environmental changes in pH, O_2 concentration and nutrient availability. Understanding the symbiotic relationship that exists between host and plaque community is essential in controlling the shift from healthy to diseased states (Marsh & Devine, 2011; Hajishengallis, 2015).

The microorganisms that inhabit dental plaque have been grouped in accordance to their association with PD (Socransky & Haffajee, 2005). Supragingival and early subgingival plaque colonisers, those widely termed 'commensal' microorganisms such as streptococci and *Actinomyces*, belong to the "Blue", "Yellow", "Green" and "Purple" categories. The "Orange" group, including *Prevotella* and *Fusobacteria* species precede the triad of "Red complex" microorganisms that are strongly associated with the onset of PD. These comprise of *Treponema denticola*, *Tannarella forsthyia* and *Porphyromonas gingivalis* which thrive in mature subgingival dental plaque (Socransky & Haffajee, 2005). Of these Red complex microorganisms, *P. gingivalis* is considered the "keystone pathogen" in PD and is referred to as the microorganism responsible for initiating dysbiosis between host and dental plaque community (Darveau et al., 2012). Figure 1.1 highlights the dysbiosis in subgingival dental plaque that is associated with PD development (Hajishengallis, 2015).

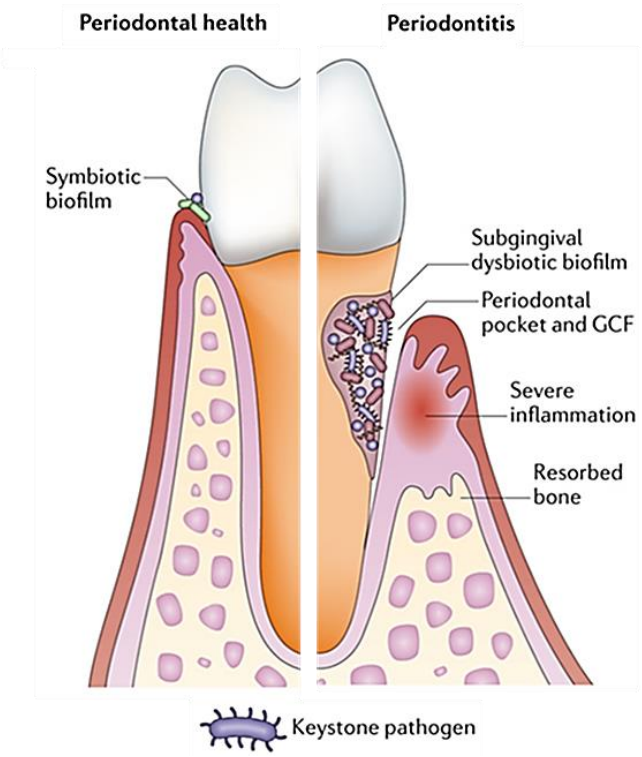

Figure 1.1 – The shift in host-microbe homeostasis is responsible for the onset of PD (adapted from Hajishengallis, 2015). The "keystone pathogen", *P. gingivalis*, thrives in subgingival dysbiotic plaque. Severe inflammation of the gingival tissue, and resorbed alveolar bone are associated with PD.

1.1.2 The role of co-aggregation in dental plaque development

The proliferation of dental plaque, and the actions of oxygen-consuming Gram positive aerobes leads to the development of anaerobic pockets within the community enabling the growth of obligate anaerobes (Marsh, 2004). The late colonising anaerobes require co-aggregation with pioneering species of dental plaque to establish themselves within the ecological niche. This unique adherence between multiple bacterial species via cell-surface receptor recognition, allows protection against the immune response and antimicrobial therapy (Jakubovics & Kolenbrander, 2010). Late colonisers lack the repertoire of cell-surface receptors responsible for attachment to the tooth surface, therefore require adhesion to species already colonised on the tooth such as the Gram positive streptococci (Kreth et al., 2009) and Gram negative *Fusobacterium nucleatum* (Whittaker et al., 1996). The act of co-aggregation also serves to aid in satisfying nutritional

requirements; oral streptococci are capable of cleaving salivary glycoprotein side-chains into smaller carbohydrates that can be utilised as a fermentable energy source by a vast array of late colonising species (Byers et al., 1999).

The "keystone pathogen" *P. gingivalis* adheres to multiple species of oral streptococci known as viridans streptococci; a unique class of microorganisms that mediate α-haemolysis on blood agar. *Streptococcus gordonii*, *Streptococcus oralis* and *Streptococcus sanguinis* each co-aggregate with *P. gingivalis* (Stinson et al., 1991). Co-aggregation between viridans streptococci and *P. gingivalis* is a multimodal interaction, mediated via the short (Mfa1) and long fimbriae (FimA) of *P. gingivalis* with the SspB protein and glyceraldehyde 3-phosphate dehydrogenase (GAPDH) cell surface enzyme of streptococci species, respectively (Chung et al., 2001; Maeda et al., 2004). The importance of such interactions has been highlighted by the observation that the development of *P. gingivalis* biofilms on streptococcal substrata is inhibited when FimA-SspB interaction is disrupted (Lamont et al., 2002).

Co-aggregation with *S. gordonii* is also considered to be essential for the colonisation of dentinal tubules in endodontic infection by the otherwise non-invasive *P. gingivalis* (Love et al., 2000). In endodontal diseases, which generally refers to inflammation of the dental pulp and periapical tissues, invasive bacteria may accumulate within the pulp, either by penetration through the dentinal tubules exposed by caries or tooth wear, or via infection of the lateral canals of the tooth (Narayanan & Vaishnavi, 2010). Oral streptococci such as *S. gordonii* are early colonisers of dentinal tubule walls via recognition of collagen type I through the antigen I/II polypeptide family (including the protein, SspB; Love et al., 1997). A shift to growth of obligate anaerobes such as *P. gingivalis* and *P. intermedia* is associated with acute root infections (Hashioka et al., 1992; Sundqvist et al., 1989), a process heavily reliant on co-aggregation with the pioneering streptococci species (Love et al., 2000).

1.2 Bacterial haem acquisition

1.2.1 Gingival crevicular fluid as a source of haem

A characteristic feature of PD is the formation of a deep crevice between the tooth and surrounding gingival tissue, which is known as the periodontal pocket. The periodontal pocket contains gingival crevicular fluid (GCF), a rich source of proteins that provides a nutrient source for the bacterial niche within the pocket, which can harbour between 10^8 and 10^{10} bacteria (Hajishengallis, 2015). Perturbation of the gingival epithelium by bacterial accumulation is responsible for the exudation of the fluid, highlighted by the positive correlation between PD status and GCF flow rate; rate of exudation can increase 30-fold in severe PD (Goodson, 2003; Griffiths, 2003). Subgingival plaque inhabitants such as *P. gingivalis* rely heavily on proteolysis of host proteins for growth, a process that is driven largely by early colonisers of supragingival plaque such as oral streptococci (Bradshaw et al., 1994; Homer & Beighton, 1992; Wickstrom et al., 2009).

An array of haem-containing and haem-carrying molecules such as haemoglobin (Hb), albumin and haemopexin flood the GCF as a result of vascular swelling and bleeding of the gingival tissue epithelium (Tew et al., 1985; Bickel et al., 1985a; Koike et al., 1989; Hanioka et al., 2005). These proteins provide an essential source of haem (iron protoporphyrin IX) to oral pathogens such as *P. gingivalis* and *P. intermedia*, two microorganisms that exhibit an absolute growth requirement for the co-factor (Marsh et al., 1994; Leung & Folk, 2002). Haem also represents a potential vital source of iron for *P. gingivalis* and *P. intermedia*; in which it is an essential element for cellular metabolism, enzyme activity and ultimately survival in the host (Messenger & Barclay, 1983; Ascenzi et al., 2005).

1.2.2 Haem biochemistry

To understand the importance of haem in bacterial pathogenicity, it is essential firstly to appreciate the complex biochemistry and behaviour of iron protoporphyrin IX species in aqueous solution. Free haem exists in equilibrium as haematin monomers (Fe(III)PPIX.OH), μ-oxo dimers ($[Fe(III)PPIX]_2O$) or π-π dimers of the

haematin monomer, depending on pH, temperature and the type of solutes present within the aqueous solution (Asher et al., 2009). The monomeric haem molecule consists of four pyrrole rings that are attached to the central iron via a nitrogen atom, and to one another by methene bridges (-CH-) (Figure 1.2). The fifth coordination site of the iron is occupied by a H_2O or OH^- ligand. Haem monomers may also spontaneously associate to form π-π dimers.

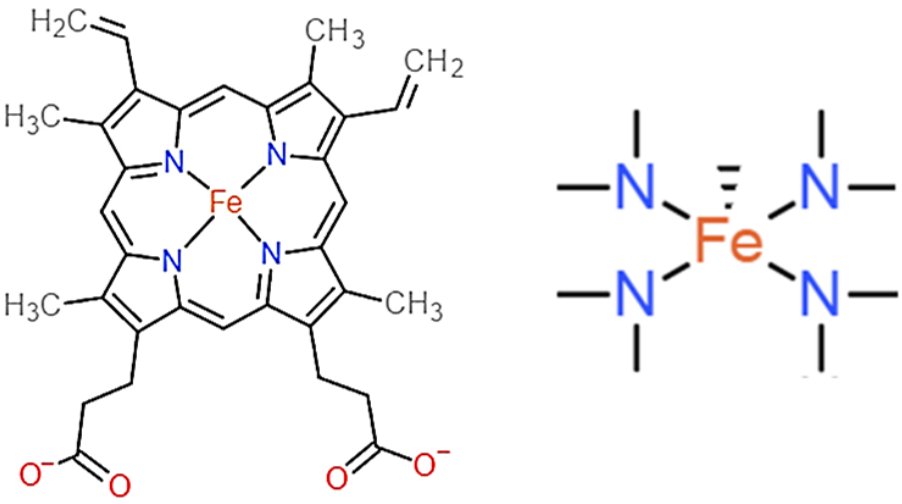

Figure 1.2 – The structure of the haem (iron protoporphyrin IX) monomer. The Fe centre is adjoined to four nitrogen atoms of the pyrrole rings. The fifth coordination site, denoted by dotted lines in the right panel, is occupied by a OH^- or H_2O ligand (not shown).

The π-π dimer will form between two haem molecules at their unligated surfaces because of π-cloud interactions between the porphyrin molecules, resulting in a 'stacking' interaction with the H_2O/OH^- ligand facing outwards (de Villiers et al., 2007). In aqueous solutions, the H_2O/OH^- ligands will solvate with water molecules, but in high salt or basic conditions formation of μ-oxo dimers will occur (Asher et al., 2009). μ-oxo dimers differ from their π-π counterparts by the formation of a reversible bond between two haems by an oxygen molecule (-O-). π-stacking between μ-oxo dimers may also occur forming large aggregates (de Villiers et al., 2007; Asher et al., 2009). The concentration of haem in solution affects the equilibrium between monomeric and dimeric haem; lowering the haem

concentration shifts the equilibrium from the dimeric to the monomeric form, whilst aggregation between the molecules is favoured as the haem concentration is raised (Asher et al., 2009).

1.2.2.1 Haem-containing and haem-carrying proteins

Free haem in the body is sequestered by haem-carrying proteins, principally albumin and haemopexin, and is also contained within haemoglobin (Hb). Hb is a 64kDa tetrameric protein consisting of four monomer subunits (specifically two αβ dimeric chains forming the Hb tetramer; Figure 1.3) and a haem molecule located within each subunit. Whilst the tetramer may dissociate into αβ dimers, these dimeric structures do not dissociate into individual α- and β- subunits under normal physiological conditions. The haem molecule contains highly hydrophilic propionate groups (-CH_2-CH_2-COO-) which protrude into the solvent, forming hydrogen bonds with basic amino acids in the globin structures (Perutz et al., 1998). The haem molecules are held in place by a covalent bond between the fifth coordination site of the haem iron with the imidazole ring of the so termed proximal histidine residue (His-87 at site F8 in α-chains and His-92 at site F8 in β-chains; Percy et al., 2005), and also by numerous other interactions between the porphyrin and other amino acids surrounding the haem pocket (Perutz, 1990). The distal histidine residues His58 in the α-chains and His63 in the β-chains are involved in stabilising the binding of oxygen molecules to the iron centre. O_2 binding is achieved via the sixth coordination site in oxygenated Hb (oxyHb) whilst in deoxygenated haemoglobin (deoxyHb), the final coordination site remains unoccupied (Olson et al., 1988).

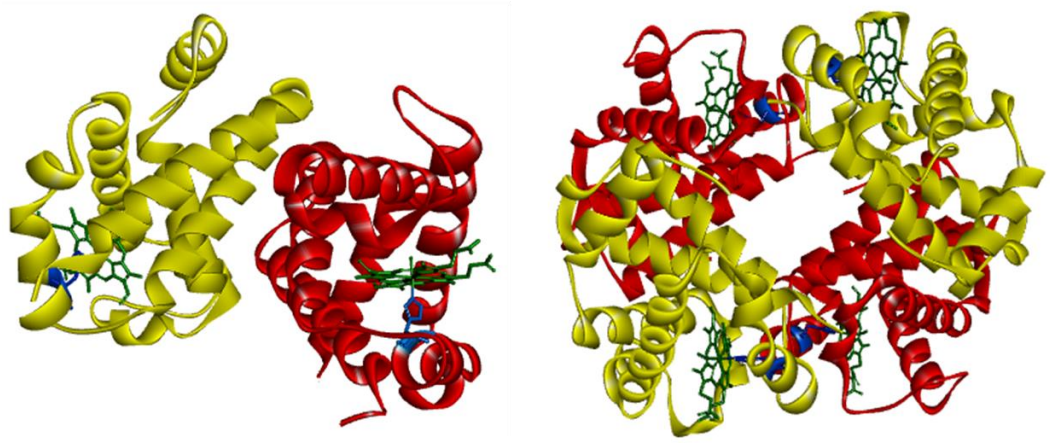

Figure 1.3 – The structure of the Hb αβ-dimer (left panel) and Hb tetramer (right panel). The haem molecule (green) is located within the haem pocket of each peptide chain, held in place by interactions with the proximal histidine (blue); His-87 for α-chain (yellow) and His-92 for β-chain (red). Constructed using PDB files; 2MHB (dimer) and 1GZX (tetramer).

Albumin and haemopexin are plasma proteins that act as haem-scavenging molecules and may be synthesised as a stress response at inflammatory sites (Smith & McCulloh, 2015). Both proteins will complex with free haem lost during denaturation of Hb. Haemopexin is in relatively low abundance in the circulation, but possesses a high affinity for haem (K_d ~10^{-13} M; Hrkal et al., 1974), while serum albumin is higher in abundance which compensates for its relatively low affinity for haem (K_d ~10^{-8} M; Beaven et al., 1974). Thus, as albumin is present in plasma at concentrations between 40 and 80-fold greater than haemopexin (Muller-Eberhard & Morgan, 1975), albumin will bind more of any free haem than will haemopexin. These haem-sequestering properties of albumin and haemopexin result in relatively low concentrations of free circulating haem (<0.1μM, Ryter & Tyrrell, 2000) which provides an initial important obstacle to microorganisms invading the body that possess a growth requirement for the co-factor.

1.2.3 Iron and haem requirements of *Porphyromonas gingivalis*

There is no evidence that *P. gingivalis* possesses a siderophore system; small compounds capable of chelating free iron (Bramanti & Holt, 1990). Therefore, haem is an essential alternative as a source of iron for vital cellular processes (Ascenzi et al., 2005). Haem is also important in other aspects of virulence for *P. gingivalis*; μ-oxo haem dimers (μ-oxo bishaem) form the black pigmentation which accumulates on the cell surface of *P. gingivalis* (Smalley et al., 1998). As *P. gingivalis* lacks catalase and peroxidase enzymes (Amano et al., 1986), it is postulated that the μ-oxo bishaem-containing pigment enables survival within the oral cavity during exposure to H_2O_2 (Smalley et al., 2000). The catalase activity of haem is well understood (Jones et al., 1973) and this may protect the organism from H_2O_2 generated by neutrophils high in number in the gingival crevice (Bondy-Carey et al., 2013) and by neighbouring plaque species such as viridans streptococci (Ryan & Kleinberg, 1995). Formation of the μ-oxo bishaem ($[Fe(III)PPIX)_2O]$; Figure 1.4) through generation of the -O- bond between haem monomers may act to utilise oxygen molecules in the immediate vicinity of the *P. gingivalis* cell and from a chemical perspective would help to promote an anaerobic micro-environment (Smalley et al., 1998). Furthermore, *P. gingivalis* lacks the full repertoire of genes responsible for the *de novo* biosynthesis of this vital co-factor (Schifferle et al., 1996; Nelson et al., 2003). Therefore, haem acquisition from the environment is essential for survival of *P. gingivalis* within the host.

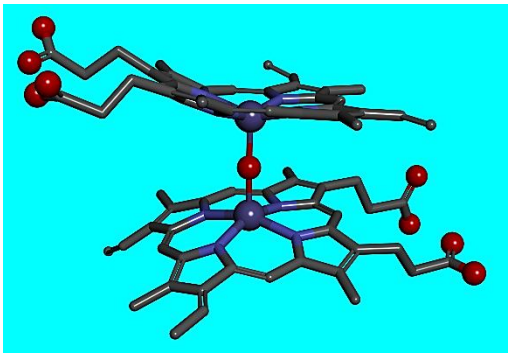

Figure 1.4 – The structure of the μ-oxo bishaem $[Fe(III)PPIX)_2O]$ which forms the black pigmentation on the surface of *P. gingivalis* (adapted from Smalley & Olczak, 2015). Formation of the μ-oxo bishaem arises through the bonding of two

haem molecules (Fe(III)PPIX) via the iron haem centres (blue) with an oxygen atom (red).

1.2.4 The gingipains of *Porphyromonas gingivalis*

Hb is the most abundant haem source in the periodontal pocket and diseased gingival crevice (Tew et al., 1985; Hanioka et al., 2005). *P. gingivalis* possesses an array of virulence factors such as gingipain proteases that can act in conjunction with one another to mediate the breakdown of Hb, and facilitate the extraction of haem for utilisation (Smalley et al., 2007; 2008; Wojtowicz et al., 2009). In addition, *P. gingivalis* is capable of agglutinating and haemolysing erythrocytes (Falkler et al., 1983) and via a cell-surface adhesion domain HagA, and the HA2 domains of the RgpA and Kgp gingipains, is capable of binding Hb and haem (DeCarlo et al., 1999; Paramaesvaran et al., 2003; Smalley & Olczak, 2015). Gingipains are 'trypsin-like' cysteine proteases that play multiple roles in *P. gingivalis* virulence (Potempa et al., 2003; O'Brien-Simpson et al., 2003). *P. gingivalis* produces two types of gingipains; the arginine- (Rgp) and lysine- (Kgp) specific forms (Pike et al., 1994). The closely related *rgpA* and *rgpB* genes belong to an almost identical proteinase domain and encode for the Arg-specific gingipain, while the Lys-specific form is the product of a single gene, *kgp* (Curtis et al., 1999). RgpA and Kgp are heteromultimeric complexes consisting of a catalytic domain and functional subunits that contain multiple haemagglutinin domains (HA1, 2, 3 and 4; Pike et al., 1994). It is postulated that the HA2 domains of RgpA and Kgp, but not RgpB which lacks the HA2 domain, act as a catalytic surface for formation of μ-oxo bishaem between two haem monomers (Figure 1.4; Smalley et al., 2006; Nhien et al., 2010; Smalley & Olczak, 2015).

1.2.4.1 Oxidation of oxyhaemoglobin to methaemoglobin; the role of gingipains in facilitating methaemoglobin formation and haem release for μ-oxo bishaem pigmentation

Normally Hb exists as oxyHb and deoxyHb (containing an Fe(II) haem) or as the physiologically inactive methaemoglobin (metHb; containing Fe(III)haem) which is incapable of binding O_2. The concentration of metHb present in circulating

erythrocytes is low, ranging from 2-6% in healthy adults (Rechetzki et al., 2012), while levels of 10-20% produce cyanosis and 20-50% may result in respiratory failure, lethargy and potential death as a consequence of its inability to transport oxygen (Camp et al., 2007). OxyHb is relatively stable due to the Fe-O_2 bond, but can spontaneously auto-oxidise into metHb when H_2O or OH^- molecules enter the haem pocket causing the nucleophilic displacement of the bound O_2 and the subsequent release of a superoxide anion (O_2^-) (Shikama, 1990; Tsuruga & Shikama, 1997). These new ligands will replace O_2 at the sixth coordination site of the haem iron with either H_2O, to form aquo- or acid metHb, or with the OH^- ion, to form hydroxyl- or alkaline metHb. Encapsulation of the haem iron within the globin moiety prevents excessive auto-oxidation (Sugawara et al., 1995). As a result, the turnover of oxyHb to metHb occurs at a low rate in the erythrocyte, whilst its intracellular enzymes cytochrome b5 and cytochrome b5 reductase are responsible for re-reduction of >95% of metHb back into oxyHb (Wright et al., 1999).

OxyHb is refractory to *P. gingivalis* proteolysis and haem release (Smalley et al., 2002; 2004; 2008), whereas metHb is the preferred form for haem acquisition due to the decreased affinity of the globin chain for Fe(III)haem (Hargrove et al., 1996). Following oxidation of oxyHb to metHb, there is an approximately 10^8-fold decrease in haem-globin affinity, which explains the increased propensity for Fe(III)haem to be transferred from metHb to serum albumin (Hargrove et al., 1996). The Arg- and Lys- specific gingipains of *P. gingivalis* work in conjunction to mediate the conversion of oxyHb to metHb, and subsequent proteolytic breakdown of the protein resulting in the release of Fe(III)haem which can be used in pigmentation by the cell (Smalley et al., 2007; 2008).

The actions of gingipains on metHb formation and haem release were first investigated by Smalley et al (2004) using the Rgp and Kgp protease deficient strains of *P. gingivalis* W50 described by Aduse-Opoku et al (2000). It was observed that RgpA and RgpB-deficient mutants (strains W501 and D7, respectively) were able to produce the black pigmentation during growth on blood agar, whereas the Kgp mutant (K1A) and double Rgp knockout (E8) were unable to develop the μ-oxo

bishaem-containing pigment (Smalley et al., 2004). Kgp-deficient mutants developed cream-coloured colonies when grown on blood agar and which were devoid of any haem, while the Rgp double knockout yielded a dark-brown pigment which possessed spectral features characteristic of a Hb haemichrome (Smalley et al., 2004); a Fe(III)haem containing Hb species that is generated by co-ordination between the haem iron and a second amino acid (in addition to the proximal histidine) within the haem pocket of the globin chain (Rifkind et al., 1994). The biochemical mechanism behind these observations was later found to involve the synergistic actions of RgpA and Kgp, in which RgpA mediated the formation of metHb from oxyHb by cleaving the arginine residues within the Hb chains (Smalley et al., 2007). MetHb is further attacked by Kgp which facilitates the release of the Fe(III)haem for pigmentation (Smalley et al., 2007; 2008). In contrast, incubation of Kgp with oxyHb alone results in the formation of a haemichrome, making it less susceptible to further degradation by either Rgp or Kgp (Smalley et al., 2007). Thus, it was shown that both Rgp and Kgp were required to mediate black pigmentation by *P. gingivalis*.

1.2.5 The HmuY haemophore and its role in haem acquisition by *Porphyromonas gingivalis*

Haem has both hydrophilic and hydrophobic properties but is unable to pass through the impermeable outer membrane of Gram negative microorganisms. Therefore, haem internalisation is mediated by a combination of haem-binding proteins and outer-membrane active transport systems (Wandersman & Delepelaire, 2012). *P. gingivalis* possesses other haem-binding proteins such as IhtB (iron haem transport protein) and HBP35 (haem-binding protein) that interact with haem for the process of iron and/or haem transportation across the membrane (Hendtlass et al., 2000; Shibata et al., 2003; Aduse-Opoku et al., 1997). IhtB is an outer membrane-located haem-binding protein involved in the assimilation of haem iron prior to internalisation (Dashper et al., 2000) while HBP35 functions in a similar manner to IhtB in addition to facilitating adhesion of *P. gingivalis* to erythrocytes as well as gingival epithelial cells (Hiratsuka et al., 2008; 2010).

P. gingivalis also produces haemophores, which are secreted or cell-surface attached proteins that act to scavenge haem and deliver it to the cell for internalisation (Wandersman & Delepelaire, 2012). The best characterised haem uptake system utilised by *P. gingivalis* is encoded by the *hmu* operon, which includes the HmuY haemophore (Olczak et al., 2005). The HmuY gene encodes a 23kDa all β-sheet protein that is anchored via lipid attachment to the outer membrane of the *P. gingivalis* cell surface, before cleavage by weak protease activity of Kgp releases the haemophore into the vicinity of the cell (Olczak et al., 2008; 2010). HmuY is a highly resilient protein, completely resistant to the proteolytic effects of RgpA, RgpB and Kgp gingipains, as well as host enzymes such as serine protease, trypsin and neutrophil elastase (Wojtowicz et al., 2009).

HmuY is capable of complexing with free haem and haem encapsulated within haem-proteins such as Hb and serum albumin (Smalley et al., 2011) and haemopexin (Smalley & Olczak, 2015). The holo-HmuY form has a unique structure which mimics a right-handed palm of a hand; the C- and N- terminus on the protein surface resembles the palm/wrist whose protruding segments represents the fingers and thumb that appear to grasp the haem from the Hb molecule (Wojtowicz et al., 2009; Figure 1.5). The haem binding cavity of the haemophore interacts with the haem molecule via two apical histidine residues, one being His-134 of the β8 sheet on the 'thumb' strand and the other at His-166 from the 'ring finger' strand, resulting in a highly symmetrical octahedral iron coordination (6 coordination sites in the haem structure and a further 2 from the HmuY). The haem molecule wedges into the cavity with the charged propionate groups pointing towards the palm and the vinyl substituents facing outwards away from the HmuY interior (Wojtowicz et al., 2009). Significantly, the haemophore forms tetramers in the apo-form, with the four binding sites buried away in the molecule; possibly offering protection from haem scavenging molecules in the host and may explain the resistance of HmuY to protease activity (Olczak et al., 2008; Wojtowicz et al., 2009).

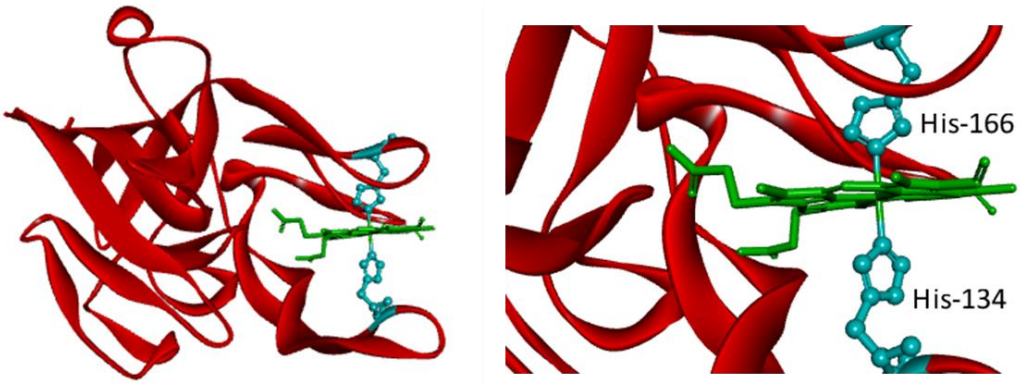

Figure 1.5 – The structure of the HmuY haemophore in complex with Fe(III)haem. The haem molecule (green) is bound by two histidine residues: His-134 and His-166 (blue). PDB access code 38HT.

The mechanism by which HmuY delivers the haem molecule to the cell for internalisation is not fully understood. However, it is proposed that HmuR, a 75-kDa barrel shaped transmembrane TonB-dependant receptor, and encoded by the same hmu operon as HmuY, is involved in the transport of haem across the outer membrane (Simpson et al., 2000; Olczak et al., 2005; Liu et al., 2006). HmuR is capable of binding haem via the His-95 and His-191 amino acid residues, an interaction that is mediated through the haem iron centre (Olczak et al., 2001). HmuR is also capable of binding Hb, and mutation of the *hmu* operon results in reduced growth of *P. gingivalis* with Hb, stemming from inefficient uptake of haem by HmuR (Simpson et al., 2000; Lewis et al., 2006). The importance of HmuY and HmuR in haem capture was demonstrated by the increased expression of the *hmu* operon in haem-depleted environments, suggesting a strong dependency on this system in providing *P. gingivalis* with a vital source of haem (Dashper et al., 2009).

1.2.6 Synergistic involvement of co-colonising species in haem acquisition by *Porphyromonas gingivalis*

It has been shown by Smalley et al (2011) that HmuY functions in synergy with gingipain proteases to facilitate haem acquisition; the first demonstration that a bacterial haemophore acts syntrophically with self-produced proteases to extract haem from Hb. This novel paradigm of haem acquisition displayed by *P. gingivalis* and the role of Rgp and Kgp in metHb formation and haem release has been

extrapolated to *P. intermedia* where the cysteine protease interpain A (InpA) is involved (Byrne et al., 2010). InpA acts in a similar way to RgpA, by facilitating the oxidation of oxyHb to metHb. It was concluded using mass spectrometry that InpA cleaves the Hb α- and β- chains at sites in the distal region of the haem pocket. This alteration in the structure of the haem pocket may enhance nucleophile entry resulting in an increased rate of auto-oxidation of the haem iron (Byrne et al., 2010). MetHb formed by the actions of InpA proteolysis can then be utilised by HmuY to form a HmuY-Fe(III)haem complex akin to that formed after exposure of oxyHb to RgpA and Kgp (Byrne et al., 2013). This was the first evidence to suggest that *P. gingivalis* may utilise a neighbouring species of dental plaque to facilitate metHb formation for haem acquisition (Byrne et al., 2013).

This unique synergistic relationship in haem acquisition was also extended to include *Pseudomonas aeruginosa* and *P. gingivalis*, both of which can co-colonise lungs of cystic fibrosis (CF) patients (Benedyk et al., 2015). Pyocyanin, a redox active phenazine compound, is a virulence factor of *P. aeruginosa*, and displays multiple biological functions during CF lung infections which include inhibition of the beating of cilia, initiation of goblet cell hyperplasia and metaplasia, and destruction of alveolar airspaces (Wilson et al., 1987; Caldwell et al., 2009). Interestingly, the phenazine class of compounds are known to mediate the oxidation of oxyHb to metHb (Minetti et al., 1993). As the fact that *P. gingivalis* and *P. aeruginosa* co-colonise the CF infected lungs, this prompted Smalley and collaborators to examine the potential role for pyocyanin in inducing metHb formation and haem pick up by HmuY. It was shown that HmuY could form the HmuY-Fe(III)haem complex from metHb induced by the action of pyocyanin (Benedyk et al., 2015). Furthermore, using a murine *in vivo* CF model, it was found that mice challenged in the lungs with pyocyanin plus *P. gingivalis* displayed signs of enhanced morbidity and eventual mortality, when compared to mice inoculated with pyocyanin or with *P. gingivalis* alone (Benedyk et al., 2015). These observations correlated with an increased concentration of metHb, total free haem level and Rgp activity in the lung tissue homogenates of the infected mice, indicating that pyocyanin had mediated an

increased availability of haem for *P. gingivalis* and an accompanying increase in virulence (Benedyk et al., 2015).

1.3 Diabetes and periodontitis

1.3.1 Diabetes; non-enzymatic glycation of host proteins and pathophysiological consequences

Diabetes is a metabolic disease arising from insufficient activity of insulin; a peptide hormone produced by the β-islet cells of the pancreas that regulates cellular uptake, storage and utilisation of circulating glucose (American Diabetes Association, 2010). There are two types of diabetes; type I (or juvenile diabetes) is characterised by the inability of the body to produce insulin, whilst type II arises from a resistance to the peptide hormone, often developing in later life (hence often termed "adult-onset diabetes"). Importantly, both forms of the disease are phenotypically associated with hyperglycaemia.

Chronic hyperglycaemia induces multiple physiological alterations such as increasing oxidative stress, promoting inflammatory cytokine production by various tissues and initiating non-enzymatic glycation of an array of host proteins including Hb (known as glycated Hb or HbA_{1c} according to location of glycation in the Hb chain, as will be discussed below; Aronson, D. [2008]). Clinically, the level of glycated Hb in circulating blood is used as a measure of diabetes severity (Makris & Spanou, 2011). In non-diabetic individuals, the concentration of glycated Hb in the blood can range up to 6%, while levels between 6 and 6.5% are associated with a high risk of developing the disease. Levels above 6.5% are largely suggestive of a diabetic state, while in diabetics with poorly-controlled glycaemia, these may increase above 10% (Selvin et al., 2010; Schlienger et al., 1982; Kahlon & Pathak, 2011).

Glycation of Hb (and other proteins) arises via a non-enzymatic condensation reaction between a glucose molecule and the N-terminal of an amino acid in the Hb molecule (Burn et al., 1976). This reaction yields two types of glycated Hb; the first is known as HbA_{1c} in which the glucose is linked to a valine residue of the β-chain,

whilst the second which is known as non-A_{1c} Hb or glycated Hb, arises from a condensation reaction between glucose and one or more lysine residues in either Hb chain (Burn et al., 1976; Shapiro et al., 1980). The most common amino acid that becomes glycated is lysine, due to the prominent exposure of the -NH_2 group (Ansari et al., 2011; Ito et al., 2011). The lysine residues that undergo glycation *in vivo*, in order of prevalence, are Lys-61(α), Lys-17(β) and Lys-66(β) (Bunn et al., 1979) whilst *in vitro*, Lys-7(α), Lys-16(α) and Lys-120(β) may also be glycated (Shapiro et al., 1980).

The generation of glycated Hb within the erythrocyte occurs slowly, first forming a glycosylamide intermediate known as a Schiff base during early exposure to glucose, before undergoing an irreversible Amadori arrangement to generate the final stable glycated product occurring after days of exposure (Ansari & Dash, 2013; see Figure 1.6). Weeks to months after exposure to glucose, the Amadori structure may react with itself or another -NH_2 group (usually of another glycated lysine residue in the Hb chain) to form carboxy-methyl lysine, to develop into Advanced Glycation End products or "AGEs". These Hb derivatives act as potent stimulators of pro-inflammatory cytokine responses (Goldin et al., 2006). As PD is largely driven by an inflammatory response, there are suggestions that an increase in AGEs and cytokine production in hyper-glycaemic individuals may be a crucial trigger and influence the onset of PD in diabetics (Grossi & Genco, 1998; Abbass et al., 2012).

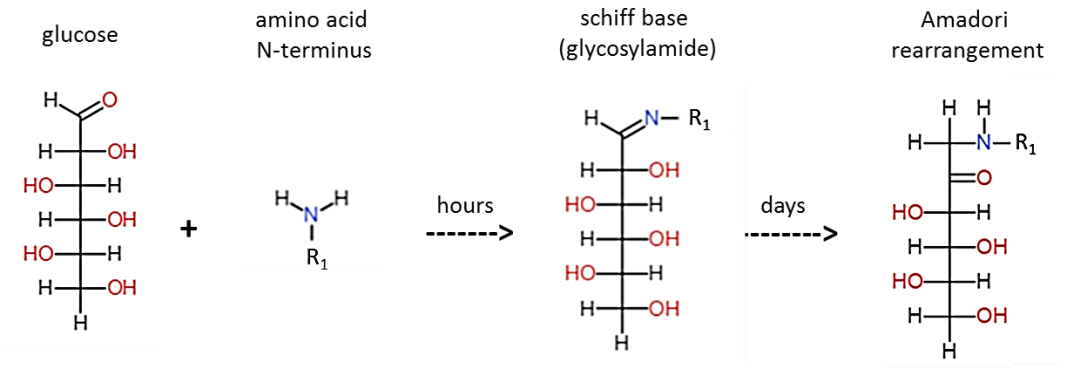

Figure 1.6 – The intermediate molecules formed during exposure of Hb to glucose (adapted from Wautier & Schmidt, 2004). The -NH_2 group represents the N-terminus of an amino acid residue (R_1 refers to the variant R-group in the amino

acid chain) located within the Hb chain. Lysine is the most common amino acid to become glycated during exposure of Hb to glucose.

1.3.2 Link between glycated Hb levels and disease severity in PD; increased colonisation by Red complex microorganisms and oral streptococci in sub- and supragingival dental plaque

An increased level of gingival tissue bleeding is seen in diabetic individuals (Ervasti et al., 1985; Bandyopadhyay et al., 2010). Correlations have been made between glycated Hb blood levels and PD severity in type II diabetic patients and also in an *in vivo* murine model of PD (Taylor et al., 1998; Cintra et al., 2013; Sanchez-Dominquez et al., 2015). Furthermore, clinical studies have demonstrated that there is an increased colonisation by Red complex microorganisms such as *P. gingivalis* in the subgingival plaque of individuals with type II diabetes (Quintero et al., 2011). The enhanced prevalence of *P. gingivalis* in subgingival plaque correlated with high levels of glycated Hb in blood (Makiura et al., 2008). However, the reasons for the elevated number of *P. gingivalis* in diabetics are not fully understood. As *P. gingivalis* displays an absolute growth requirement for haem (Marsh et al., 1994), the above finding would suggest that this parallels an increased haem availability in the gingival crevice and periodontal pocket of diabetics resulting in enhanced numbers of *P. gingivalis*. Indeed, it has been shown using murine models of *P. gingivalis*-induced PD that diabetes exacerbated the extent of alveolar bone loss associated with severe PD (Lalla et al., 1998; Li et al., 2013).

There is also evidence that numbers of oral streptococci are elevated in supragingival plaque and saliva of diabetic individuals (Hintao et al., 2007; Kampoo et al., 2014). Again, the reasons for this increased colonisation are not known, although there is a suggestion that a higher glucose content in the GCF of hyperglycaemic patients (Ficara et al., 1975) may contribute to the increased prevalence of streptococci in the supragingival plaque, since oral streptococci may utilise carbohydrates derived from the GCF as an energy source (Ohlrich et al., 2010). As GCF is also rich in host-proteins (such as transferrin, albumin and Hb) it is likely that oral streptococci will encounter glycated Hb in the gingival crevice and

periodontal pocket of diabetic individuals. However, there is no work investigating the biochemical interactions between oral streptococci and glycated host-proteins, such as glycated Hb.

A history of diabetes may also predispose the host to a more symptomatic endodontic infection (Fouad et al., 2002a; Fouad & Burleson, 2003; Marotta et al., 2012). A study by Fouad et al (2002b) used polymerase chain reaction identification of the microbiota isolated from root canals with necrotic pulps. They reported an increased bacterial load in the teeth from type I and II diabetics compared to non-diabetics, and also an increased prevalence of two *Porphyromonas* species; *P. endodontalis* and *P. gingivalis* (Fouad et al., 2002b). The numbers of other bacterial species such as *Streptococcus mitis* have also been found to be elevated in root canal infections (Fouad et al., 2003; Noronha et al., 2015).

1.3.3 Stability of the haem-globin linkage in glycated Hb; haem and iron release

Glycated Hb and myoglobin have weakened haem-globin linkages resulting in the increased transfer of haem from Hb to albumin (Sen et al., 2005; Roy et al, 2004). Circular dichroism analysis of the structure of glycated Hb suggests that there is a reduction in the number of α-helices of the peptide chains following glycation. It was proposed that this loss of α-helical content results in subtle changes to the protein quaternary structure and a small degree of unfolding of the haem pocket, thus impacting on haem-globin stability (Sen et al., 2005). In addition, the haem molecule in glycated Hb is more prone to degradation by oxidative species (e.g. H_2O_2) resulting in an increased iron release (Sen et al., 2005). It was suggested that the protein unfolding in glycated Hb may enhance entry of H_2O_2 into the haem pocket to facilitate degradation of the haem molecule, and the subsequent release of iron (Sen et al., 2005).

Importantly, in the context of haem liberation from glycated Hb, it should be noted that both glycated oxyHb and oxymyoglobin have an increased susceptibility to auto-oxidise compared to their un-glycated counterparts (Sen et al., 2005; Roy et al, 2004), which in turn further decreases the haem-globin affinity due to metHb

formation (Hargrove et al., 1996). The mechanism by which this occurs is not fully understood, but it is likely that a structural alteration to the glycated protein may enhance nucleophile (OH^- or H_2O) entry into the haem pocket, increasing oxidation of the Fe(II)haem iron to Fe(III) (Springer et al., 1989). If indeed an increased haem abundancy is responsible for enhanced colonisation of *P. gingivalis* in the subgingival plaque of diabetics, the weakened stability of the haem-globin linkage in glycated Hb may present an opportunity to *P. gingivalis* for haem release via increased ease of gingipain attack and/or haemophore extraction.

1.4 Aims of the current study

The aims of the current study were to identify two possible mechanisms which could promote haem availability to *P. gingivalis* whilst considering the physiological conditions that may be encountered in the periodontal pocket and diseased gingival crevice. Specifically, the main aims were as follows;

1) To determine the nature of the oxidised Hb species present in α-haemolytic zones mediated by *S. gordonii* cells when grown on blood agar under aerobic, microaerobic and anaerobic conditions.
2) Investigate the effects of *S. gordonii* cell suspensions on purified oxyHb.
3) Assess the ability of the HmuY haemophore of *P. gingivalis* to acquire haem from the oxidised Hb species generated by *S. gordonii* cells.
4) To compare the rates of haem acquisition by the HmuY haemophore from glycated and un-glycated Hb.
5) Analyse the structures of glycated and un-glycated Hb using circular dichroism and mass spectroscopy.

Chapter 2 Materials and Methods

2.1 Bacteria growth conditions

S. gordonii strains 35.1 (clinical isolate; Smalley et al., 1994) and DL1 were initially used to assess α-haemolytic activity. *S. gordonii* 35.1 exhibited more prominent α-haemolysis and as a result was used throughout the study. Generally, for analysis of the α-haemolytic effects, *S. gordonii* strain 35.1 was routinely grown aerobically at 37^{o}C on blood agar comprising fresh defribinated horse blood (5% v/v; TCS Biosciences; blood agar base; Oxoid Ltd). For some experiments, growth was also carried out under anaerobic and micro-aerobic conditions at 37^{o}C. Micro-aerobic conditions were produced using an air-tight candle jar, whilst anaerobic growth was carried out in the Don Whitley anaerobic workstation (MG1000; Don Whitley Scientific) under standard atmospheric conditions (10% H_2, 10% CO_2 and 80% N_2).

S. gordonii cell suspensions were produced by sub-culturing pure colonies from blood agar into liquid BHI broth (Fluka Analytical, Sigma Aldrich) and incubating aerobically overnight at 37^{o}C, whilst stirring at 200 rpm. After 24 hours of growth in liquid media, the cells were centrifuged at 12,000 x g for 10 minutes at 5^{o}C, washed three times with 0.14M NaCl, 0.1M Tris-HCl buffer, pH 7.5, then used immediately, or, for some experiments, stored at -80^{o}C in the above buffer.

2.2 Preparation of haemoglobin species

2.2.1 Oxyhaemoglobin purification

OxyHb was prepared as previously described (Smalley et al., 2002) from fresh de-fribinated horse blood. In short, erythrocytes were pelleted by centrifugation at 5000 x g, the pellet washed three times in isotonic buffered saline (0.14M NaCl, 0.1M Tris-HCl, pH 7.5) to remove plasma components, and to allow for the removal of the buffy coat layer which was pipetted off. The packed erythrocytes were then freeze-thawed then lysed by re-suspension in 1 mM Tris-HCl buffer (pH 7.0) for 20 minutes at 20°C. Next, the cell membranes were removed from the haemolysate by centrifugation (20,000 x g for 20 minutes at 5°C) and the Hb-containing supernatant was stored in NaCl-Tris buffer, pH 7.5, as a stock solution (approximately 1mM with respect to Hb tetramer) until required at -80^{o}C to minimise any auto-oxidation.

2.2.2 Methaemoglobin formation

MetHb formed by the action of *S. gordonii* cells was produced by incubating 4µM oxyHb (tetramer) with suspensions of cells at various densities (1.00, 0.50 and 0.33 OD_{600}) in BHI broth at 37°C for 4-6 hours. MetHb generated by exposure of oxyHb to H_2O_2 was carried out by reacting 4µM oxyHb (tetramer) with glucose oxidase (GOX; 0.01µM) and glucose (50mM) for 1-4 hours at 20°C (Giulivi & Davies, 1990). Control metHb generated without exposure to H_2O_2 was made via auto-oxidation of 1mM oxyHb for 48-72 hours at 37°C in NaCl-Tris buffer, pH 7.5. All metHb samples were used immediately or stored at -80°C until required. Such preparations remain stable at -80°C for several months.

2.2.3 Deoxyhaemoglobin preparation by reduction of metHb with sodium dithionite

Sodium dithionite ($Na_2S_2O_4$) is a strong reducing agent, capable of converting metHb (Fe(III)haem) into deoxyHb (Fe(II)haem) and depleting O_2 in aqueous solution (Dalziel & O'Brien, 1957). For this, freshly prepared 100mM stock solutions of $Na_2S_2O_4$ in NaCl-Tris buffer, pH 7.5, were made and used within one hour of preparation to avoid decomposition of $Na_2S_2O_4$ upon contact with any dissolved O_2. $Na_2S_2O_4$ was added to a final concentration of 10mM to 4µM Hb (tetramer basis) and the formation of deoxyHb was confirmed spectroscopically by the appearance of a Soret band λ_{max} at 430nm and Q band at 555nm (Antonini & Brunori, 1971).

2.2.4 Preparation of glycated Hb by affinity chromatography

Glycated Hb was produced using a modified protocol previously described by Ch'ng and Marinah (1988). In short, 200µl of 0.5mM oxyHb containing 250mM glucose plus 100U/ml penicillin and 100µg/ml streptomycin in NaCl-Tris buffer, pH 7.5, was applied to Whatman grade 1 filter papers (47mm diameter) and incubated in sterile petri dishes for 7 days at 37°C. Un-glycated control Hb was produced under the same conditions but without glucose addition. Following the 7-day incubation, the Hb which had dried into the filter paper was extracted by rotating the papers gently for 30 minutes at 20°C in 3ml of the above buffer. Residual glucose and buffer

constituents were removed from the glycated Hb preparations by dialysis in cellulose membrane dialysis tubing (10mm width; Sigma Aldrich) at 5^{o}C. For this, Hb samples were dialysed firstly versus 500ml dH_2O for two hours, then against 500ml ammonium acetate buffer (pH 8.5, 0.25M) for two hours, before one final hour against 500ml of the above buffer containing 20mM magnesium chloride. This last step was carried out for purification of the glycated protein using phenylboronic acid (PBA) affinity resin (Middle et al., 1983; section 2.2.5).

2.2.5 Phenylboronic acid affinity (PBA) resin purification of glycated Hb

The separation of glycated Hb using immobilised PBA resin was done as previously described by Middle et al (1983). The PBA resin binds compounds containing cis-diol moieties with high affinity through a reversible boronate formation (Springsteen & Wang, 2002). 1ml of glycated and un-glycated Hb (approximately 100µM with respect to tetramer, prepared as described in section 2.2.4) were each added separately to 1ml of the PBA resin (Sigma Aldrich; A8530). The Hb samples were gently mixed by rotation for 1 hour at 20^{o}C to allow for the glycated Hb to bind to the PBA, then samples were centrifuged at 12,000 x g for 10 minutes to pellet the resin carrying the reversibly bound glycated Hb. For the control Hb samples treated without glucose, the supernatants containing unbound Hb was saved and used as un-glycated control Hb samples throughout. Resin-bound Hb (and hence glycated) was desorbed from the resin by the addition of 1ml of 0.25M ammonium acetate (pH 8.5) containing 0.2M sorbitol, which acts as a competing diol, binding with higher affinity to the PBA resin, and forcing release of the glycated Hb. Samples were gently mixed by rotation for 1 hour at 20^{o}C to allow for the sorbitol to compete with the glycated Hb bound to the resin. Following centrifugation at 12,000 x g for 10 minutes, the glycated Hb-containing supernatants were dialysed against 500ml dH_2O for 2 hours at 5^{o}C, to remove residual sorbitol in the solution. The degree of Hb glycation was determined as described in section 2.4.3.

2.3 Spectroscopical analysis of Hb species

2.3.1 UV-visible spectroscopy

All UV-visible spectroscopy work was completed at 20^{o}C on an Ultrospec 2000 spectrophotometer (Pharmacia Biotech), using either 1ml plastic semi-micro cuvettes (VWR International), or UV-transparent microcuvettes (70-200µl; Brand, GMBH, Wertheim, Germany) both with 1cm path lengths. Where appropriate, absorbance spectra were corrected by subtraction of the control buffer.

2.3.1.1 Determination of oxyhaemoglobin oxidation

The conversion of oxyHb to metHb is observable spectroscopically by the blue shift in the Soret band from 414nm to approximately 405nm, and loss of peak intensities in the Q band region at 541nm and 577nm (Winterbourn et al., 1976). For some experiments, oxyHb oxidation was depicted as a change in A_{577nm} plotted against time as previously described (Smalley et al., 2007). For other measurements, difference spectra were produced by subtracting initial time zero spectrum from spectra at each subsequent time point. The summed integrated peak areas of 348-411nm and trough areas between 411-472nm were also used as an indirect measure of the amount of metHb formed (Zhang et al., 1996; Kelm et al., 1997; Byrne et al., 2010).

2.3.1.2 Calculation of concentrations of oxyHb, metHb and haemichrome species

The simultaneous equations used to calculate the concentrations of oxyHb and metHb were derived from Winterbourn et al (1976), and rearranged to give the following expressions;

$$[\text{oxyHb}] = 0.0156.A_{577nm} - 0.0168.A_{630nm} \quad (1)$$

$$[\text{metHb}] = 0.0726.A_{630nm} - 0.0011.A_{577nm} \quad (2)$$

However, the millimolar extinction coefficients at 577nm and 630nm used for oxyHb and metHb were: $\varepsilon\text{oxyHb}_{577nm} = 65$, $\varepsilon\text{oxyHb}_{630nm} = 1$, $\varepsilon\text{metHb}_{577nm} = 15$ and

$\varepsilon metHb_{577nm}$ = 14, respectively, and were determined previously using 4µM horse Hb reference samples in NaCl-Tris buffer, pH 7.5 (Smalley et al., 2007).

Where appropriate the concentrations of haemichrome were calculated using manipulations of the above expressions to account for the change at A_{560nm} associated with haemichrome formation, as described by Byrne (2011).

$$[oxyHb] = 29.75.A_{577nm} – 9.75.A_{630nm} – 22.25.A_{560nm} \quad (3)$$

$$[metHb] = 7.00.A_{577nm} + 76.75.A_{630nm} – 13.75.A_{560nm} \quad (4)$$

$$[haemichrome] = 58.25.A_{560nm} – 28.25.A_{577nm} – 28.50.A_{630nm} \quad (5)$$

2.3.2 Circular Dichroism

Circular dichroism analysis of Hb was carried out on a Jasco 1100 circular dichroism spectrometer. Far- and near-UV data analysis was completed for the 180-260nm and 260-320nm wavelength regions, respectively, using 1cm path length quartz cells. Experiments were conducted at 20^{o}C using Hb concentrations of 0.5µM and 5µM (with respect to tetramer), for far- and near-UV analysis, respectively. All Hb preparations were dialysed against 500ml of 0.1M NaH_2PO_4/Na_2HPO_4 buffer (pH 7.4) prior to data collection, due to the propensity of Cl^- ions and Tris molecules to absorb light at 180-200nm. Hb samples were scanned 25 times and corrected against control buffer minus Hb.

2.3.3 Mass spectrometry

Liquid chromatography mass spectrometry data analysis was kindly performed by Dr. Rosalind Jenkins, Institute of Translational Medicine, The University of Liverpool. The procedure was carried out using the Triple TOF 5600 mass spectrometer (Sciex). In brief, the Hb samples (16µM tetramer of glycated Hb and control Hb minus glucose addition, respectively) were diluted 1:10 in 0.1M NaH_2PO_4/Na_2HPO_4 buffer, pH 7.4 and 0.5µg trypsin (MS grade; Sigma Aldrich) was added before incubation overnight at 37^{o}C. Hb samples were desalted by reversed-phase chromatography using ZipTips (Millipore) before delivery to the mass spectrometer by automated in-

line reversed phase liquid chromatography. Protein sequence coverage was determined by means of ProteinPilot software v4.0 (Sciex) using the ParagonTM algorithm (Shilov et al., 2007) and the most recent version of the SwissProt database as visited on December 2015 (http://www.uniprot.org/).

2.4 Analytical methods

2.4.1 Colorimetric assay for haem

Haem content was determined using the Triton-X100-methanol assay described by Pandey et al (1999). In this assay, 0.1 ml haem-containing samples were mixed with 0.9 ml of Triton-X100 (2.5% v/v dissolved in methanol). Under these conditions, Triton-X100 forms a green coloured complex with haem having a Soret band λ_{max} at 397nm which has an extinction coefficient (ε) of 165 mM^{-1} cm^{-1} (Pandey et al., 1999).

2.4.2 H_2O_2 assay using the Fe(III)-xylenol orange method

The Fe(III)-xylenol orange method for H_2O_2 detection relies on a colorimetric reaction, whereby H_2O_2 will react with sorbitol and, via formation of the OH^- ion, will oxidise the Fe(II) of a solution of ammonium ferrous (II) sulphate to Fe(III), which, in turn, forms a complex with the xylenol orange reagent, changing the dye to a purple colour (Jiang et al., 1990). The protocol and reagent concentrations specified by the Pierce™ Quantitative Peroxide Assay was followed. In short, the working reagent was prepared by mixing 1 volume of 2.5M H_2SO_4 in dH_2O containing 25mM ammonium ferrous (II) sulphate, with 10 volumes of dH_2O containing 100mM sorbitol and 125µM xylenol orange. 10 volumes of working reagent was added to 1 volume of sample containing unknown H_2O_2 concentrations, mixed and incubated at 20°C, before samples were analysed spectroscopically after 15-20 minutes. In the presence of H_2O_2, the purple chromogen yields a peak λ_{max} at 560nm. Unknown H_2O_2 concentrations were calculated against a standard curve produced by serial dilutions of a stock solution of H_2O_2 (30% v/w) which were confirmed using the extinction coefficient (ε) of 43.6

M^{-1} cm^{-1} at 240nm for H_2O_2 (Beers & Sizer, 1952). The working range of the Fe(III)-xylenol orange method is 1µM-1mM.

2.4.3 5-hydroxymethylfurfural assay as a measure of Hb glycation

Thiobarbituric acid (TBA) is used universally to determine the concentration of 5-hydroxymethylfurfural (5-HMF), a breakdown product of glucose, in samples of glycated proteins including Hb (Fluckiger & Winterhalter, 1976). To hydrolyse the glycated moieties from the protein, 0.25ml of oxalic acid (1.5M) was added to 0.5ml of purified glycated Hb and un-glycated Hb samples and heated at 100^{o}C for 4 hours in heat-resistant screw-cap Eppendorf tubes. Next, 0.25ml of 40% v/v trichloroacetic acid was added to each Hb sample and left for 5 minutes at 20^{o}C to precipitate the protein, then centrifuged at 12,000 x g for 5 minutes. 0.8 ml of the protein-free supernatant was incubated for 1 hour at 40°C with 0.2 ml TBA (50mM in dH_2O). In the presence of glycated products, a colorimetric reaction occurs between the TBA and 5-HMF resulting in a yellow chromogen with 443nm λ_{max}. The absorbance of the cooled sample was read at A_{443nm} against a control ammonium acetate buffer (0.25M, pH 8.5) minus Hb and 5-HMF concentration was determined against a standard curve generated for serial dilutions of 5-Hydroxymethyl-2-furaldehyde (Sigma Aldrich).

2.4.4 Colorimetric ferrozine-based assay for the quantitation of iron

The colorimetric ferrozine-based assay detects Fe(II) iron in solution at low pH values. The yellow-coloured ferrozine working reagent (100mg of thiosemicarbazide, 1g of ascorbic acid, and 100mg of ferrozine, dissolved in dH_2O and diluted to a final volume of 100ml with 0.1mol/L HCl) was prepared according to previous work (Ceriotti & Ceriotti, 1980). The working reagent was mixed with samples of unknown iron concentration, in a ratio of 1:2, and incubated at 37^{o}C for 20 minutes. In the colorimetric reaction, ascorbic acid will reduce Fe(III) to Fe(II) iron, and ferrozine will chelate Fe(II) iron under acidic conditions yielding a magenta-coloured complex with 562nm λ_{max} and extinction coefficient (ε) of 28

mM^{-1} cm^{-1}. All readings were corrected by the subtraction of control blanks produced by preparing the above working reagent but omitting ferrozine.

2.5 HmuY purification and isolation

The apo-HmuY haemophore of *P. gingivalis* was kindly provided by Professor Teresa Olczak (Laboratory of Biochemistry, Institute of Biochemistry and Molecular Biology, University of Wroclaw, Poland). It was purified from the soluble fraction of the *Escherichia coli* lysate as previously described (Olczak et al., 2008). In brief, the HmuY gene lacking the first 25 residues was amplified on *P. gingivalis* A7436 genomic DNA and cloned into the NcoI and HindIII restriction sites of the pTriEx-4 vector (Novagen), resulting in a pHMUY11 plasmid that was transformed into ER2566 *E. coli* cells. HmuY was purified from the lysate by ion-exchange chromatography and gel filtration chromatography. Stock solutions of 1.06mM were stored at -20^{o}C.

2.6 Data graphing and statistical analysis

All graphs were produced using Prism 3.03 (GraphPad software) unless specified otherwise. Where appropriate, Student's unpaired t-test was used for statistical analysis. Molecular structure diagrams were produced from Protein Data Bank (PDB) files using the Accelrys Discovery Studio 2016 Client (BIOVIA) visualizer program (http://accelrys.com/products/collaborative-science/biovia-discovery-studio).

Chapter 3 Methaemoglobin formation by *Streptococcus gordonii* cells

3.1 Introduction

There is little data that describes the Hb species formed from the process of α-haemolysis mediated by *S. gordonii* during growth on blood agar. α-haemolysis is usually manifest as a yellow or yellow-green zone around the colonies of *S. gordonii* during aerobic growth. Working on *S. gordonii*, Barnard & Stinson (1996) concluded that H_2O_2 was the "α-haemolytic agent" responsible for the discoloration associated with this effect. However, as their work primarily concerned identification of the agent responsible they only proposed that the haemolytic effect was accompanied by Hb Fe(II)haem oxidation. This was based upon the observation that the UV-visible spectrum of the Hb species showed a blue shift in the Soret band from 414nm to 403nm and a decrease in peak intensity at 578nm; characteristic of an oxidised form of Hb. These spectral changes were observed after incubation of suspensions of sheep erythrocytes with spent liquid growth medium from *S. gordonii* or upon addition a bolus of H_2O_2. The addition of catalase to the above incubations abrogated the α-haemolytic effects of both the spent growth medium of *S. gordonii* and H_2O_2. From these observations, it was concluded that H_2O_2 was responsible for α-haemolysis (Barnard & Stinson, 1996).

As discussed above, metHb is the preferred substrate from which *P. gingivalis* derives haem via gingipain-mediated proteolysis and/or extraction by HmuY (Smalley et al., 2007; 2011; Wojtowicz et al., 2009). Therefore, as α-haemolysis by *S. gordonii* appears to be accompanied by Hb oxidation, it is possible that this bacterial species may provide *P. gingivalis* with a source of Fe(III)haem should these two species co-aggregate in an environment where oxyHb becomes available e.g., the periodontal pocket following gingival tissue bleeding. Therefore, a more detailed spectroscopic examination of the Hb species produced as a result of α-haemolysis brought about by *S. gordonii* under aerobic conditions was undertaken to determine the exact composition of the Hb present. Furthermore, as co-aggregates of *P. gingivalis* plus *S. gordonii* may experience reduced O_2 levels depending on periodontal pocket depth and disease status (Loesche et al., 1983; Mettraux et al., 1984; Tanaka et al., 1998), it was pertinent to analyse α-haemolysis mediated by *S. gordonii* under microaerobic and anaerobic environments,

consistent with conditions that may exist *in vivo* within the periodontal pocket. Finally, in this chapter, studies will be described which examine the effects of cell suspensions of *S. gordonii* on isolated oxyHb.

3.2 Materials and methods

3.2.1 Analysis of horse blood agar extracts resulting from α-haemolysis mediated by *S. gordonii*

S. gordonii was grown under aerobic, microaerobic (candle jar) and anaerobic conditions on horse blood agar. A total of three agar extracts from the blood agar plate were taken aseptically from zones of α-haemolysis, removed as plugs using the widest ends of sterile glass pasteur pipettes. These plugs were suspended in 1ml of 0.14M NaCl, 0.1M Tris-HCl buffer, pH 7.5, and freeze-thawed between room temperature and -20^{o}C for a total of three cycles, before the agar was pelleted by centrifugation (12,000 x g for 5 minutes at 20^{o}C), yielding a Hb-containing supernatant which was analysed spectroscopically.

3.2.2 Incubation of oxyHb with *S. gordonii* cells

S. gordonii cells were aerobically grown on blood agar overnight and sub-cultured under aerobic conditions in BHI broth for a further 24 hours at 37^{o}C. Following centrifugation (12,000 x g for 10 minutes, at 5^{o}C), the *S. gordonii* pellets were washed three times in NaCl-Tris buffer, pH 7.5, and re-suspended in BHI broth to yield suspensions with final cell densities of 1.00, 0.50 and 0.33 OD_{600}, respectively. 4μM oxyHb (tetramer basis) was added to each cell suspension and incubated aerobically at 37^{o}C. OxyHb controls were made in BHI broth without bacterial inoculum.

3.2.3 Incubation of oxyHb with cell-free growth medium of *S. gordonii*

S. gordonii cells were grown aerobically to 1.00 OD_{600} in BHI broth at 37^{o}C and pelleted by centrifugation (12,000 x g for 10 minutes at 5^{o}C), then filter sterilised through 0.2μm Acrodisc membranes (Gelman Sciences) to remove any residual *S. gordonii* cells. To assess the extent of metHb formation by spent growth medium,

4µM oxyHb (tetramer basis) was incubated with the cell-free supernatants from the above cultures for 4 hours at 37°C, and monitored spectroscopically.

3.2.4 Measurement of *S. gordonii*-generated H_2O_2 by Fe(III)-xylenol orange

S. gordonii cells were grown on blood agar overnight and sub-cultured in BHI broth for 24 hours (both aerobically), then pelleted and washed in NaCl-Tris buffer, pH 7.5, as above. Cells were resuspended to an OD_{600} of 0.25 and 1.00 in either NaCl-Tris buffer, pH 7.5, containing 100mM glucose, or in BHI broth alone, then incubated for 4 hours at 37°C. At intervals, 150µl of the samples were centrifuged (12,000 x g for 10 minutes at 20°C) to pellet the cells and 100µl of the supernatant was added to 1ml of Fe(III)-xylenol orange assay working reagent. The A_{560nm} was measured after correction by subtraction of the absorbance of a control containing NaCl-Tris buffer, pH 7.5, plus 100mM glucose, or BHI broth alone without bacterial inoculum. H_2O_2 concentrations were calculated using a standard curve produced by serial dilutions of H_2O_2, which were confirmed using the extinction coefficient (ε) of 43.6 M^{-1} cm^{-1} at 240nm for H_2O_2 (Beers & Sizer, 1952).

3.2.5 α-haemolysis and metHb formation mediated by H_2O_2 generated via the glucose/glucose oxidase (G/GOX) enzymatic reaction

Glucose incubation with glucose oxidase (GOX) was used as a model system for the generation of H_2O_2 (Beers & Sizer, 1952). 100µl of a solution of glucose (50mM) and GOX (2µM) in NaCl-Tris buffer, pH 7.5, were added together to 0.5mm diameter wells made using the wide ends of sterile glass pasteur pipettes in horse blood agar plates and incubated aerobically at 37°C. Zones of α-haemolysis surrounding the wells were removed aseptically from the agar and freeze-thawed as described above to extract Hb before spectroscopic analysis.

3.2.6 Identification of ferrylhaemoglobin during metHb generation by *S. gordonii* cell suspensions

Sulphaemoglobin (sulpHb) can be used as a surrogate measure for the presence of ferrylhaemoglobin (ferrylHb; Giulivi & Davies, 1994). To detect ferrylHb generation

by *S. gordonii* cells, 4μM oxyHb was incubated with *S. gordonii* cells in BHI broth (1.00 OD_{600}) for 6 hours at 37°C. After the cells were pelleted by centrifugation (12,000 x g for 10 minutes at 5°C), 1μM bovine catalase was added to the Hb-containing supernatants to scavenge any residual H_2O_2. Hb samples were then analysed spectroscopically for the characteristic Q band at 618nm which is indicative of sulpHb (Giulivi & Davies, 1994; Herold & Rehmann, 2003), immediately before and after addition of 200μM sodium sulphide (Na_2S; Sigma Aldrich). All spectra were compared against control metHb samples produced in BHI broth formed by auto-oxidation without the actions of H_2O_2.

3.3 Results

3.3.1 Hb species present in α-haemolytic zones produced by *S. gordonii* on horse blood agar

In order to study the Hb species from zones of α-haemolysis produced by *S. gordonii*, cells (strains 35.1 and DL1) were grown overnight under aerobic conditions at 37°C on fresh horse blood agar (in which there was an initial 97% oxyHb prior to incubation). *S. gordonii* strain 35.1 mediated very clear α-haemolysis surrounding bacterial colonies after 16 hours, manifest as a yellow-straw discolouration on the blood agar (Figure 3.1). Although α-haemolysis was observed during growth of *S. gordonii* strain DL1, after 16 hours this was minimal compared to strain 35.1, and so the latter strain was used throughout the study. After 16 hours, control plates without bacterial inoculum maintained a bright red colour typical of oxygenated blood (oxyHb). The agar from the control plate and from zones of α-haemolysis surrounding *S. gordonii* strain 35.1 colonies were aseptically removed using pasteur pipettes as above, and freeze-thawed in 1ml of NaCl-Tris buffer, pH 7.5, to release proteins into solution. Following centrifugation (12,000 x g for 10 minutes at 5°C), the Hb-containing supernatants were analysed spectroscopically (Figure 3.2). The UV-visible spectrum of the extract from the control plate was indicative of the presence of oxyHb (412nm Soret λ_{max} and prominent Q band features at 541nm and 577nm). In comparison, spectroscopic features characteristic of metHb were observed in the Hb extract from α-haemolytic

zones adjacent to the colonies i.e., a blue shift in the Soret band λ_{max} to 405nm, the loss of 577nm and 541nm peak intensities, and increase at 500nm and 630nm. The A_{560nm}, A_{577nm} and A_{630nm} values for both Hb extracts derived from the spectra were used in the three-component analysis expression to measure the relative oxyHb, metHb and haemichrome concentrations (section 2.3.1.2). These calculations indicated that the major Hb species from α-haemolytic zones was metHb (92%), with 8% oxyHb, whilst no haemichrome was detected. In contrast, the Hb species in the control blood agar extract was predominantly oxyHb with approximately 8% metHb and no haemichrome present. This confirmed that α-haemolysis mediated by *S. gordonii* was accompanied by metHb formation. It is noteworthy that similar spectral features were observed for the Hb species in an agar extract surrounding *S. gordonii* DL1 colonies, although there was significantly less metHb after incubation for 16 hours compared to *S. gordonii* 35.1 (42%; data not shown).

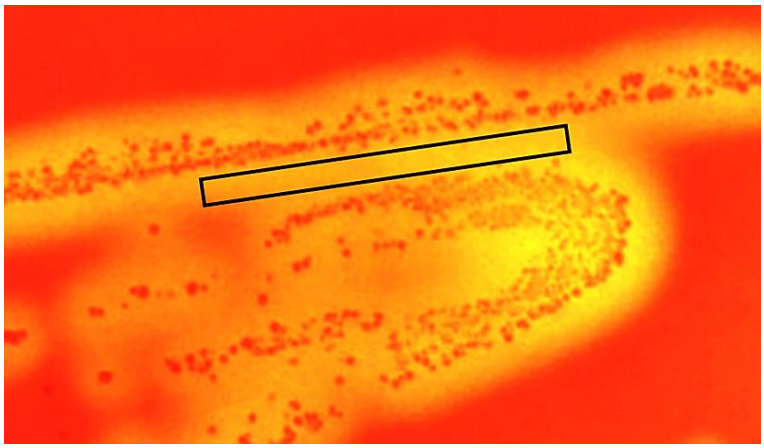

Figure 3.1 – α-haemolysis mediated by *S. gordonii* strain 35.1 after aerobic growth on horse blood agar at 37°C. The black rectangle denotes the α-haemolytic zone adjacent to the *S. gordonii* colonies removed for extraction of the Hb species following 16-hour incubation.

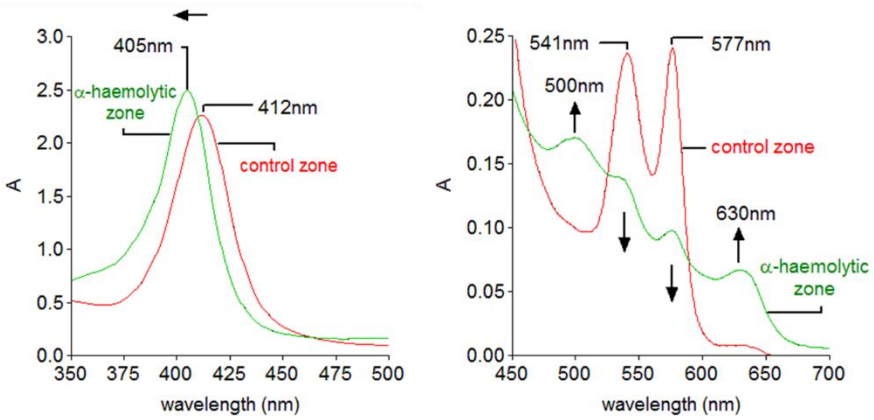

Figure 3.2 – UV-visible spectra of the Hb species extracted from α-haemolytic zones produced by *S. gordonii* grown aerobically on horse blood agar at 37°C. After 16 hours, the agar was removed from α-haemolytic zones adjacent to the colonies (black rectangle, Figure 3.1) and a control plate minus bacterial inoculum. A soluble Hb fraction was extracted from the agar following 3 cycles of freeze-thawing in NaCl-Tris buffer, pH 7.5. Arrows denote the change in peak intensities of Soret and Q band regions associated with metHb.

The blood agar extracts were treated with 10mM sodium dithionite ($Na_2S_2O_4$), to simultaneously reduce the Hb Fe(III)haem (in metHb) to Fe(II) (in deoxyHb) and deplete the O_2 present in the buffer (Dalziel & O'Brien, 1957). The resulting spectrum with 430nm Soret band and 555nm Q band was indicative of deoxyHb (Figure 3.3). Using ε430nm of 136.5mM^{-1} cm^{-1} (with respect to Hb subunit) for deoxyHb, the concentration of deoxyHb in the solution was calculated as 4μM (tetramer basis) which corresponded to the total concentration of oxyHb plus metHb in the α-haemolytic zone, confirming all the Hb in the extract had been

converted to deoxyHb. This verified that metHb had originally been formed as a consequence of α-haemolysis.

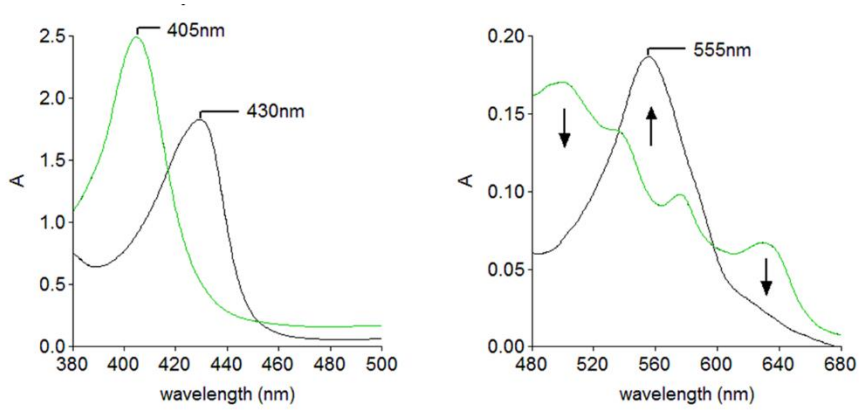

Figure 3.3 – Effect of chemical reduction of the Hb extracts from α-haemolytic zones mediated by *S. gordonii*. The Hb extract from α-haemolytic zones (green line) was reduced using 10mM $Na_2S_2O_4$ (black line). The 430nm Soret and 555nm Q band are typical of deoxyHb.

3.3.2 MetHb formation during α-haemolysis produced by *S. gordonii* under microaerobic and anaerobic conditions

During the maturation of supragingival and subgingival dental plaque, O_2 tension levels can decline (Mattreux et al., 1984; Loesche & Grossman, 2001). As a result, *S. gordonii* may encounter microaerobic and anaerobic environments, and therefore in the following sections, the extent of α-haemolysis of *S. gordonii* under these conditions was investigated. It is noteworthy that, to simulate microaerobic conditions that may occur *in vivo* in dental plaque and the periodontal pocket, the candle jar technique has been shown to generate an atmosphere of approximately 5-10% O_2 and 3-5% CO_2, respectively (Mukherjee, 2010). After 16 hours, *S. gordonii* cells mediated α-haemolysis when grown on horse blood agar under microaerobic (candle jar) and anaerobic conditions at 37°C. Hb in the agar extracts from zones of α-haemolysis produced by *S. gordonii* cells under aerobic, microaerobic and anaerobic conditions were removed and analysed spectroscopically as above. Compared to the control blood agar, metHb was also the major form of Hb in α-haemolytic zones produced by *S. gordonii* under both microaerobic and anaerobic

conditions (Figure 3.4). The % of metHb in α-haemolytic zones produced under aerobic conditions were 94.4 ± 0.8% compared to 8.1 ± 1.1% in the control plate extracts. Under microaerobic conditions, metHb was 85.8 ± 1.9% compared to 22.2 ± 1.3% from the un-inoculated plate extracts. α-haemolytic zones generated during anaerobic growth of *S. gordonii* contained 76.1 ± 2.0 % metHb, while the control plate extracts comprised of 41.7 ± 0.9% metHb. The remaining Hb species under aerobic, microaerobic and anaerobic conditions was oxyHb. It should be noted that the increase in metHb formation in the control plate extracts under microaerobic and anaerobic conditions was likely due to the enhanced rate of auto-oxidation of oxyHb under reduced O_2 conditions (Balagopalakrishna et al., 1996; Rifkind & Nagababu, 2013). Nonetheless, there was significantly more metHb generated in zones of α-haemolysis mediated by *S. gordonii* under microaerobic and anaerobic conditions, compared to control plate extracts. Taken together, these findings show that *S. gordonii* mediated α-haemolysis accompanied with formation of metHb under aerobic, microaerobic and anaerobic conditions.

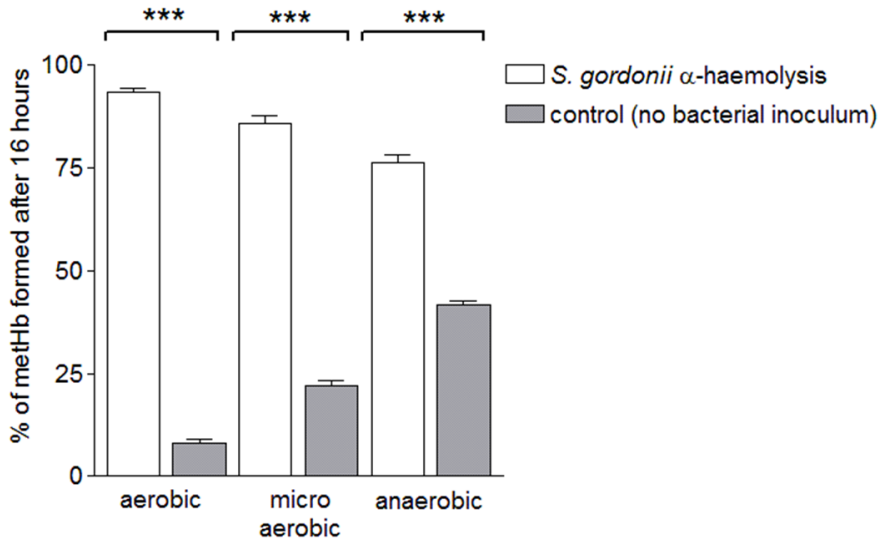

Figure 3.4 – Relative levels of metHb in α-haemolytic zones mediated by *S. gordonii* under aerobic, microaerobic and anaerobic conditions. *S. gordonii* cells were grown on horse blood agar for 16 hours at 37°C. Error bars denote standard error; n= 3. Significant differences were determined by unpaired t test (*** $p < 0.001$).

3.3.3 MetHb formation during incubation of oxyHb with *S. gordonii* cell suspensions

The following section assesses the ability of the *S. gordonii* cells to generate metHb when incubated with isolated oxyHb in the absence of other constituents such as serum albumin which can scavenge Fe(III)haem from metHb (Hargrove et al., 1996). *S. gordonii* cells were cultured in BHI broth for 24 hours at 37^{o}C, and following centrifugation (12,000 x g for 10 minutes at 5^{o}C), pellets were washed three times in NaCl-Tris buffer, pH 7.5, to remove overnight growth medium constituents and secreted components, then resuspended to an OD_{600} of 1.00 in either BHI broth, or in the above buffer containing 100mM glucose. OxyHb was added to the above cell suspensions to a final concentration of 4μM (tetramer), and samples were incubated aerobically at 37^{o}C.

After 4 hours of incubation with *S. gordonii* in BHI broth, there was spectroscopic evidence of metHb formation i.e., a Soret blue shift from 414nm to 405nm (Figure 3.5, left panel), increases in peak intensity at 500 and 630nm, and decreases at 541 and 577nm Q bands (Figure 3.5, right panel). From these spectra, the relative concentrations of oxyHb, metHb and haemichrome were calculated, revealing that metHb was the most abundant species (95%) with the remaining 5% in the form of haemichrome. In comparison, control oxyHb incubations in BHI broth minus *S. gordonii* contained 33% metHb, with the remaining Hb species in the form of oxyHb. However, the incubation of oxyHb with *S. gordonii* cells in NaCl-Tris buffer, pH 7.5, containing 100mM glucose generated a similar amount of metHb (36%) as the un-inoculated control, with the remaining Hb species consisting of largely oxyHb (64%). Taken together, these findings indicated that *S. gordonii* cells resuspended in BHI broth mediated metHb formation from oxyHb.

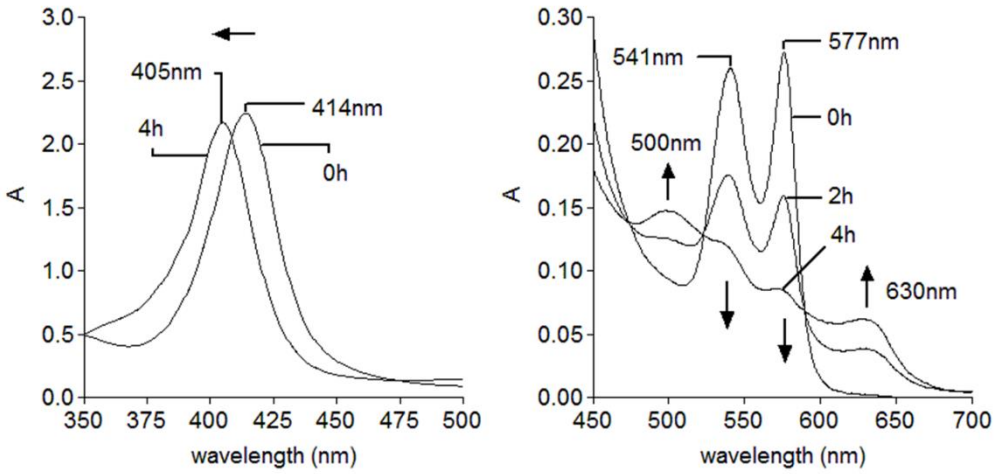

Figure 3.5 – Conversion of oxyHb into metHb by *S. gordonii* cell suspensions. 4µM oxyHb was incubated aerobically with *S. gordonii* cells (1.00 OD_{600}) suspended in BHI broth for 4 hours at 37°C. Arrows denote changes in peak intensities associated with metHb formation.

3.3.4 MetHb formation during exposure of oxyHb to *S. gordonii* cell-free spent growth medium

To investigate whether metHb formation by *S. gordonii* required direct contact between Hb and whole cells to facilitate metHb formation, oxyHb was incubated with *S. gordonii* cell-free spent growth medium. *S. gordonii* (1.00 OD_{600}) was cultured aerobically as above in BHI broth for 16 hours at 37°C and, following centrifugation (12,000 x g for 10 minutes at 5°C), the supernatant was filter sterilised through 0.2µm membranes to ensure no cells remained in the suspension. 4µM oxyHb was then incubated with 1ml of cell-free growth medium aerobically at 37°C for 4 hours. Sequential spectra (Figure 3.6) indicated that metHb was formed (blue shift in the Soret band to 406nm, and absorbance increases at 500nm and 630nm, and decreases at 541nm and 577nm). After 4 hours, there was 73% metHb in the suspension with the remainder oxyHb (25%) and haemichrome (2%). Control oxyHb incubated in BHI broth alone contained 33% metHb and 67% oxyHb, respectively (data not shown).

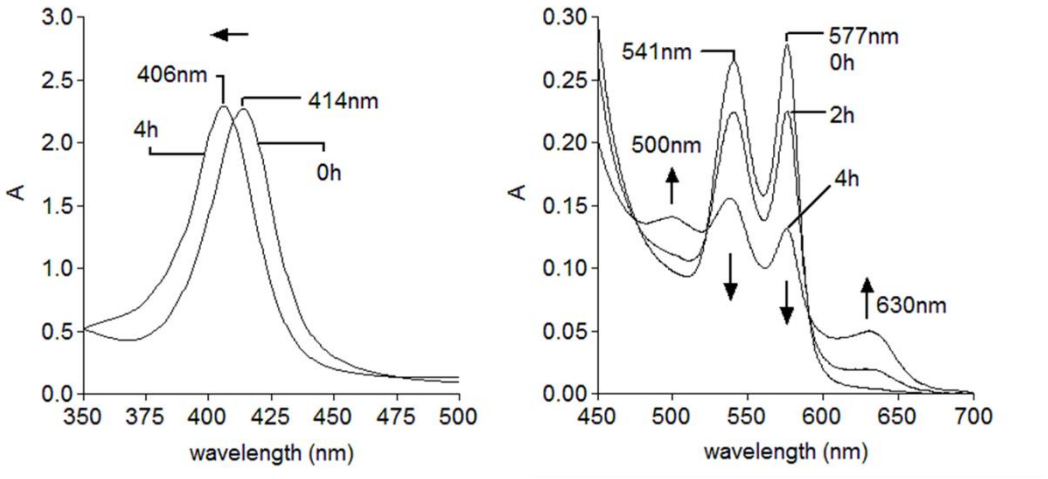

Figure 3.6 – MetHb formation by the cell-free spent growth medium of *S. gordonii*. 4µM oxyHb was incubated aerobically for 4 hours at 37°C with 1ml of cell-free growth medium from overnight culture of 1.00 OD_{600} *S. gordonii* cell suspensions.

Difference spectra were derived from the spectra shown in Figures 3.5 and 3.6, and from spectra of an oxyHb control by subtracting the initial time zero spectrum from those at each subsequent time point to reveal changes in the Soret band region (Figure 3.7). The summed integrated peak areas of 348-411nm and trough areas between 411-472nm were used as an indirect measure of the amount of metHb formed as previously described (Kelm et al., 1997; Zhang et al., 1996; Byrne et al., 2010).

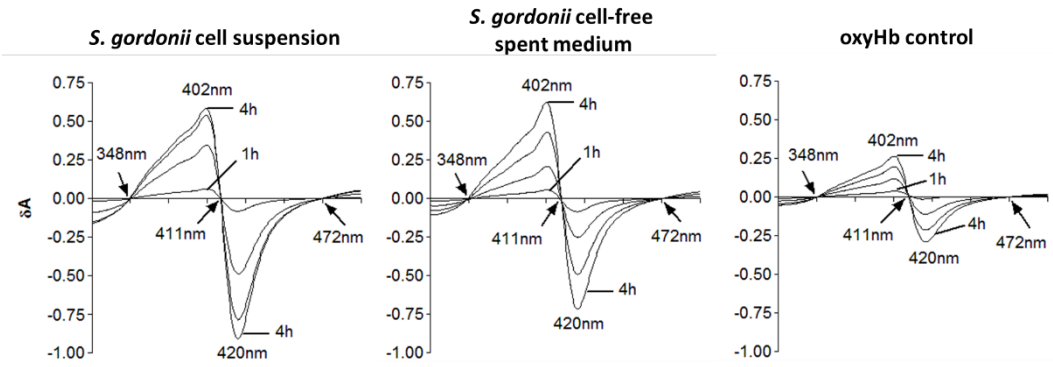

Figure 3.7 – The progressive changes in the absorbances of the Soret band region during incubation of oxyHb with *S. gordonii* cell cultures. 4µM oxyHb was incubated with *S. gordonii* cells (1.00 OD_{600}; left panel), *S. gordonii* cell-free growth

medium taken from overnight growth of *S. gordonii* or in BHI broth alone, for 4 hours at 37°C. The peak and trough areas were summed between 348-411nm, and 411-472nm, respectively (see Figure 3.8).

The summed integrated peak and trough areas of the overall absorbance changes in the Soret bands were plotted against time to give relative measures of metHb formation (Figure 3.8). These showed that both *S. gordonii* cell suspensions and *S. gordonii* cell-free growth medium increased metHb formation at rates greater than the oxyHb auto-oxidation control.

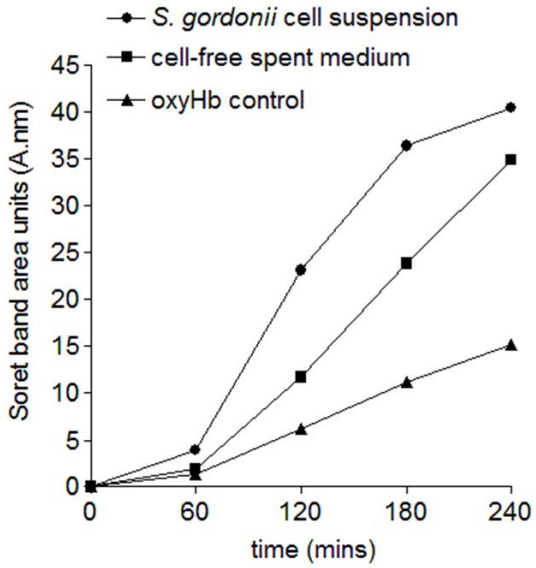

Figure 3.8 – MetHb formation mediated by *S. gordonii* cultures. The sum of the integrated area of the peaks and troughs (348-411nm and 411-472nm, respectively) derived from difference spectra presented in Figure 3.7 were used as an indirect measure of metHb formation.

3.3.5 Inhibition of metHb formation by *S. gordonii* by catalase

The observation that metHb formation was mediated by both the cell-free spent growth medium and cell suspensions of *S. gordonii* (1.00 OD_{600}) indicated that the compound responsible was released by the cells during growth. Barnard & Stinson (1996) identified H_2O_2 as the α-haemolytic agent of *S. gordonii*, and described, in part, the apparent generation of an oxidised Fe(II)Hb species by cell-free growth medium during incubation with whole erythrocytes. Therefore, based on these

observations, metHb formation by *S. gordonii* should be inhibited by catalase, since catalase decomposes H_2O_2 into H_2O and O_2.

To test this, *S. gordonii* cells were grown overnight on horse blood agar and sub-cultured into BHI broth for 24 hours, centrifuged (12,000 x g for 10 minutes at 5^oC) and washed in NaCl-Tris buffer, pH 7.5, then resuspended to 1.00 OD_{600} in BHI broth. 4μM oxyHb was incubated aerobically with two *S. gordonii* cell suspensions at 37^oC and following 2 hours of incubation, bovine catalase (to final concentration of 1μM) was added to one of the suspensions and to an oxyHb control minus bacterial inoculum (Figure 3.9). The decrease in peak intensity at A_{577nm} was then monitored as a measure of metHb formation as previously described (Smalley et al., 2007).

Catalase addition inhibited metHb formation mediated by *S. gordonii* cell suspensions, reducing the δA_{577nm} to a similar gradient observed in the oxyHb control. The relative % of metHb in each sample following a total of 6 hours of incubation were as follows; *S. gordonii* cell suspensions and oxyHb minus catalase contained 73% metHb, *S. gordonii* cell suspensions and oxyHb plus catalase consisted of 48% metHb, whilst the oxyHb control contained 23% metHb. This showed that H_2O_2 generated by *S. gordonii* was responsible for metHb formation and corroborated the observations of Barnard & Stinson (1996).

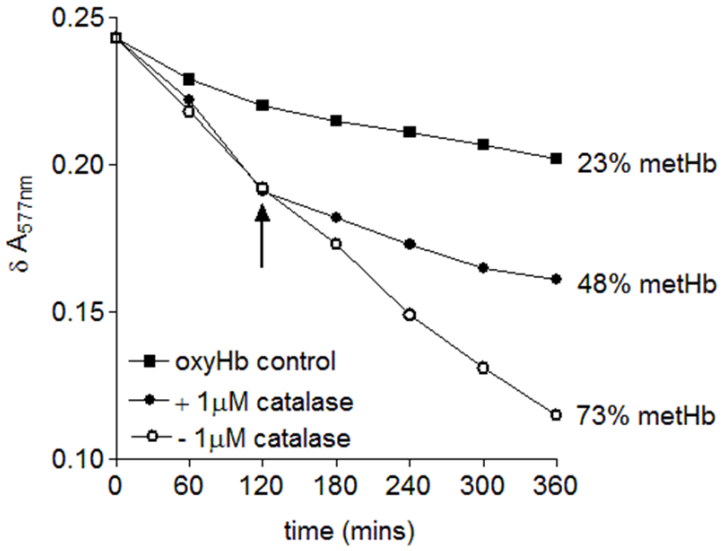

Figure 3.9 – Effects of bovine catalase on metHb production by *S. gordonii*. 4μM oxyHb was incubated with *S. gordonii* cell suspensions (1.00 OD_{600}) at 37°C in BHI broth and metHb formation was measured as a function of decrease in A_{577nm}. The arrow denotes time of addition of bovine catalase (1μM) to one *S. gordonii* cell suspension and the oxyHb control. The relative level of metHb in each sample following a 6-hour incubation is indicated.

3.3.6 Dose dependence between *S. gordonii*-generated H_2O_2 and metHb formation

S. gordonii mediated metHb formation accompanied with α-haemolysis when grown under aerobic, microaerobic and anaerobic conditions. However, *S. gordonii* growth on horse blood agar was visibly diminished under microaerobic and anaerobic conditions, as was both the extent of α-haemolysis surrounding colonies and metHb formation (see section 3.3.2). This is likely due to a reduced production of H_2O_2 by *S. gordonii* when grown under anaerobic conditions (Barnard & Stinson, 1999). Thus, to investigate whether metHb formation was dependent on the level of cellular H_2O_2 production, oxyHb was incubated for 4 hours with different densities of *S. gordonii* cells (0.33, 0.50 and 1.00 OD_{600}) grown as described above, and the change at A_{577nm} was monitored as a measure of metHb formation (Smalley et al., 2007). There was a decrease in peak intensity at A_{577nm} in all three cell densities, an effect that was greatest in the 1.00 OD_{600} cell suspension, and the

δA_{577nm} decreased proportionately in lower cell densities (Figure 3.10). The relative percentages of metHb formed were 87%, 66% and 50% for 1.00, 0.50 and 0.33 OD_{600}, respectively. The remaining Hb species in each sample was oxyHb, but including 4% haemichrome in the densest cell suspension. The control oxyHb in BHI broth minus bacterial inoculum contained 23% metHb. This indicated a correlation between cell density and metHb formation.

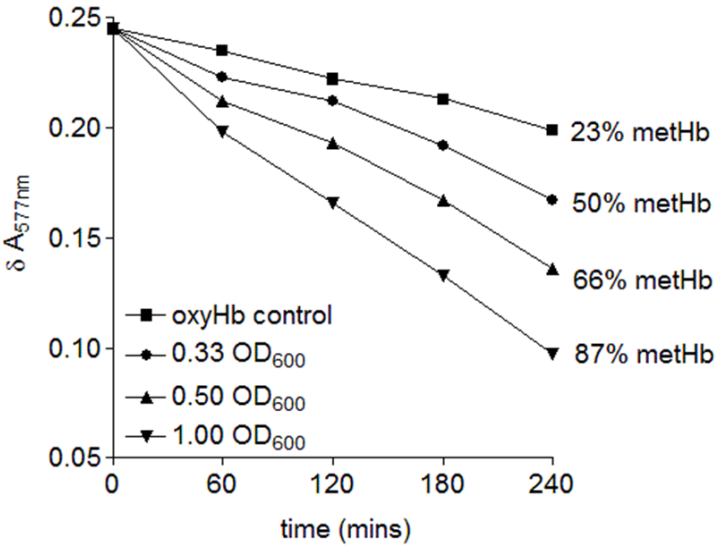

Figure 3.10 – MetHb formation by *S. gordonii* at different cell densities. OxyHb (4µM) was incubated with *S. gordonii* cell suspensions (0.33, 0.50, 1.00 OD_{600}) in BHI broth at 37°C. Control contained oxyHb in BHI broth minus bacterial inoculum. MetHb formation was expressed as a decrease in A_{577nm}. The relative level of metHb in each sample after 6-hour incubation is indicated.

The positive relationship between metHb production and *S. gordonii* cell density was further confirmed by measuring the total metHb relative to the maximal H_2O_2 concentration produced by the different *S. gordonii* cell suspensions. Cell suspensions of 1.00, 0.50 and 0.33 OD_{600} were prepared as above in BHI broth and after 4-hour incubation, cells were pelleted and 100µl of the cell-free supernatant mixed with 1ml of Fe(III)-xylenol orange working reagent and assayed for H_2O_2. This showed a positive linear relationship between *S. gordonii*-generated H_2O_2 and the level of metHb (Figure 3.11).

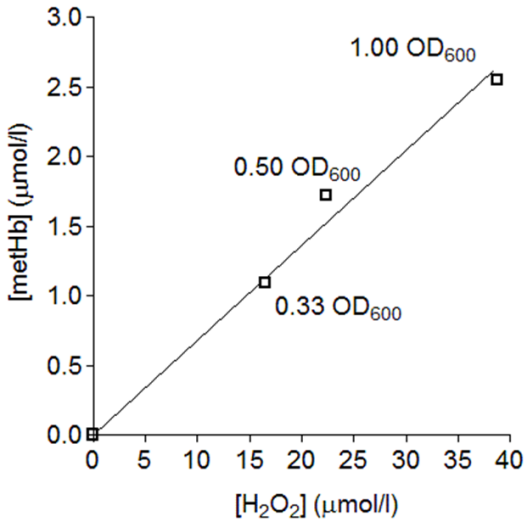

Figure 3.11 – Correlation between metHb formation and *S. gordonii* H_2O_2 production at different cell densities. 4µM oxyHb was incubated aerobically with *S. gordonii* cell suspensions in BHI broth for 4 hours at 37°C and [H_2O_2] and [metHb], the latter after correction for any metHb derived from oxyHb auto-oxidation.

3.3.7 Continuous rather than bolus addition of H_2O_2 is responsible for metHb formation by *S. gordonii* cells

The preceding sections in this chapter demonstrated that metHb was formed by incubating 4µM oxyHb with *S. gordonii* cell suspensions in which H_2O_2 was generated at concentrations of <50µmol/l. Interestingly, it has previously been shown that incubation of 5µmol/l oxyHb with 2.1µmol/l H_2O_2 failed to mediate the formation of metHb (Salehi et al., 2014). However, relative H_2O_2 and oxyHb concentrations as above but H_2O_2 generated as a continuous flux via the glucose and glucose oxidase (G/GOX) enzymatic reaction, did bring about oxidation of oxyHb to metHb (Giulivi & Davies, 1990). In the following sections, the effects of bolus addition versus a continuous flux of H_2O_2 upon α-haemolysis and oxyHb oxidation was compared. Firstly, bolus aliquots of H_2O_2 were added to 4µM oxyHb at concentrations produced maximally after 4 hours by 0.33, 0.50 and 1.00 OD_{600} *S. gordonii* cell suspensions (i.e., 16.6, 22.4 and 38.8µmol/l; see Figure 3.11); these being prepared from 30% w/w H_2O_2 in NaCl-Tris buffer, pH 7.5. However, there was no apparent increase in the rate of metHb formation compared to the oxyHb

control minus H_2O_2, even at the highest H_2O_2 concentration used (38.8µmol/l; data not shown), although metHb formation was observed at H_2O_2 concentrations above 100µmol/l. This observation was in line with the work of Salehi et al (2014) as discussed above, that bolus addition of H_2O_2 to oxyHb (at equimolar concentrations of both, respectively) did not mediate the formation of metHb.

H_2O_2 is generated by *S. gordonii* as a continuous flux during growth in a mono-species biofilm (Liu et al., 2011). Indeed, it was shown here that two cell densities of *S. gordonii* (1.00 and 0.25 OD_{600}) produced H_2O_2 in a continuous flux (Figure 3.12). H_2O_2 production by *S. gordonii* cells incubated aerobically in BHI broth was assayed using the Fe(III)-xylenol orange method at time-points during 4-hour incubations. At 20 minute intervals, 150µl of both suspensions were pelleted (12,000 x g for 10 minutes at 5^{o}C), before 100µl of the cell-free supernatants were assayed for H_2O_2 production. *S. gordonii* cells resuspended in NaCl-Tris buffer, pH 7.5, containing 100mM glucose and incubated aerobically for 4 hours did not produce a detectable level of H_2O_2 using the Fe(III)-xylenol orange method. This absence of H_2O_2 production may explain why *S. gordonii* cells in NaCl-Tris buffer, pH 7.5, containing 100mM glucose did not generate metHb when incubated with oxyHb (section 3.3.3). Taken together, these results suggest that metHb may be generated by *S. gordonii* cell suspensions in BHI broth via a continuous production of H_2O_2.

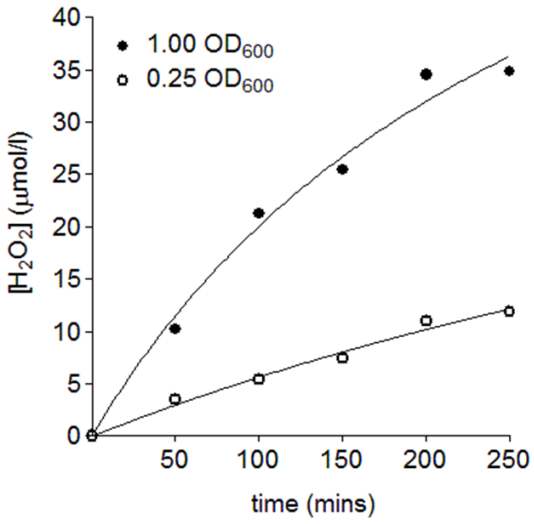

Figure 3.12 – Continuous H_2O_2 production by *S. gordonii* cell suspensions. *S. gordonii* cell densities (1.00 and 0.25 OD_{600}) were incubated in BHI broth at 37°C. H_2O_2 was detected using the Fe(III)-xylenol orange method.

3.3.8 α-haemolysis and accompanying metHb formation is mediated via a continuous flux of H_2O_2 produced by the glucose/GOX enzymatic reaction

A continuous flux of H_2O_2 production by *S. gordonii* cells is likely responsible for metHb formation (sections 3.3.6 and 3.3.7). Thus, this section investigated whether a continuous production of H_2O_2 generated via the G/GOX reaction would also mediate α-haemolysis and metHb formation. This was done by comparing the effects of both a bolus addition, and a continuous flux of H_2O_2 on horse blood agar. H_2O_2 concentrations equivalent to, and exceeding those maximally produced by *S. gordonii* cells (Figure 3.1; 5µmol/l-1mmol/l) were prepared in NaCl-Tris buffer, pH 7.5, and added to 0.5mm diameter wells made aseptically on horse blood agar plates (containing approximately 97% oxyHb) then incubated aerobically for 2 hours at 37°C. The bolus addition of H_2O_2 at all concentrations (5µmol/l-1mmol/l) failed to mediate α-haemolysis. However, 100µl of a mixture of 50mM glucose and 2µM GOX added to the blood agar and incubated for 2 hours at 37°C resulted in α-haemolytic zones surrounding the wells (Figure 3.13A), which was accompanied with the formation of metHb (97%; Figure 3.13B). In comparison, a control blood agar extract contained 93% oxyHb whilst a well containing 50mM glucose, 2µM GOX plus

4µM bovine catalase displayed a reduced zone of α-haemolysis (results not shown). Therefore, it can be concluded from these results that α-haemolysis was mediated by a continuous flux of H_2O_2 produced by the G/GOX enzymatic reaction and not by bolus addition of H_2O_2.

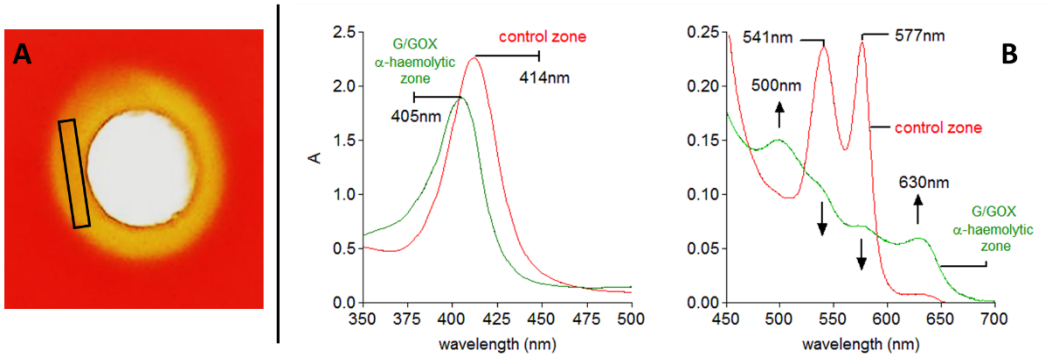

Figure 3.13 – The α-haemolytic effect of H_2O_2 generated via the G/GOX enzymatic reaction. The Hb species in the α-haemolytic zones surrounding wells containing glucose (50mM) and GOX (2µM; black rectangle, A) gave rise to a spectrum (B) indicative of metHb (97%). Horse blood agar plates were incubated aerobically at 37°C for 2 hours.

3.3.9 Reaction mechanism of metHb formation by *S. gordonii*

The reaction of H_2O_2 with oxyHb and metHb can result in the production of an intermediate known as ferrylhaemoglobin (ferrylHb) in which the haem iron is of a higher oxidation state i.e., Fe(IV) (Winterbourn, 1990). However, ferrylHb is indistinguishable spectroscopically from metHb formed during this process (Giuluvi & Davies, 1990), possibly due to the propensity of the unstable Fe(IV) centre to mediate oxidation of certain amino acid residues and in doing so returning to the Fe(III) state (e.g., metHb; Silva et al., 2009). FerrylHb can however be detected by the addition of sodium sulphide (Na_2S) which reacts with the ferryl intermediate resulting in the formation of sulphaemoglobin (sulpHb) where the sulphur atom will bind across a β-β double bond on one of the pyrrole rings in the haem structure (Pietri et al., 2011). To investigate whether ferrylHb was formed during the reaction between *S. gordonii* and oxyHb, *S. gordonii* cell suspensions (1.00 OD_{600}) were firstly incubated aerobically in BHI broth with oxyHb (4µM) for 4 hours at 37°C (resulting

in 75% metHb). Following centrifugation (12,000 x g for 10 minutes at 5°C), catalase (1µM, final concentration) was added to the metHb-containing supernatants to remove residual H_2O_2 and Na_2S (final concentration of 200µM) was added and the spectrum recorded immediately. This revealed a 618nm peak characteristic of sulpHb (Giulivi & Davies, 1994; Herold & Rehmann, 2003; Figure 3.14, left panel), and indicated that ferrylHb was produced during the reaction. The 618nm Q band was absent from a control oxyHb sample minus *S. gordonii* following addition of Na_2S (data not shown). A similar result was obtained when metHb (90%) was allowed to form via the G/GOX enzymatic reaction (50mM glucose and 0.01µM GOX) with 4µM oxyHb, in which a flux of H_2O_2 was generated at similar levels as that made by a 1.00 OD_{600} *S. gordonii* cell suspension (i.e., 5-50µmol/l) (Figure 3.14, right panel). Taken together, these results demonstrated that ferrylHb was formed as an intermediate during oxidation of oxyHb to metHb via H_2O_2 production by *S. gordonii* cell suspensions.

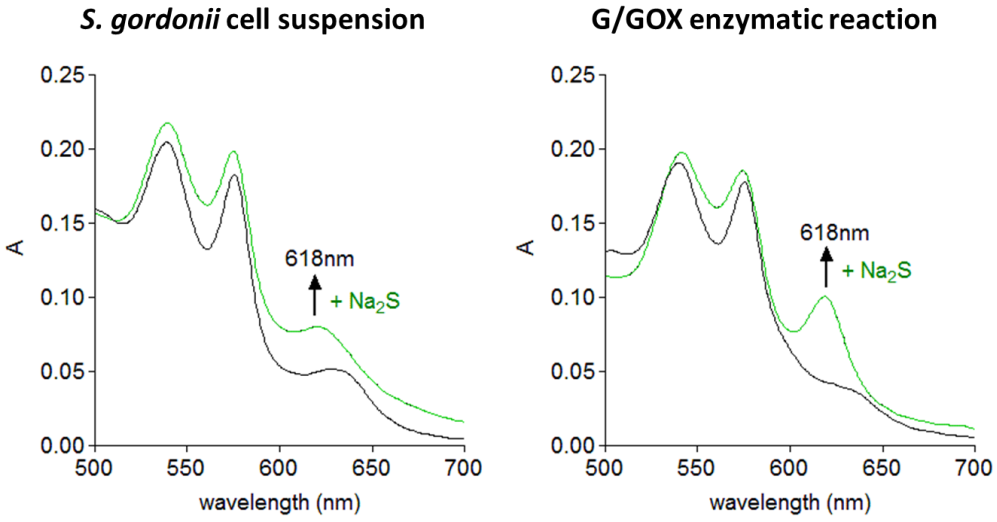

Figure 3.14 – Detection of sulphaemoglobin after addition of Na_2S to metHb formed by incubation of oxyHb with *S. gordonii* cells or glucose/GOX. MetHb was generated by incubation of oxyHb (4µM) with *S. gordonii* cell suspensions (1.00 OD_{600}) for 4 hours at 37°C, or with G/GOX (50mM glucose and 0.01µM GOX, respectively) for 2 hours at 20°C. 1µM catalase, and then 200µM Na_2S, were added to each metHb sample and spectra recorded immediately. The 618nm Q band is characteristic of sulpHb.

3.4 Discussion and conclusions

α-haemolysis on blood agar mediated by viridans streptococci is a phenomenon that was first described over a 100 years ago (Andrewes & Horder, 1906). However, there is little data on the characterisation of the Hb species present in the α-haemolytic zones. Thus, the primary aim of work described in this chapter was to identify the major Hb species mediated by *S. gordonii* during the α-haemolytic process. *In vivo*, microorganisms such as *S. gordonii* may encounter erythrocytes during periods of gingival and periodontal ligament bleeding which is clinically associated with PD (Loesche & Grossman, 2001). Hanioka et al (1989; 2005) showed that exudates from gingival tissue following bleeding contained Hb which was up to 80% O_2 saturated, and thus following bleeds it is likely that subgingival organisms may be exposed to Hb which is largely oxyHb. In all experiments here, the Hb used was minimally 97% oxyHb, and although incubation of control blood agar at 37^{o}C resulted in some auto-oxidation, metHb was the overwhelming component (>90%) in agar extracts from the α-haemolytic zones after aerobic growth of *S. gordonii*.

There was no evidence of haemichrome Hb in the agar extracts from the α-haemolytic zones after growth of *S. gordonii*. Haemichrome species are denatured Fe(III)Hb species in which the haem molecule becomes co-ordinated to an additional amino acid residue in the Hb chain, (Rachmilewitz et al., 1972). The altered molecular structures of haemichromes are likely the reason why they cannot be degraded by the *P. gingivalis* K-gingipain (Smalley et al., 2007; 2008). Therefore, the observation that metHb is formed by *S. gordonii* in zones of α-haemolysis may be of importance since metHb is the preferred Hb substrate from which *P. gingivalis* can extract haem.

The periodontal pocket exhibits a range of atmospheric O_2 conditions depending on pocket depth; deep pockets (7-10mm) clinically associated with PD display a lower pO_2 (11.6mmHg) than moderately deep sites (5-6mm; 15.0mmHg pO_2) (Mettraux et al., 1984), and this may influence the extent of metHb formation by *S. gordonii* since α-haemolysis is reduced during growth under anaerobic conditions (Barnard & Stinson, 1999; results in this study). To partly mimic such atmospheric conditions, α-

haemolysis mediated by *S. gordonii* was investigated under aerobic, microaerobic (candle jar) and anaerobic environments. α-haemolysis was observed under all above conditions, but was less extensive during microaerobic and anaerobic growth. This is likely as *S. gordonii* is a facultative anaerobe and although the organism will grow anaerobically, its growth yield under such conditions will be reduced and hence H_2O_2 production/α-haemolysis will be diminished. Nonetheless, the Hb in α-haemolytic zones formed during microaerobic and anaerobic growth was largely metHb (approx. 86% and 76%, respectively).

S. gordonii cell suspensions mediated metHb formation from isolated oxyHb. Barnard & Stinson (1996) found that α-haemolysis was mediated by H_2O_2 released by *S. gordonii* cells, and here it was shown that spent growth medium could oxidise oxyHb to metHb, indicating that direct cell contact with Hb is not necessary. Therefore, *S. gordonii* may facilitate metHb formation within dental plaque biofilms which are permeable to solutes (Stewart, 2003), with H_2O_2 diffusing through the extracellular plaque matrix. This may be of particular importance as previous work using scanning electron microscopic imaging of diseased periodontal pocket epithelium has shown that erythrocytes tend to associate with bacterial aggregates in dental plaque (Verderame et al., 1989). Interestingly, in this context, H_2O_2 at concentrations of 100-200µmol/l generated by *S. gordonii* (2-4 fold higher concentrations than those produced by the densest cell suspension of *S. gordonii* in this study) has been shown to diffuse up to 200 micrometres through a mono-culture biofilm of *S. gordonii* (Liu et al., 2011).

Catalase inhibited metHb formation by *S. gordonii* cell suspensions confirming that H_2O_2 was responsible for the oxidation effect. Furthermore, the *S. gordonii* cell density correlated with both H_2O_2 production and metHb formation. Although *S. gordonii* was capable of generating metHb, it is likely that other viridans streptococci (including *S. oralis*, *S. intermedius* and *S. sanguinis*) may also have the potential to mediate metHb formation through H_2O_2 production.

The oxidation of oxyHb to metHb by H_2O_2 is a complex biochemical process which involves entry of H_2O_2 into the haem pocket to facilitate oxidation of the Fe(II)haem in oxyHb to Fe(III)haem in metHb (Winterbourne et al., 1976; 1985). OxyHb may

also undergo spontaneous auto-oxidation as a result of the entry of a molecule of H_2O or OH^- into the haem pocket inducing the nucleophilic displacement of the superoxide ion (O_2^-; Shikama, 1990). O_2^- may continue to further oxidise Hb, or be converted into H_2O_2 (via the action of superoxide dismutase) and this can also mediate metHb formation (Winterbourne et al., 1976). However, this process is slow due to the stable nature of the Fe(II)O_2 bond in oxyHb (Shikama, 1985). As the auto-oxidation of oxyHb is slow, *P. gingivalis* may normally encounter only low concentrations of auto-oxidised metHb. Enhanced generation of metHb by *S. gordonii* may therefore have important implications for haem acquisition by *P. gingivalis*.

Importantly in the context of the plaque ecology, auto-oxidation of oxyHb is also dependent on the pH of the immediate environment. The rates of oxidation of both α- and β- chains is lowest between pH 7.5-9 (Tsuruga et al, 1998). As the inflamed gingival crevice and diseased periodontal pocket are slightly alkaline (reported to be approximately pH 7.5-8; Bickel & Cimasoni, 1985b), the concentrations of metHb formed via normal auto-oxidation would be relatively low. The observation that *S. gordonii* can mediate metHb formation rapidly at pH 7.5 strengthens the potential role the organism may play in aiding haem acquisition by *P. gingivalis in vivo* in a pocket or sulcus environment.

Interestingly, whilst *S. gordonii* cells mediated metHb formation in BHI broth, metHb formation and H_2O_2 production was not observed when cells were resuspended in NaCl-Tris buffer, pH 7.5, containing 100mM glucose. H_2O_2 production by *S. gordonii* is mediated largely via pyruvate oxidase (encoded by the *SpxB* gene), which is part of the glycolytic pathway. Pyruvate oxidase converts pyruvate into acetyl phosphate which results in the release of H_2O_2 and CO_2 (Lunt & Vander Heiden, 2011). Therefore, although glucose was provided as a substrate in the buffer, it may be that *S. gordonii* requires other constituents of BHI broth to grow and generate H_2O_2 to mediate metHb formation. Conversely, it could be that the concentrations of H_2O_2 generated by *S. gordonii* cells in buffer containing 100mM glucose were too small to be detected via the Fe(III)-xylenol orange assay (the working range of the assay was 1µM-1mM). Indeed, other work has shown that

S. gordonii cells suspended in phosphate buffer, pH 7.0, containing between 10µM-1000mM glucose, produced H_2O_2 only at nanomolar concentrations (Barnard & Stinson, 1999). However, these H_2O_2 concentrations were detected using a more sensitive assay employing 2,2'-azino-bis(3-ethylbenzothiazoline-6-sulphonic acid) and horseradish peroxidase.

The generation of metHb from oxyHb by *S. gordonii* cell suspensions in BHI broth appeared to be dependent on a continuous flux of H_2O_2 production and that addition of bolus concentrations of H_2O_2 equivalent to those produced maximally after 4 hours by *S. gordonii* cell suspensions did not produce the same effect. Previous work has shown that bolus addition of micromolar concentrations of H_2O_2 to oxyHb (0.2-2.1µM of H_2O_2 and 5.0µM Hb; Salehi et al., 2014) did not result in metHb formation. This could explain why only a higher molar ratio of bolus H_2O_2 to Hb (e.g., >100µM of H_2O_2 to 4µM oxyHb, respectively) facilitated metHb formation upon incubation with oxyHb, and that metHb formation was not observed upon bolus addition of lower concentrations of H_2O_2.

The enzymatic reaction between glucose and GOX generates H_2O_2 in a continuous flux similar to *S. gordonii* cell suspensions in BHI broth. This enzyme reaction was useful in demonstrating that α-haemolysis and metHb formation is mediated via exposure to a continuous production of H_2O_2. Although H_2O_2 is released by *S. gordonii* in a continuous flux during biofilm growth (Liu et al., 2011), this work is the first to show that α-haemolysis was mediated by a flux of H_2O_2. Importantly it has been shown by Smalley et al (2000) that *P. gingivalis* can survive during exposure to H_2O_2 when cultured with µ-oxo bishaem (the dimeric form of Fe(III)haem present in the black pigment). *P. gingivalis* also remains viable during exposure to 1mM H_2O_2 (Smalley et al., 2000), which is 20-fold higher than those produced here by *S. gordonii* cell suspensions (<50µmol/l). This protection against H_2O_2 is likely due to the "catalase" activity of ferrihaem species (Jones et al., 1973). The continuous release of H_2O_2 by *S. gordonii* may therefore provide *P. gingivalis* with a vital source of Fe(III)haem (via metHb generation) for pigmentation, but at a concentration which is endured by *P. gingivalis*.

The final section of this chapter served to identify a possible reaction mechanism by which *S. gordonii* mediated α-haemolysis and metHb formation. As H_2O_2 is capable of diffusing across mammalian cell membranes via aquaporin channels (Bienert et al., 2006), it is likely that the compound enters the erythrocyte via this route. Work on the effects of hydroperoxides on erythrocyte stability suggested that H_2O_2 may damage membrane elasticity and protein skeleton functionality (Snyder et al., 1985; Hale et al., 2011). Furthermore, it is proposed that erythrocyte haemolysis is facilitated by the formation of irreversible haemichromes (Fe(III)Hb species unable to be converted to Fe(II)Hb by reducing agents). Such haemichromes may weaken the membrane skeleton leading to cell destruction (Jarolim et al., 1990). However, spectroscopic analysis of *S. gordonii* α-haemolytic agar extracts indicated that the prominent Hb species present was metHb with no evidence for the presence of haemichromes.

The detection of ferrylHb produced as an intermediate during the conversion of oxyHb to metHb could offer an alternative explanation for the reaction mechanism of α-haemolysis. FerrylHb arises via a comproportionation reaction which involves oxyHb first being converted into the Fe(IV)Hb intermediate during exposure to H_2O_2 (reaction 6), and then ferrylHb reacts with either oxyHb or H_2O_2 to form metHb (reactions 7 and 8; Giulivi & Davies, 1990);

$$HbFe(II)O_2 \text{ (oxyHb)} + H_2O_2 + H^+ \rightarrow HbFe(IV)\text{-}OH \text{ (ferrylHb)} + H_2O_2 + O_2 \quad (6)$$

$$Hb(IV)\text{-}OH \text{ (ferrylHb)} + H_2O_2 + H^+ \rightarrow HbFe(III) \text{ (metHb)} + H_2O + OH_2^{\bullet} \quad (7)$$

$$HbFe(IV)\text{-}OH \text{ (ferrylHb)} + HbFe(II)O_2 \text{ (oxyHb)} \rightarrow 2HbFe(III) \text{ (metHb)} + O_2 \quad (8)$$

It is proposed by Giuluvi & Davies (1990) that reactions (6) and (7) will occur when oxyHb is exposed to continuous flux of H_2O_2, while reactions (6) and (8) are likely in the presence of a high concentration of oxyHb (Giuluvi & Davies., 1990). Reactions (7) and (8) both lead to the formation of metHb. The exact physiological effect of ferrylHb when generated within the erythrocyte is unknown, although Sztiller et al (2006) have shown that the ferrylHb binds to erythrocyte membranes, with a two-fold greater avidity than metHb, and mediates small changes to membrane structure. Therefore, haemolysis may be mediated by the accumulation of these

ferrylHb species in the erythrocyte membrane, resulting in the loss of structural integrity and eventual degradation of the erythrocyte and release of Hb.

To conclude, results from this chapter indicated that *S. gordonii* mediated the formation of metHb via H_2O_2 production under aerobic, microaerobic and anaerobic conditions. This is the first study to provide conclusive spectroscopic evidence that metHb is present in zones of α-haemolysis mediated by *S. gordonii* on horse blood agar. α-haemolysis on blood agar and metHb formation by *S. gordonii* cell suspensions arose through a continuous production of H_2O_2 by the organism. Interestingly, in the context of this study, metHb is the preferred substrate for haem acquisition by *P. gingivalis* and circumvents the refractory nature of oxyHb (in which the haem is in the Fe(II) state) to *P. gingivalis* proteases (Smalley et al., 2002; 2004; 2008). The following chapter investigates the ability of the *P. gingivalis* HmuY haemophore to acquire Fe(III)haem from metHb generated by *S. gordonii*.

Chapter 4 HmuY-Fe(III)haem complex formation from methaemoglobin generated by *Streptococcus gordonii*

4.1 Introduction

Haem is a vital co-factor for growth and virulence of *P. gingivalis* (Marsh et al., 1994; Smalley & Olczak, 2015). However, as *P. gingivalis* lacks the full repertoire of genes involved in *de novo* biosynthesis of haem porphyrin (Roper et al., 2000, Nelson et al., 2003), it must first scavenge haem from the surrounding environment. This is achieved via a combination of haem-binding proteins, proteases (gingipains) and haemophores. HmuY, the most extensively studied haemophore of *P. gingivalis*, will bind haem and deliver it to the cell surface before uptake via the lipoprotein receptor, HmuR (Olczak et al., 2005). HmuY is capable of binding free Fe(III)haem, as well as extracting it from host haemoproteins, including Hb, albumin and haemopexin (Smalley et al., 2011; Smalley & Olczak, 2015). The novel Hb haem acquisition mechanism described for *P. gingivalis* firstly involves oxidation of oxyHb by RgpA to metHb, followed by haem extraction via the actions of Kgp and/or the HmuY haemophore (Smalley et al., 2002, 2004, 2007, 2008, 2011; Wojtowicz et al., 2009). The HmuY haemophore is the first to be discovered to work in tandem with proteases involved in mediating metHb formation, and subsequent haem release (Smalley et al., 2011).

There is recent evidence to suggest *P. gingivalis* may utilise the biochemical activities of neighbouring species to facilitate metHb formation. *P. intermedia*, a co-aggregating species with *P. gingivalis* in dental plaque (Kamaguch et al., 2001), produces a cysteine protease called interpain A (InpA) which acts in a similar way to the R-gingipain of *P. gingivalis*, in mediating oxyHb oxidation (Byrne et al., 2010), and as a result facilitates extraction of Fe(III)haem by HmuY from metHb (Byrne et al., 2013). *P. aeruginosa*, a co-coloniser of the cystic fibrotic (CF) lung with *P. gingivalis* and other oral anaerobes (Rogers et al., 2004; Tunney et al., 2008; Caldas et al., 2015), produces pyocyanin, a blue phenazine redox compound that is involved in virulence properties such as inhibiting the beating of cilia and destroying alveolar airspaces in the CF lung (Wilson et al., 1987; Caldwell et al., 2009). Recently, pyocyanin has been shown by Smalley and colleagues to mediate metHb formation from oxyHb. This enhanced total Fe(III)haem availability to the cell and

for pick up by HmuY resulting in virulence upregulation of *P. gingivalis* by increased protease activity (Benedyk et al., 2015).

In line with the above synergistic paradigm between *P. gingivalis* and neighbouring species, this chapter will primarily investigate whether Fe(III)haem can be extracted by HmuY from metHb which has been generated by *S. gordonii*, either extracted from α-haemolytic zones from blood agar or during exposure of oxyHb to bacterial cell suspensions. In addition, a comparison will be made of the rates of Fe(III)haem acquisition by HmuY from auto-oxidised metHb vs. that generated by *S. gordonii* cell suspensions or by exposure to H_2O_2 produced by the G/GOX enzymatic reaction. Finally, near- and far-UV circular dichroism (CD) analysis will be used to compare the protein structures of metHb generated by auto-oxidation or via the influence of H_2O_2.

4.2 Material and methods

4.2.1 MetHb preparations

MetHb was prepared by incubation of 4μM oxyHb (tetramer) with *S. gordonii* cell suspensions (1.00 OD_{600}) in BHI broth at 37^{o}C for 4-6 hours. Cells were removed by centrifugation (12,000 x g for 10 minutes), and Hb-containing supernatants filter sterilised through 0.2μm membranes. MetHb generated by H_2O_2 in the absence of *S. gordonii* cells was prepared by incubating 4μM oxyHb with 50mM glucose and 0.01μM GOX in NaCl-Tris buffer, pH 7.5, for 4 hours at 37^{o}C. Auto-oxidised metHb samples were produced by incubating 4μM oxyHb for 72 hours at 37^{o}C in the above buffer or BHI broth. For comparative purposes, all Hb samples contained approximately 90% metHb before use for incubations with HmuY.

4.2.2 UV-visible spectroscopic detection of HmuY-Fe(III)haem complex formation from incubations of Fe(III)haem or metHb with HmuY

Stock samples of HmuY (1054μM) were diluted to 64μM in NaCl-Tris buffer, pH 7.5. Equimolar concentrations of HmuY and Fe(III)haem or metHb (i.e., 16μM with respect to Hb subunit) were incubated together at 20^{o}C for 2-6 hours. Spectra were recorded, and difference spectra were produced for each sample by subtracting the

time zero spectrum from spectra at each subsequent time point. Where applicable, the integrated area increases of the 525nm and 560nm Q bands (between x-axis intercepts at approximately 510nm and 590nm) were plotted against time and used as a comparison for the rate of HmuY-Fe(III)haem complex formation. All spectra were corrected for any spectral changes occurring in each control metHb sample during incubation.

4.2.3 Triton-X100-methanol assay for detection of free Fe(III)haem in the filtrate of metHb generated by *S. gordonii* cells

MetHb samples produced by *S. gordonii* cell suspensions as above were filtered through 30kDa cut-off membranes by centrifugation (12,000 x g, for 30 minutes at 5^{o}C). 1 volume of Hb-free filtrate was added to 10 volumes of Triton-X100 (2.5% v/v in methanol; Pandey et al., 1999) to test for any free Fe(III)haem.

4.2.4 Determination of the stability of the HmuY-Fe(III)haem complex in the presence of H_2O_2

A stock solution of the HmuY-Fe(III)haem complex (16µM) was produced by incubating equimolar concentrations of HmuY with Fe(III)haem for 1 hour at 20^{o}C. A range of H_2O_2 concentrations (5, 10, 25 and 50 µmol/l, respectively) were prepared from H_2O_2 (30% w/w) in NaCl-Tris buffer, pH 7.5, and standardised by reference to the extinction coefficient (ε) of 43.6 M^{-1} cm^{-1} at 240nm (Beers & Sizer, 1952). The HmuY-Fe(III)haem complex was incubated with each H_2O_2 concentration for 2 hours at 37^{o}C, and the decrease in the Soret band λ_{max} (A_{411nm}) was used as an indication of complex dissociation (Byrne et al., 2013).

4.2.5 Circular dichroism analysis of metHb generated by exposure to H_2O_2 produced via the glucose/GOX enzymatic reaction

MetHb was prepared by incubation of 4µM oxyHb with G/GOX or by auto-oxidation (section 4.2.1), and dialysed against 0.1M NaH_2PO_4/Na_2HPO_4 buffer, pH 7.4 for 2 hours to remove chloride ions and Tris molecules that may interfere with absorbance readings during the CD analysis (Kelly et al., 2005). MetHb samples

were analysed in the far-UV (180-260nm) and near-UV (260nm-320nm) regions. All spectra were produced using 1cm path length quartz cells at 20°C at metHb concentrations of 0.5µM and 5µM (tetramer basis), for far- and near- UV analysis, respectively. Samples were scanned 25 times and spectra corrected against a NaH_2PO_4/Na_2HPO_4 buffer control.

4.3 Results

4.3.1 HmuY-Fe(III)haem complex formation

The reaction of equimolar concentrations of HmuY and Fe(III)haem results in the formation of a bis-histidine HmuY-Fe(III)haem complex, which possesses a unique UV-spectrum (Olczak et al., 2008; Smalley et al., 2011). Here, this was achieved by incubation of HmuY and Fe(III)haem (16µM) at 20°C, yielding a stable spectrum with a Soret λ_{max} at 411nm, and Q bands at 525nm and 560nm after 2 hours (Figure 4.1).

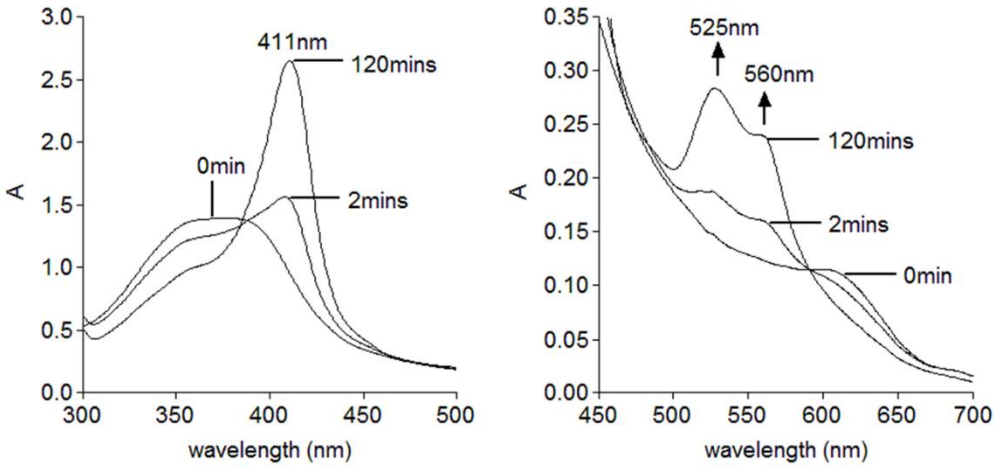

Figure 4.1 – UV spectrum showing formation of HmuY-Fe(III)haem complex from Fe(III)haem. An equimolar concentration of Fe(III)haem and HmuY (16µM) were incubated together for 120 minutes at 20°C. The resulting HmuY-Fe(III)haem complex possesses unique spectroscopic characteristics at 411nm, 525nm and 560nm. t0 represents the spectrum of free Fe(III)haem prior to HmuY addition.

4.3.2 HmuY-Fe(III)haem complex formation from metHb extracted from α-haemolytic zones mediated by *S. gordonii* cells on horse blood agar

MetHb was the major Hb species in zones of α-haemolysis mediated by *S. gordonii* (section 3.3.1). As metHb is the preferred form of Hb for haem pick up by the HmuY haemophore, (Smalley et al., 2011) this section investigates whether the metHb species formed during α-haemolysis could be utilised for Fe(III)haem extraction by HmuY. It was essential to do this as there is evidence to suggest that exposure of oxyHb to H_2O_2 can result in both protein and haem degradation (Nagababu & Rifkind, 2000). If this occurred during α-haemolysis as a consequence of H_2O_2 production, then this might compromise haem extraction from the protein and/or subsequent haem extraction and binding by the haemophore. For this, the Hb was extracted from zones of α-haemolysis mediated by *S. gordonii* by the freeze-thawing method described in section 3.2.1. This extract contained approximately 92% metHb, with the remainder in the oxyHb form. The Hb species was incubated with equimolar concentrations of HmuY (16μM with respect to Hb subunit) for 4 hours at 20^{o}C. Difference spectra were then produced (Figure 4.2) which gave rise to a trough at 390nm and a peak at 421nm as a result of the red shift in the Soret band λ_{max} from 405nm in metHb to 411nm associated with the HmuY-Fe(III)haem complex (Smalley et al., 2011). The troughs formed at 500nm and 630nm were indicative of the loss of metHb from the sample.

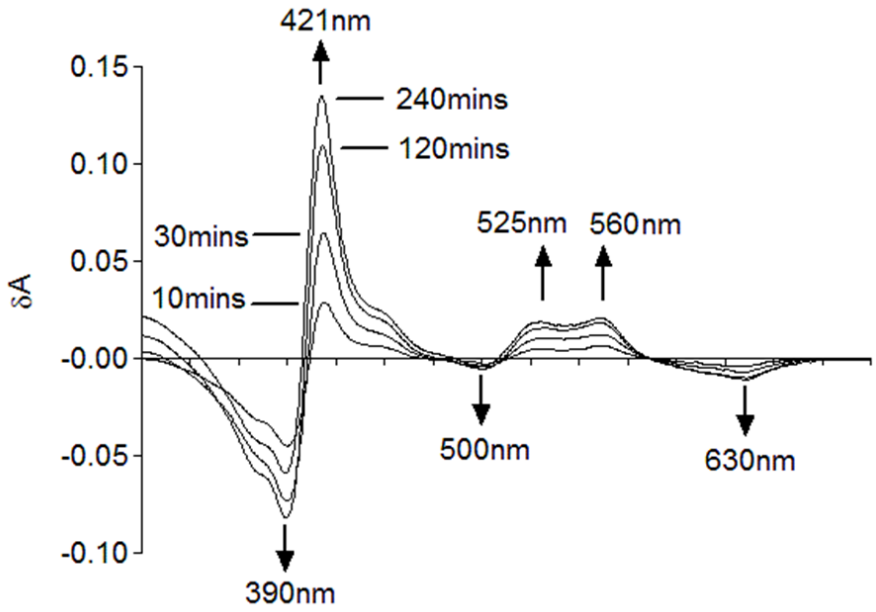

Figure 4.2 – Difference spectra showing changes in absorbance of Soret and Q band regions during formation of the HmuY-Fe(III)haem complex from metHb extracted from blood agar in α-haemolytic zones produced by *S. gordonii*. Hb (16µM with respect to subunit, containing 92% metHb) was extracted from α-haemolytic zones mediated by *S. gordonii* cells grown aerobically at 37°C for 16 hours, then incubated with 16µM HmuY for 4 hours at 20°C.

4.3.3 HmuY-Fe(III)haem complex formation from metHb generated by *S. gordonii* cell suspensions during incubation with oxyHb

The following section investigated whether haem could be picked up easily by HmuY from metHb formed by *S. gordonii* cell suspensions. OxyHb (4µM) was incubated with a 1.00 OD_{600} *S. gordonii* cell suspension in BHI broth for 6 hours at 37°C, after which the *S. gordonii* cells were pelleted by centrifugation (12,000 x g for 10 minutes) and the Hb-containing supernatant (90% metHb, 5% oxyHb and 5% haemichrome, respectively) was incubated with HmuY (16µM) for 4 hours at 20°C. Difference spectra produced as above gave rise to the characteristic peaks at 421nm, 525nm and 560nm indicative of HmuY-Fe(III)haem complex formation (Figure 4.3).

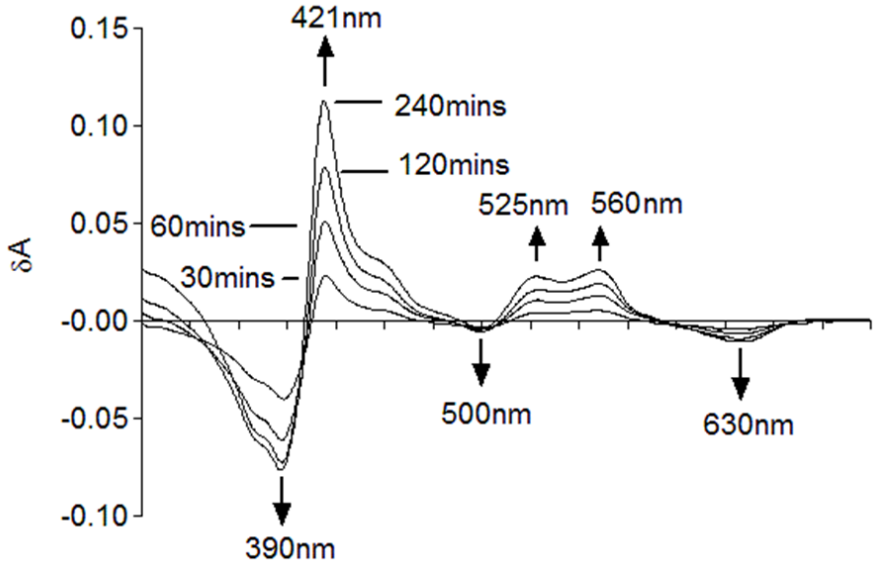

Figure 4.3 – Difference spectra showing the HmuY-Fe(III)haem complex formation from metHb generated during incubation of oxyHb with *S. gordonii* cell suspensions. Hb (containing 90% metHb) generated after a 6-hour incubation of oxyHb with a 1.00 OD_{600} suspension of *S. gordonii* cells was mixed with an equivalent concentration of HmuY and incubated for 4 hours at 20°C.

4.3.4 Rates of HmuY-Fe(III)haem complex formation from metHb formed by *S. gordonii* cell suspensions vs. that from auto-oxidation

The oxidation of oxyHb or oxymyoglobin to its met-forms via H_2O_2 exposure may result in oxidative events occurring at tyrosine residues in the protein chains, some of which have been identified in the haem pocket (Svistunenko et al., 2002). As an alteration to the structure of the haem pocket could theoretically weaken the haem-globin linkage in the protein (Hargrove et al., 1996), this could enhance haem capture by HmuY. Thus, to investigate whether haem could be acquired more readily by HmuY from metHb generated by exposure to H_2O_2, the relative rates of Fe(III)haem pick up by HmuY from metHb formed by *S. gordonii* cell suspensions and auto-oxidised metHb were determined. This was done by calculating the integrated peak areas of the 525nm and 560nm bands of the HmuY-Fe(III)haem complex of three independent experiments, after incubation of HmuY with Hb as above for 4 hours at 20°C, and plotting these against time. The Hb species formed by *S. gordonii* cells contained 92% metHb (plus 4% oxyHb and 4% haemichrome,

respectively) whilst the auto-oxidised Hb sample, prepared in BHI broth, was metHb 95%, and 5% oxyHb. Using GraphPad Prism, a one-phase exponential association curve as described by Gao et al (2010) for the *P. gingivalis* HusA haemophore haem binding was fitted to the data to assess the rate of HmuY-Fe(III)haem complex formation (Figure 4.4). This showed that the HmuY-Fe(III)haem complex formed at a faster rate from metHb formed as a result of *S. gordonii*-mediated oxidation than from auto-oxidised metHb (32.6 ± 1.1 x 10^{-3} s^{-1} compared to 18.5 ± 0.8 x 10^{-3} s^{-1}).

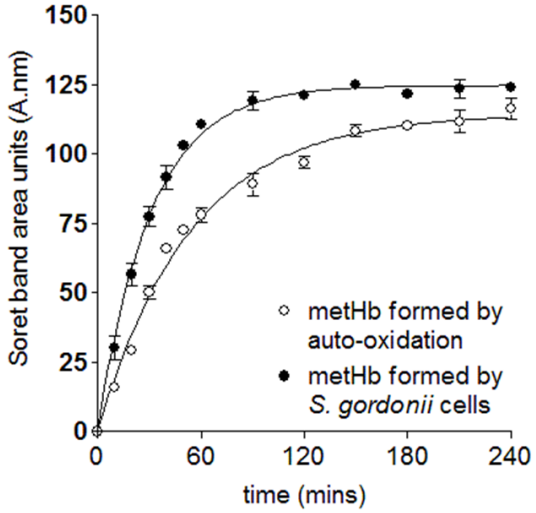

Figure 4.4 – Time course of HmuY-Fe(III)haem complex formation for metHb formed by *S. gordonii* cells compared with that from auto-oxidation. Equimolar concentrations of HmuY were incubated with metHb generated by *S. gordonii* cell suspensions (1.00 OD_{600}) for 6 hours, or by auto-oxidation in BHI broth for 72 hours at 37°C. Error bars denote standard error of readings from three separate experiments.

Nagababu & Rifkind (2000) showed that exposure of oxyHb to H_2O_2 can result in the degradation of the protein, and the subsequent release of haem. Therefore, it was determined if the increased rate of Fe(III)haem pickup by HmuY from metHb mediated by *S. gordonii* cells was not as a result of any free Fe(III)haem in solution originating from any degraded Hb following exposure to H_2O_2. The metHb generated by *S. gordonii* cell suspensions was ultra-filtered through 30kDa membranes, and the Hb-free filtrate was analysed for the possible presence of free Fe(III)haem using the Triton-X100-methanol assay (Pandey et al., 1999) which would

indicate that haem had been released during exposure of the oxyHb to H_2O_2. To do this, 1 volume of Hb-free filtrate was added to 10 volumes of Triton-X100 (2.5% v/v in methanol); free Fe(III)haem in the filtrate would complex with the Triton-X100 in solution, giving rise to a green compound that could be analysed spectroscopically (Pandey et al., 1999). However, no free Fe(III)haem was found in the filtrate indicating that the increased rate of haem pick up by HmuY from metHb generated by *S. gordonii* cells was not due to H_2O_2-mediated haem loss.

4.3.5 HmuY-Fe(III)haem complex formation from metHb mediated by H_2O_2 via the glucose/GOX enzymatic reaction

It was tentatively proposed in the above section, that oxidative events in the Hb haem pocket arising from exposure to H_2O_2 mediated by *S. gordonii* (which could theoretically weaken the haem-globin linkage; Hargrove et al., 1996), may be a means which enables HmuY to pick up Fe(III)haem from metHb at a greater rate than from auto-oxidised metHb (section 4.3.4). If this effect was indeed mediated by H_2O_2, then a similar rate of HmuY-Fe(III)haem complex formation compared to *S. gordonii*-mediated metHb should be observed using metHb generated via H_2O_2 produced by the G/GOX system. To do this, 4µM oxyHb was incubated with 50mM glucose and 0.01µM GOX in NaCl-Tris buffer, pH 7.5, for 4 hours at 20^oC. These concentrations of glucose and GOX generated a flux of H_2O_2 at similar levels to those produced by a 1.00 OD_{600} *S. gordonii* cell suspension (i.e., 5-50µmol/l). The resulting oxidised Hb samples which contained 95% metHb and 5% oxyHb, respectively, were filtered on 30kDa centrifugation devices (12,000 x g at 20^oC for 10 minutes) then dialysed against dH_2O for two hours at 5^oC to remove glucose, GOX and residual H_2O_2. An auto-oxidised control, produced in NaCl-Tris buffer, pH 7.5, containing the same relative concentration of metHb as above was employed as a comparison. Upon addition of an equimolar concentration of HmuY to both metHb samples (16µM with respect to Hb subunit), there was evidence of an increased rate of HmuY-Fe(III)haem complex formation from metHb generated via G/GOX, compared to auto-oxidised metHb (Figure 4.5). The relative haem binding constant by HmuY from metHb generated via G/GOX was 11.3 ± 0.6 x 10^{-3} s^{-1}

compared to 5.0 ± 0.5 x 10^{-3} s^{-1} for auto-oxidised metHb. Moreover, the increased rate of HmuY-Fe(III)haem complex formation was not considered to be a consequence of haem lost from the Hb following exposure to H_2O_2, since no free haem was detected in the filtrates of metHb formed by H_2O_2 generated via the G/GOX reaction. Taken together, this and the results from the preceding section indicated that Fe(III)haem was more readily extracted by HmuY from metHb generated by exposure to a continuous flux of H_2O_2, either via *S. gordonii* cells or the G/GOX enzymatic system.

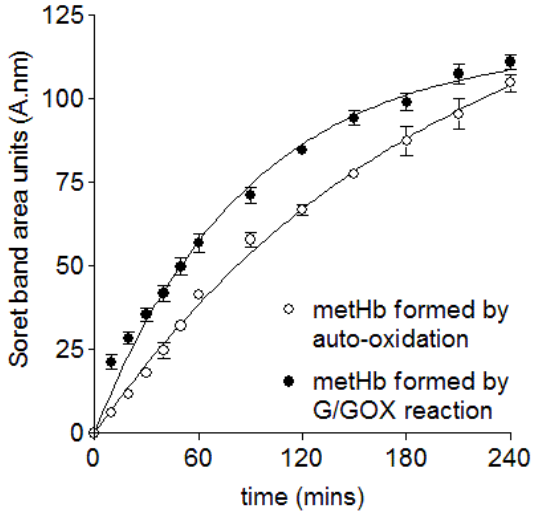

Figure 4.5 – Comparison of rates of HmuY-Fe(III)haem complex formation from auto-oxidised metHb and metHb generated via the glucose/GOX reaction. HmuY was mixed with metHb formed by incubation of 4µM oxyHb with 50mM glucose and 0.01µM GOX in NaCl-Tris buffer, pH 7.5, for 4 hours at 20°C, or via auto-oxidation for 72 hours at 37°C. Error bars denote standard error of triplicate readings.

4.3.6 Circular dichroism analysis of metHb mediated by exposure to H_2O_2 produced via glucose/GOX reaction

Fe(III)haem was acquired more readily by HmuY from metHb generated via exposure to H_2O_2 (either via *S. gordonii* cells or by the G/GOX enzymatic reaction) compared to auto-oxidised metHb. Since H_2O_2 may oxidise amino acid residues in the Hb-chains (Svistunenko et al., 2002), it is possible that the observation of

increased haem pickup by HmuY from H_2O_2-mediated metHb relate to an alteration to the structure of Hb as a consequence of exposure of the protein to H_2O_2. Therefore, near- and far-UV circular dichroism analysis was used to compare the protein structures of metHb produced by H_2O_2 generated via the G/GOX enzymatic reaction or by auto-oxidation. MetHb samples were prepared as above (section 4.3.5) in NaCl-Tris buffer, pH 7.5, but which were dialysed against 500ml dH_2O for 1 hour, then against 500ml NaH_2PO_4/Na_2HPO_4 buffer, pH 7.4, for 2 hours, to remove the chloride ions and Tris since these absorb light strongly below 200nm (Kelly et al., 2005). Next, the Hb samples were filtered through 30-kDa cut-off membranes, and diluted in NaH_2PO_4/Na_2HPO_4 buffer, pH 7.4, to give 0.5µM and 5µM, respectively, for analysis in far- (180-260nm) and near-UV regions (260-320nm). 25 repeat scans were completed for each sample and corrected by subtraction of control buffer spectra.

The far- UV region depicts the changes occurring in the peptide bonds of the Hb molecule, which give rise to the secondary structure of the protein i.e., α-helix and β-sheets. Figure 4.6 (left panel) shows the far-UV region of the Hb samples, with the peak between 180-200nm, and the trough at approximately 220nm, characteristic of the α-helical nature of Hb. The high similarity between the two spectra indicates that metHb formed during exposure to H_2O_2 generated via the G/GOX reaction possesses an almost identical secondary structure to that of auto-oxidised metHb. Meaningful CD spectral data could not be obtained for metHb generated via *S. gordonii* cell suspensions since these samples were prepared through incubating oxyHb with cell suspensions in BHI broth and as a consequence contained peptides from the growth which interfered with the spectra in the far-UV region (results not shown).

The near- UV region is important in determining the presence of aromatic amino acid side chains such as tryptophan (Trp), phenylalanine (Phe) and tyrosine (Tyr), as well as the spatial disposition of neighbouring amino acid chains (Kelly et al., 2005). Each aromatic side chain possesses a characteristic wavelength profile, with the peak between 260-270nm representing the Phe residues present in the Hb protein, while the Trp and Tyr residues are distinguishable by absorbance between 275-

285nm and 285-305nm, respectively (Kelly et al., 2005). Figure 4.6 (right panel) shows the near-UV region of both metHb samples. There are subtle differences in the two spectra in the Phe residue region, with a slight reduction to the shoulder at 268-270nm, and small alterations to the trough between 285-295nm (denoted by the arrows in Figure 4.6, right panel), which may indicate an alteration in the Tyr residues in the H_2O_2-mediated metHb. These changes, albeit small, indicate that there may have been structural alterations to the topology of the aromatic amino acid residues, specifically at the Phe and Tyr residues during exposure to H_2O_2. This observation is in line with work which described an oxidative reaction occurring between hydroperoxides (H_2O_2) and aromatic amino acids within haem-containing proteins such as Hb (Svistunenko, 2005).

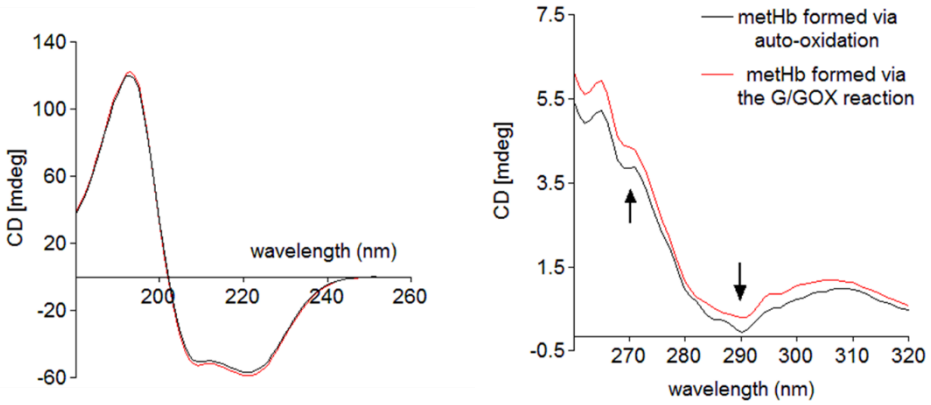

Figure 4.6 – Near- and far-UV region CD spectra of auto-oxidised metHb and that generated by H_2O_2 via the glucose and GOX reaction. MetHb concentrations were 0.5 and 5.0µM, for far- and near-UV regions, respectively. Spectra were generated with 25 scan repeats at room temperature and corrected against NaH_2PO_4/Na_2HPO_4 buffer, pH 7.4. Arrows in the right panel denote the wavelengths at which subtle changes were observed in the spectra of the metHb preparations formed by the G/GOX reaction e.g., 268-270nm and 285-295nm.

4.3.7 Stability of the HmuY-Fe(III)haem complex following exposure to bolus additions of H_2O_2

The apo- and holo- forms of HmuY are completely resistant to the proteolytic effects of the gingipains of *P. gingivalis*, InpA of *P. intermedia*, as well as the host-

derived trypsin and neutrophil elastase (Wojtowicz et al., 2009; Byrne et al., 2013). However, it is not known whether the HmuY-Fe(III)haem complex is stable when exposed to H_2O_2, specifically at concentrations produced by *S. gordonii* cells. To investigate this, H_2O_2 concentrations that were equal to and exceeded the maximal H_2O_2 production by *S. gordonii* cell suspensions i.e., 5, 10, 25, 50µmol/l (Chapter 3; Figure 3.11) were prepared from 30% H_2O_2 (w/w) in NaCl-Tris buffer, pH 7.5. 16µM HmuY-Fe(III)haem complex was incubated with this range of H_2O_2 concentrations for 1 hour at 20°C, and the decrease at A_{411nm} Soret band monitored as a measure of complex loss (Figure 4.7). The 411nm peak intensity was observed to decrease at higher H_2O_2 concentrations (25 and 50µmol/l) although importantly, it was observed to remain stable (approximately 80% of the original) after 2-hour incubation in the presence of 50µmol/l H_2O_2. Therefore, it can be concluded from this that the HmuY-Fe(III)haem complex is structurally stable at the highest concentrations of H_2O_2 produced by *S. gordonii* cell suspensions when delivered as a bolus.

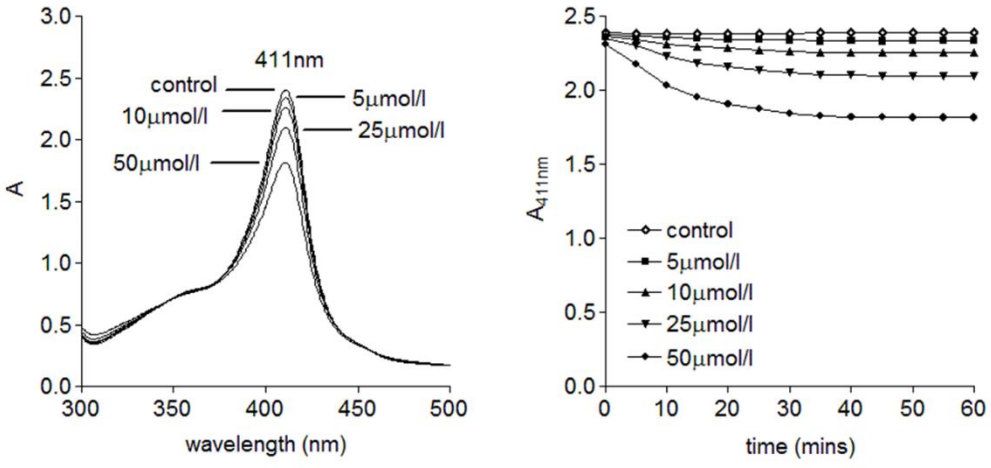

Figure 4.7 – HmuY-Fe(III)haem complex stability in presence of H_2O_2. 16µM HmuY-Fe(III)haem complex was incubated with bolus additions of 5, 10, 25, 50µmol/l H_2O_2 for 1 hour at 20°C. The HmuY-Fe(III)haem complex has a characteristic λ_{max} peak at 411nm (left panel) and the decrease in peak intensity of the Soret band was monitored as measure of haem-haemophore complex loss (right panel).

4.4 Discussion and conclusions

The main source of haem in the human body is in the form of Hb and to obtain haem from it, *P. gingivalis* must mediate its release via the aid of RgpA, Kgp and haemophores such as HmuY and HusA (Smalley et al., 2007; 2008; 2011; Gao et al., 2010). RgpA is important in mediating oxyHb oxidation, providing metHb for further globin degradation by K-gingipain and eventual Fe(III)haem extraction by HmuY (Smalley et al., 2011). However, this study has demonstrated that metHb mediated via H_2O_2 generated by *S. gordonii* represents a potential mechanism through which *P. gingivalis* might gain Fe(III)haem from Hb without the involvement of the gingipain proteases.

Formation of HmuY-Fe(III)haem complex from free Fe(III)haem occurs rapidly and is observed spectroscopically as the appearance of a 411nm Soret band and Q bands at 525 and 560nm (Smalley et al., 2011), and can be clearly distinguished from free Fe(III)haem with a flattened Soret band with a 385nm λ_{max} (Figure 4.1). However, HmuY-Fe(III)haem complex formation from metHb is slower due partly to encapsulation of the iron protoporphyrin XI within the Hb haem pocket. Furthermore, under conditions employed here, complete complexation between HmuY and Fe(III)haem from metHb may take up to 24 hours (Smalley et al., 2011), thus it was necessary to visualise any changes by deriving difference spectra. This showed that metHb generated by *S. gordonii* via H_2O_2 production could be utilised by HmuY to form the HmuY-Fe(III)haem complex. This is an important observation as it has been shown that Hb and haem may be prone to structural changes or complete degradation during exposure to H_2O_2 (Gutteridge, 1986; Nagababu & Rifkind, 2000; Li et al., 2006).

Interestingly, HmuY-Fe(III)haem complex formation occurred more rapidly from metHb mediated by *S. gordonii* than that generated via auto-oxidation (section 4.3.4; Figure 4.4) and a similar trend was observed with metHb produced via the G/GOX reaction (section 4.3.5; Figure 4.5). There was approximately a two-fold increase in the rate of haem acquisition by HmuY from metHb generated by exposure to H_2O_2 compared to auto-oxidised metHb. This was seen by applying a

one-phase exponential association curve to the data to calculate the haem binding constants by HmuY from the metHb incubations. The haem binding constant for metHb generated by *S. gordonii* cells vs auto-oxidised metHb in BHI broth was 32.6 ± 1.1 x 10^{-3} s^{-1} compared to 18.5 ± 0.8 x 10^{-3} s^{-1}, respectively, whilst for metHb generated by G/GOX it was 11.3 ± 0.6 x 10^{-3} s^{-1}, compared to 5.0 ± 0.5 x 10^{-3} s^{-1} for metHb auto-oxidised in NaCl-Tris buffer, pH 7.5. As discussed above, Hb is prone to degradation following exposure to H_2O_2 (Nagababu & Rifkind, 2000), and so it was important to demonstrate that increased Fe(III)haem pickup by HmuY from metHb (formed by H_2O_2) was not as a result of Hb breakdown and loss of Fe(III)haem into solution. Indeed, no free haem was observed in such preparations and thus it can be concluded that the HmuY-Fe(III)haem complex formation was from Fe(III)haem extracted directly from the Hb molecule.

CD spectroscopy in the far-UV region did not reveal any major structural differences between metHb generated by H_2O_2 compared to that produced through natural auto-oxidation. On the contrary, near-UV CD spectroscopy of the metHb generated via H_2O_2 exposure showed subtle differences to that of auto-oxidised metHb (specifically pointing to changes arising from spatial alterations in Phe and Tyr residues), which may offer a potential explanation for increased haem pick up by HmuY. Interestingly, a continuous flux of H_2O_2 has been shown capable of oxidising Tyr residues in Hb subunits (Giulivi & Davies, 1993), and which were subsequently identified as Tyr-42(α), Tyr-35(β), Tyr-130(β) or Tyr-145(β) (Svistunenko et al., 2002). Of these, Tyr-42(α) is located in the haem pocket but is also surface-exposed to the external environment (Reeder et al., 2008; see Figure 4.8). The detection of ferrylHb produced during the oxidation of oxyHb to metHb by H_2O_2 generated by *S. gordonii* (Chapter 3, section 3.3.9) strengthens the possibility that the Tyr-42(α) residue had become oxidised; the unstable ferryl haem (IV) iron has the propensity to oxidise amino acid residues in the haem pocket to return to the ferric (III) state (Reeder et al., 2008; Silva et al., 2009). If this is the case, it is possible that the ferrylHb generated during exposure to H_2O_2 will be rapidly re-reduced to metHb by an electron transfer from the Tyr-42(α) residue which, in turn, becomes oxidised (Reeder et al., 2008).

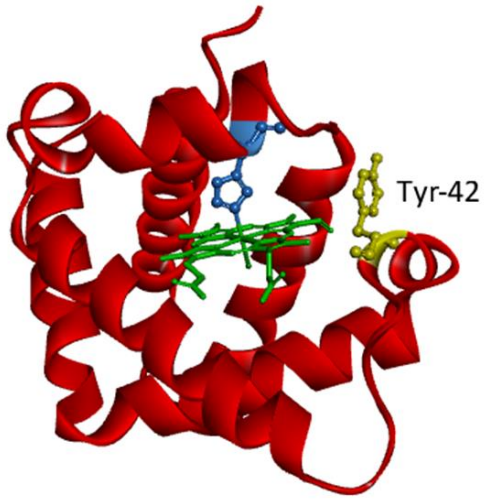

Figure 4.8 – The location of the Tyr-42 amino acid residue in the vicinity of the haem pocket in the α-chain of human Hb. The Tyr-42(α) residue (yellow) located close to the haem molecule (green) and proximal histidine (His-87; blue). Diagram produced using PDB file 2MHB.

Due to the vicinity of the Tyr-42(α) residue to the haem pocket, an oxidative event at this amino acid may influence the ease of haem extraction by HmuY, since an alteration to the structure of haem pocket has been shown to weaken the haem-globin linkage (Hargrove et al., 1996). In myoglobin, the covalent bond between the haem and globin chain (specifically referred to as the proximal His(F8)-haem iron linkage), is essential in maintaining the association equilibrium constant for globin-haem binding of ~ 10^{14} M^{-1} (Hargrove et al., 1996). Structural alterations to the haem pocket which alter the normal functioning of the proximal histidine can weaken the haem-globin linkage; e.g., the protonation and subsequent rotation of the imidazole ring of the proximal histidine results in increased haem dissociation (Yang & Phillips, 1996; Barrick, 1994). Interestingly, evidence suggests that the phenolic ring in tyrosyl residues in Hb, arising from H_2O_2 exposure, can rotate around the C^{β}-C^{1} bond (Svistunenko et al., 2002; Figure 4.9), which could result in the subtle alteration to the Hb structure that could likely be detected in near-UV CD. A more sensitive spectroscopic method such as electron paramagnetic resonance could be used in future work to identify specific oxidised amino acids in the metHb formed by exposure to H_2O_2 (Cooper et al., 2013). However, at this juncture, it is likely that an oxidative event at a tyrosine residue within the Hb chain,

and possibly the haem pocket (e.g., Tyr-42(α)), may weaken the stability of the haem-globin linkage in metHb mediated by exposure to H_2O_2 and which could explain the increased haem pick up by HmuY from H_2O_2 generated- compared to auto-oxidised-metHb.

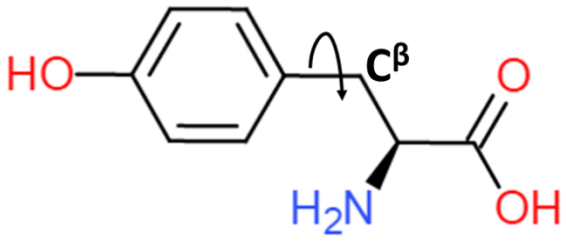

Figure 4.9 – The structure of the tyrosine amino acid. The phenol ring may rotate around the C^{β} bond in a tyrosyl radical formed during the reaction of Hb with H_2O_2 (adapted from Svistunenko et al., 2002).

The stability of the HmuY-Fe(III)haem complex during exposure to H_2O_2 at concentrations similar to those produced by *S. gordonii* cell suspensions was investigated; an important consideration should holo- or apo-HmuY be exposed to H_2O_2 *in vivo* as a result of co-aggregation between *P. gingivalis* and *S. gordonii*. It was observed that the HmuY-Fe(III)haem complex remained largely unaffected after 1-hour exposure to 50µmol/l H_2O_2. As HmuY delivers bound haem to the membrane bound transport protein HmuR for internalisation of the essential co-factor (Olczak et al., 2005), the HmuY-Fe(III)haem complex must remain stable to perform this function. The haemophore has previously been shown to be resistant to gingipain and InpA protease activity as well as chemical and thermal degradation (Wojtowicz et al., 2009; Byrne et al., 2013), whilst here it was demonstrated that the protein (at least when in complex with Fe(III)haem) was also largely resilient to any H_2O_2-mediated damage.

P. gingivalis is capable of generating metHb through the actions of self-produced gingipains; the HmuY-Fe(III)haem complex forms readily from metHb mediated through the proteolytic attack by RgpA on oxyHb (Smalley et al., 2011). However, this work has extended a recently described synergistic paradigm by which *P. gingivalis* can utilise the biochemical properties of co-colonised species to facilitate

metHb formation, and enhance Fe(III)haem availability to the organism (Byrne et al., 2013; Benedyk et al., 2015). So far, the observations from this work that *S. gordonii* can mediate formation of metHb is significant as the natural conversion of oxyHb to metHb via auto-oxidation is minimal, and lowest at neutral to slightly alkaline pH (Shikama, 1998) i.e., the pH range of the diseased gingival crevice and periodontal pocket (Eggert et al., 1991; Bickel & Cimasoni 1985b). Thus, the availability of metHb to haem-requiring organisms such as *P. gingivalis* may under such conditions be naturally low, and which highlights the need for a mechanism by which metHb is made available. Thus, co-aggregation with *S. gordonii* in the periodontal pocket may be an efficient way for *P. gingivalis* to overcome this initial biochemical obstacle of accessing metHb, and hence obtaining a vital supply of haem for growth, survival and virulence.

Chapter 5 HmuY-Fe(III)haem complex formation from glycated haemoglobin

5.1 Introduction

Poorly controlled diabetes is associated with an increased level of gingival tissue bleeding and correlates with an enhanced severity of PD (Ervasti et al., 1985; Bandyopadhyay et al., 2010). A positive link also exists between circulating glycated Hb levels and the severity of PD; with high glycated Hb levels (>9% of total Hb) correlating with an increased risk of PD-associated alveolar bone loss (Taylor et al., 1998). It has also been reported that moderately high glycated Hb levels (>6.5% of total Hb) correlated with an increased propensity for periapical PD, which is an inflammatory lesion caused by bacterial infection of the pulp canal system (Sanchez-Dominquez et al., 2015). Type II diabetic patients also have an increased colonisation by Red complex microorganisms such as *P. gingivalis* in subgingival dental plaque (Quintero et al., 2011). Interestingly, numbers of *P. gingivalis* isolated from subgingival plaque were higher in individuals with high blood glycated Hb levels (Makiura et al., 2008). However, the mechanisms by which *P. gingivalis* prevalence is increased in such individuals, and how this contributes to an increased propensity to develop PD, remains unclear. Furthermore, the numbers of oral viridans streptococci species such as *S. intermedius* and *S. oralis* are also increased in subgingival plaque of individuals with diabetes mellitus (Kampoo et al., 2014).

Haem is vital for the growth and virulence of *P. gingivalis* (Marsh et al., 1994). Therefore, it could be postulated that the enhanced colonisation of *P. gingivalis* in subgingival plaque of diabetics may be driven by an increased source of haem. It has been shown that both glycated Hb and myoglobin possess a weakened haem-globin linkage, which results in increased rates of haem transfer to serum albumin (which normally binds Hb haem) (Roy et al, 2004; Sen et al., 2005). These findings raise the possibility that the HmuY haemophore of *P. gingivalis*, which picks haem from metHb due to its lower binding affinity for the co-factor than oxyHb, may acquire haem more readily from glycated Hb, and feature as a mechanism through which haem acquisition by the bacterium is increased. Intriguingly, destruction of Hb by H_2O_2 is also accelerated after Hb becomes glycated (Sen et al., 2005). The breakdown of glycated Hb and liberation of free iron (an essential element for

streptococci species; Romero-Espejel et al., 2013) via the action of H_2O_2 generated by *S. gordonii* and other H_2O_2-producing organisms may aid streptococcal growth. Thus, H_2O_2-mediated iron release from glycated Hb will also be examined.

5.2 Material and methods

5.2.1 Glycation of Hb

In vitro glycation of Hb was achieved using a modified protocol previously described by Ch'ng and Marinah (1988). In short, 200µl of 0.5mM oxyHb (tetramer basis) containing 250mM glucose plus 100U/ml penicillin and 100µg/ml streptomycin in NaCl/Tris-HCl buffer, pH 7.5, was applied to Whatman grade 1 filter papers (47mm diameter), allowed to dry, then maintained in sterile petri dishes for 7 days at 37^{o}C. Un-glycated control Hb was produced by incubation under the same buffer conditions as above but without glucose. The dried Hb was then extracted from the filter papers by desorption in 3ml of the above buffer, by rotating gently for 30 minutes at 20^{o}C. Residual glucose was removed from the glycated Hb preparations by dialysis in cellulose membrane dialysis tubing at 5^{o}C, firstly versus dH_2O for two hours, then against ammonium acetate buffer (pH 8.5, 0.25M) for two hours. Finally, the last buffer was exchanged for ammonium acetate (pH 8.5, 0.25M) containing 20mM magnesium chloride to prepare the sample for the next purification step using phenylboronic acid affinity resin (see below). It was shown by Middle et al (1983) that slightly alkaline buffers (e.g., pH 8.5) were optimum for Hb-PBA resin complexation, and Mg^{2+} ions enhanced binding of glycated Hb to the PBA resin further.

5.2.2 Purification of glycated Hb using phenylboronic acid affinity (PBA) resin

The protocol for purification of glycated Hb using PBA resin was used as previously described (Middle et al., 1983). The immobilised PBA resin binds compounds containing diol moieties with high affinity through a reversible boronate formation (Figure 5.1; adapted from Springsteen & Wang, 2002).

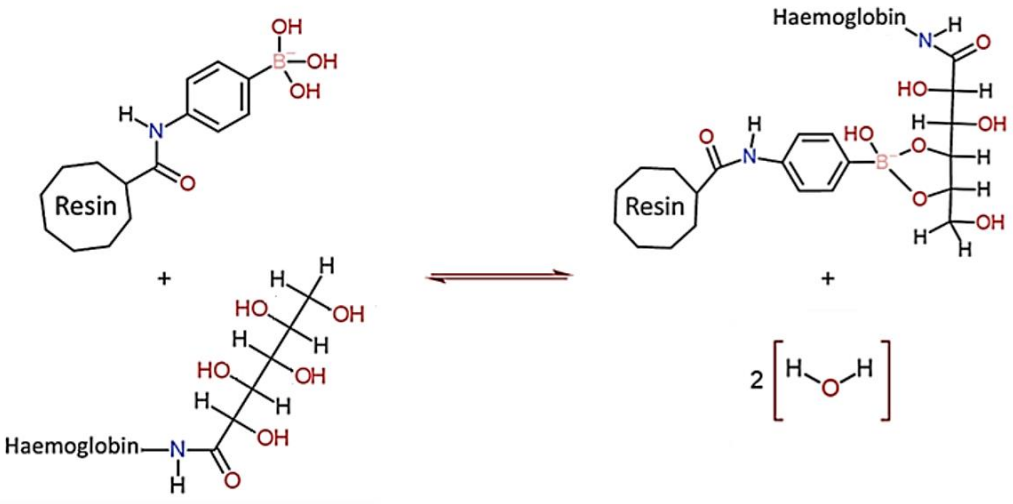

Figure 5.1 – The mechanism of boronate ester formation between diol moieties in the glycated Hb chain and the phenylboronic acid resin. The boronate will complex with two diol moieties (-OH) located in the Hb chain (the glucose molecule will link to the -NH terminal domain of an amino acid residue in Hb) resulting in the release of two molecules of H_2O.

1ml of glycated and un-glycated Hb preparations as prepared above (approximately 100µM with respect to tetramer) were added separately to 1ml of the PBA resin (Step 1; Figure 5.2) and mixed for 1 hour at 20^{o}C to allow for boronate-diol complexation (Middle et al., 1983). Samples were centrifuged (12,000 x g for 10 minutes at 5^{o}C) to pellet the resin and attached Hb, and the unbound Hb fraction still present in the glycated Hb preparation not retained on the resin was discarded (Step 2; Figure 5.2). The glycated Hb fractions bound to the resin were desorbed by the addition of 1ml of ammonium acetate (pH 8.5, 0.25M) containing 0.2M sorbitol (Step 3; Figure 5.2) which acts as a competing diol, binding with higher affinity to the PBA resin, and forcing release of the glycated, diol-containing Hb. This was achieved by mixing the resin with the ammonium acetate buffer containing sorbitol for 1 hour at 20^{o}C, and centrifuging the sample at 12,000 x g for 10 minutes at 5^{o}C. The desorbed fraction was termed glycated Hb (Step 4, Figure 5.2). The same procedure was repeated with the control Hb preparation minus glucose, although the unbound Hb from steps 1 and 2 was used throughout as un-glycated, control Hb.

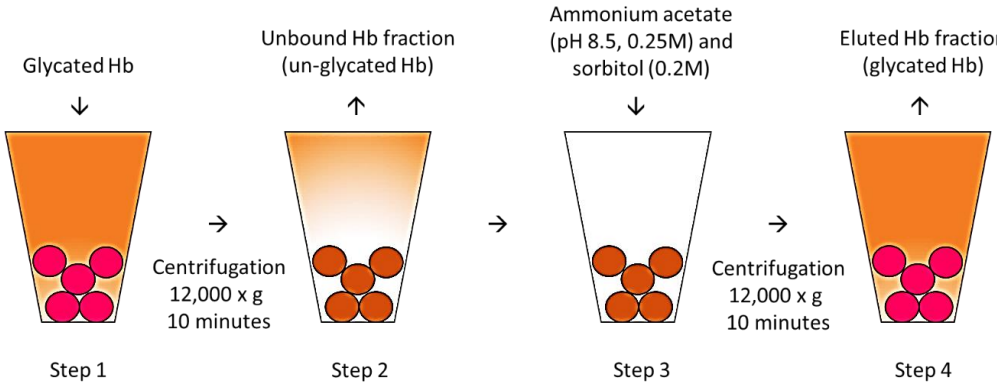

Figure 5.2 – Scheme showing the purification steps for glycated Hb using phenylboronic acid resin. The supernatant from step 4 was retained as 'glycated Hb'.

5.2.3 Mass spectrometry analysis of Hb glycation sites

16µM (tetramer basis) of glycated and un-glycated Hb samples were prepared and purified as above (sections 5.2.1 and 5.2.2) and dialysed against 0.1M NaH_2PO_4/Na_2HPO_4 buffer, pH 7.4, for two hours at 5^{o}C. Hb samples were diluted 1:10 in the above buffer and 0.5µg trypsin (MS grade) was added before incubation overnight at 37^{o}C. Samples were desalted by reversed phase chromatography using ZipTips (Millipore) prior to delivery to the mass spectrometer. Glycated peptides were identified using PeakView software to extract parent ions of the appropriate m/z for peptide plus hexose (simple sugar addition), and the area under the curve of each peak was used to assess the relative abundance of glycated peptides. Glycation sites at specific amino acid residues within the Hb chains were compared to the publications studying Hb glycated *in vitro* and *in vivo* (Shapiro et al., 1980; Zhang et al., 2001; Delpierre et al., 2004; Ito et al., 2011).

5.2.4 Quantification of relative abundance of Hb glycation using the colorimetric 5-hydroxymethylfurfural assay

5-hydroxymethylfurfural (5-HMF) is a breakdown product of glucose which can be detected in glycated Hb preparations (Fluckiger & Winterhalter, 1976) and is used routinely as a measure of peptide glycation. Oxalic acid (0.25ml; 1.5M) was added to 0.5ml of purified glycated and un-glycated Hb samples (final Hb concentrations

ranging from 136-304µM, with respect to tetramer) and heated at 100°C for 4 hours to hydrolyse the glycated moieties from the Hb and mediate catalytic conversion of glucose to 5-HMF (Figure 5.3).

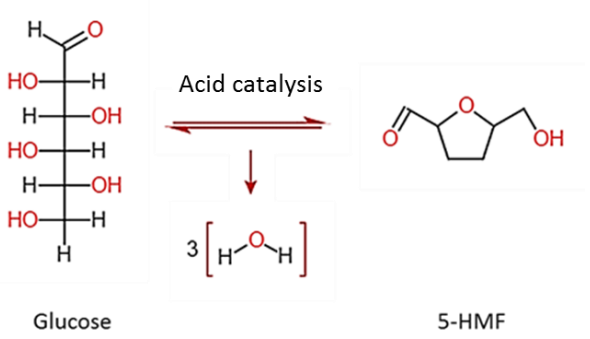

Figure 5.3 – The oxalic acid catalysed generation of 5-HMF.

Next, 0.25ml of 40% v/v trichloroacetic acid (TCA) was added to each Hb sample and left for 5 minutes at 20°C to denature and precipitate the protein which was removed after centrifugation at 12,000 x g for 5 minutes at 20°C. The protein-free supernatant (0.8 ml) was then incubated for 1 hour at 40°C with 0.2 ml thiobarbituric acid (TBA; 50 mM in dH_2O). In the presence of glycated products, a colorimetric reaction occurs between the TBA and 5-HMF resulting in a yellow chromogen with λ_{max} 443nm. The absorbance of the cooled samples were read spectroscopically at A_{443nm} against the control (ammonium acetate buffer; 0.25M, pH 8.5) and the 5-HMF concentration was determined against a standard curve generated for serial dilutions of 5-hydroxymethyl-2-furaldehyde.

5.2.5 UV-visible spectroscopic detection of HmuY-Fe(III)haem complex formation from glycated and un-glycated Hb

Equimolar concentrations of HmuY plus glycated and un-glycated Hb (16µM with respect to Hb tetramer) were incubated at 20°C for 4 hours. The integrated area changes of the 525nm and 560nm Q bands (taken from the intersection of the x axis at 510nm and 590nm, respectively) were used as a measure of the rates of HmuY-Fe(III)haem complex formation.

5.2.6 Triton X-100-methanol method for detection of free Fe(III)haem in the filtrate of glycated and un-glycated Hb

Glycated and un-glycated Hb samples were filtered on 30-kDa cut-off membranes by centrifugation at 12,000 x g, for 30 minutes at 5^{o}C to produce a Hb-free filtrate and 1 volume of this was added to 10 volumes of Triton-X100 (2.5% v/v in methanol; Pandey et al., 1999) to test for the presence of free Fe(III)haem.

5.2.7 Structural analysis of glycated and un-glycated Hb using far-and near-UV circular dichroism

Glycated and un-glycated Hb samples were purified as outlined in sections 5.2.1 and 5.2.2. Following dialysis against NaH_2PO_4/Na_2HPO_4 buffer, pH 7.4, for two hours at 5^{o}C, to remove chloride ions or Tris present in the samples, Hb preparations were analysed using near- (260-320nm) and far- UV (200-260nm) CD spectroscopy. Data collection was conducted at 20^{o}C using Hb concentrations of 0.5µM and 5µM (tetramer basis), for far- and near-UV analysis, respectively. All samples were scanned 25 times resulting in an averaged spectrum.

5.2.8 Colorimetric ferrozine-based assay for the quantitation of iron release from glycated and un-glycated Hb after exposure to H_2O_2

The ferrozine-based assay for determination of iron release from glycated and un-glycated Hb after exposure to H_2O_2 followed a similar protocol outlined by Kar & Chakraborti (2001). 1ml of 200µM glycated or un-glycated Hb (tetramer basis) was incubated with 50mM glucose and 0.01µM GOX at 37^{o}C for 24 hours. The concentrations of glucose and GOX used here generated a continuous flux of H_2O_2 equivalent to that produced by a 1.00 OD_{600} *S. gordonii* cell suspensions (Chapter 3; section 3.3.6) i.e., 5-50µmol/l over 4 hours. Next, 0.25ml trichloroacetic acid (40% v/v) was added to 0.5ml of Hb sample for 5 minutes at 20^{o}C to precipitate protein. Following centrifugation, 0.5ml of supernatant was incubated with 1ml ferrozine working reagent for 20 minutes at 37^{o}C, and A_{562nm} used to determine the iron content using the extinction coefficient (ε) of 28 mM^{-1} cm^{-1} for the ferrozine-iron complex (Ceriotti & Ceriotti, 1980).

5.3 Results

5.3.1 Identification of glycated amino acid residues using mass spectrometry

Liquid-chromatography mass spectrometry was used to identify the glycation sites on the amino acid residues in the Hb chains. Glycated and un-glycated Hb samples were prepared, purified and digested as above (sections 5.2.1 and 5.2.2) and following desalting using ZipTips were delivered via reversed phase chromatography to mass spectrometry. The spectral data (not presented) showed there was a total of 8 glycation sites in the α-chain, and a further 10 in the β-chain; all located on lysine residues (summarised in Table 5.1). These results were derived by using PeakView software; in short, the parent ions of the appropriate m/z for horse Hb plus a simple sugar addition (e.g., hexose; $C_6H_{12}O_6$) were calculated, and the area under the curve of each peak was used to assess the presence or absence of the glycation. The glycation sites were compared to those identified by Shapiro et al (1980) for glycated human Hb *in vitro* and *in vivo*, Zhang et al (2001) for human Hb glycated *in vivo*, Delpierre et al (2004) and Ito et al (2011) for human Hb glycated *in vitro*. As Hb was purified from horse blood in this study, it is noteworthy that horse and human Hb were comparable; all the lysine residues being located at the same sites in the α- and β-chains of the Hb of both species (Figure 5.4).

Table 5.1 – Glycated residues in horse Hb samples glycated *in vitro* as identified using mass spectrometry. The location of the glycated lysine residues detected by mass spectrometry in the horse Hb preparations in this study are compared to those for both *in vitro* (Shapiro et al., 1980; Delpierre et al., 2004; Ito et al., 2011) and *in vivo* glycated human Hb (Shapiro et al., 1980; Zhang et al., 2001).

Lysine residue	Detected in this study	Shapiro et al (1980) *in vivo* and *in vitro* glycated Hb	Zhang et al (2001) *in vivo* glycated Hb	Delpierre et al (2004) *in vitro* glycated Hb	Ito et al (2011) *in vitro* glycated Hb
7(α)	-	✓	✓	-	-
11(α)	-	-	-	-	-
16(α)	✓	✓	✓	✓	✓
40(α)	✓	✓	✓	-	-
56(α)	-	-	✓	-	✓

60(α) 61(α)	✓	✓	-	✓	-
90(α)	✓	-	-	-	-
99(α)	✓	-	-	-	-
127(α)	✓	-	✓	-	-
139(α)	✓	-	✓	✓	-
8(β)	✓	✓	✓	-	✓
17(β)	✓	✓	✓	✓	-
59(β)	✓	-	-	✓	-
61(β)	-	-	✓	-	-
65(β) 66(β)	✓	✓	✓	✓	-
82(β)	✓	-	-	✓	✓
95(β)	✓	-	-	✓	-
120(β)	✓	✓	-	✓	-
132(β)	✓	-	✓	✓	-
144(β)	✓	✓	✓	✓	✓

```
                1
HORSEα          VLSAADKTNVKAAWSKVGGHAGEYGAEALERMFLGFPTTKTYFPHFDLSHGSAQVKAHGK
HUMANα          VLSPADKTNVKAAWGKVGAHAGEYGAEALERMFLSFPTTKTYFPHFDLSHGSAQVKGHGK

               61
HORSEα          KVADGLTLAVGHLDDLPGALSDLSNLHAHKLRVDPVNFKLLSHCLLSTLAVHLPNDFTPA
HUMANα          KVADALTNAVAHVDDMPNALSALSDLHAHKLRVDPVNFKLLSHCLLVTLAAHLPAEFTPA

              121
HORSEα          VHASLDKFLSSVSTVLTSKYR
HUMANα          VHASLDKFLASVSTVLTSKYR

                1
HORSEβ          VQLSGEEKAAVLALWDKVNEEEVGGEALGRLLVVYPWTQRFFDSFGDLSNPGAVMGNPKV
HUMANβ          VHLTPEEKSAVTALWGKVNVDEVGGEALGRLLVVYPWTQRFFESFGDLSTPDAVMGNPKV

               61
HORSEβ          KAHGKKVLHSFGEGVHHLDNLKGTFAALSELHCDKLHVDPENFRLLGNVLALVVARHFGK
HUMANβ          KAHGKKVLGAFSDGLAHLDNLKGTFATLSELHCDKLHVDPENFRLLGNVLVCVLAHHFGK

              121
HORSEβ          DFTPELQASYQKVVAGVANALAHKYH
HUMANβ          EFTPPVQAAYQKVVAGVANALAHKYH
```

Figure 5.4 – Primary amino acid sequences of horse and human α- and β- chains showing the positions of lysine residues (K). Amino acid sequence alignment was generated by Protein BLAST software (https://blast.ncbi.nlm.nih.gov) using Universal Protein Resource Knowledge Base (UniProtKB) protein access codes P68871 and P69905 for human α- and β- chains, P01958 and P02062 for horse α- and β- chains, respectively.

Using Accerlys software to produce a 3D rendering of the glycated Hb molecule (PDB access code 1MHB), it was possible to visualise the positions of the lysine residues which had been glycated in the Hb structure in this study. It is evident from the examination of Figure 5.5 that the glycated residues are located mainly on the surface of the Hb molecule, and include Lys-16(α), Lys-8(β), Lys-82(β) and Lys-144(β). Note also that the glycated residues Lys-61(α), Lys-90(α), Lys-66(β) and Lys-95(β) were positioned in the haem pocket. Specifically, Lys-61(α) and Lys-66(β) are located on the E helix of the α- and β- chains which contain the histidine residues (His58 and His63, respectively) involved in oxygen binding to the haem iron, whilst Lys-90(α) and Lys-95(β) are positioned on the same F8 helix-loop as the proximal histidines (His-87(α) and His-92(β), respectively) which are essential in covalently linking the haem molecule to the Hb chains.

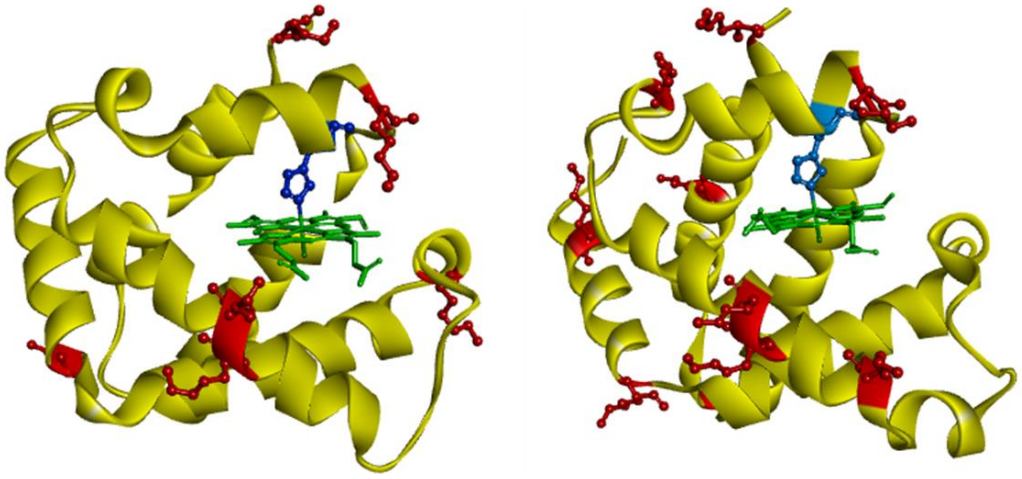

Figure 5.5 – Glycated lysine residues in the α-chain (left panel) and β-chain (right panel) of horse Hb. The figure was produced using Accerlys software (PDB access code 1MHB). Glycated lysine residues (red), the haem molecule (green) and proximal histidine; His-87(α) and His-92(β) (blue) are all shown.

5.3.2 Quantification of the relative abundance of Hb glycations in the glycated and un-glycated Hb preparations using the 5-hydroxymethylfurfural assay

The relative abundance of glycated Hb was calculated from the 5-hydroxymethylfurfural (5-HMF) assay in three separate preparations of glycated and un-glycated Hb. The results were determined by calculating the total

concentration of 5-HMF in the sample (as determined from a standard curve for 5-HMF) relative to the total concentration of Hb in each preparation. From this, glycated Hb preparation 1 contained 161µM 5-HMF/136µM Hb, glycated Hb preparation 2 contained 356µM 5-HMF/304µM Hb whilst glycated Hb preparation 3 contained 333µM 5-HMF/257µM Hb. These results indicated that the glycated Hb preparations each contained approximately 1 glycation per Hb (subunit basis). It is noteworthy that 5-HMF was also detected in the un-glycated Hb samples, likely arising from natural *in vivo* glycation of Hb in normal non-diabetic individuals (Bunn et al., 1976). However, the concentration of 5-HMF in the un-glycated preparations was relatively low (un-glycated Hb preparation 1, 29µM 5-HMF/136µM Hb; preparation 2, 48µM 5-HMF/238µM Hb; preparation 3, 45µM 5-HMF/224µM Hb), averaging at one glycation per 4-5 Hb molecule (subunit basis).

5.3.3 Fe(III)haem is more readily acquired by HmuY from glycated Hb than from un-glycated Hb

Non-enzymatic glycation of Hb results in the weakening of Hb-haem linkage and the subsequent increased transfer of haem from glycated Hb to serum albumin (Sen et al., 2005). Thus, it is reasonable to assume that haem may be more easily extracted by HmuY from glycated Hb compared to un-glycated Hb. It should be noted that during the 7-day *in vitro* preparation of the glycated and un-glycated Hb, the samples were highly auto-oxidised (the glycated Hb comprising 95% metHb, and the un-glycated Hb composed of 97% metHb, with the remaining Hb species in each preparation in the form of haemichrome; Figure 5.6). Given the ability of HmuY to extract haem from metHb (Smalley et al., 2011) it would be expected that both glycated and un-glycated Hb (each being in the metHb form) would be equally susceptible to haem sequestration by the haemophore.

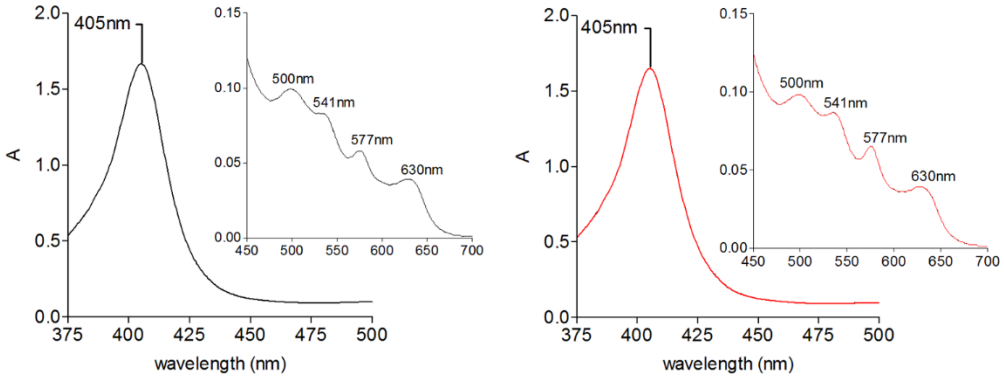

Figure 5.6 – The UV-visible spectra of the glycated Hb (left panel) and un-glycated Hb (right panel) after PBA resin purification. Both Hb samples contained almost equal amounts of metHb; 95% for glycated Hb and 97% for un-glycated Hb with the remainder haemichrome in both preparations.

However, the rates of HmuY-Fe(III)haem complex formation from these Hb samples (measured by integrating the 525nm and 560nm Q band areas, and the rate constant of HmuY-Fe(III)haem binding calculated using a one-phase exponential association curve as previously described by Gao et al [2010]) were different (Figure 5.7). Specifically, the HmuY-Fe(III)haem complex formed more rapidly from glycated Hb than from un-glycated Hb (relative haem binding constant for HmuY of 16.6 ± 1.0 x 10^{-3} s^{-1} from glycated Hb compared to 11.3 ± 0.7 x 10^{-3} s^{-1} for un-glycated Hb, respectively). Thus, although the Hb preparations contained almost equal concentrations of metHb, there was an approximate 1.5-fold increase in haem acquisition rate by HmuY from glycated Hb compared to un-glycated Hb over a 4-hour reaction.

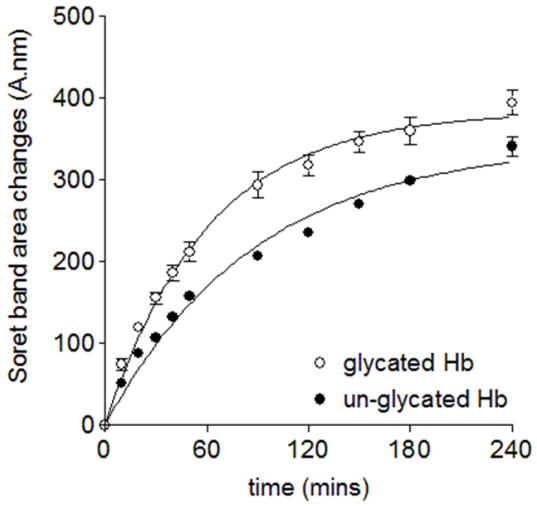

Figure 5.7 – Comparison of HmuY-Fe(III)haem complex formation from glycated and un-glycated Hb. Hb (64µM subunit basis) was incubated with an equimolar concentration of HmuY for 4 hours at 20°C. The combined integrated areas of 525 and 560nm Q bands (from difference spectra) were used as a measure of HmuY-Fe(III)haem complex formation.

It should be pointed out here that the increased rate of HmuY-Fe(III)haem complex formation from glycated Hb was not a result of free Fe(III)haem lost from the protein during glycation. This was determined from the observation that free Fe(III)haem was not detected in the filtrates of either glycated and un-glycated Hb. Therefore, it can be concluded that the increase in HmuY-Fe(III)haem complex formation from glycated Hb may have arisen from direct extraction of haem from the protein, most likely as a result of the weakened haem-globin linkage as previously reported for glycated Hb by Sen et al (2005).

5.3.4 Structural analysis of glycated and un-glycated Hb using near- and far-UV circular dichroism

The increase in HmuY-Fe(III)haem complex formation from glycated Hb may have resulted from subtle change(s) to the structure of the Hb molecule in which the haem-globin linkage is weakened. The work of Sen et al (2005) provided evidence that glycated human Hb possessed a different secondary structure to that of its un-glycated counterpart. Thus, this section will analyse the structures of the glycated

and un-glycated Hb samples using CD spectroscopy. In these experiments, glycated and un-glycated Hb samples were prepared and purified as above (sections 5.2.1 and 5.2.2), and diluted to 0.5µM and 5.0µM in NaH_2PO_4/Na_2HPO_4 buffer, pH 7.4, for far-and near-UV CD spectroscopic analysis, respectively (Figure 5.8).

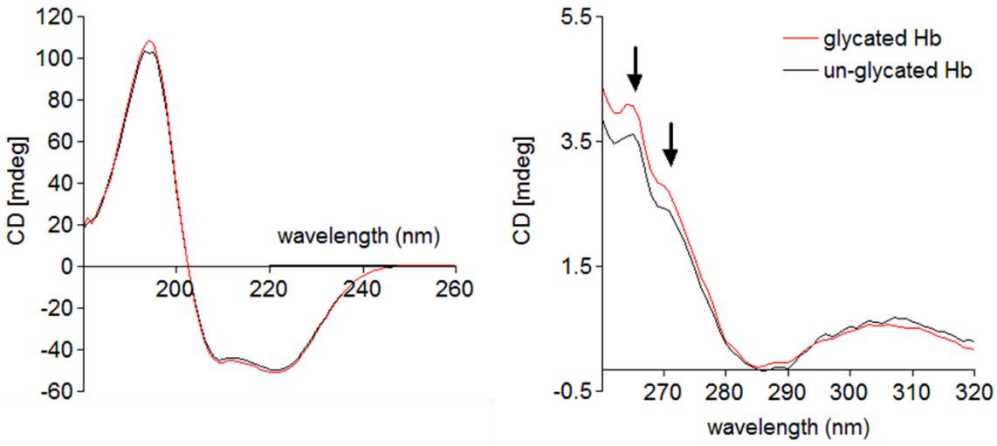

Figure 5.8 – Near- and far-UV CD spectral analysis of glycated and un-glycated Hb. The spectra depict the average of 25 scan repeats for the far-UV (left panel) and near-UV regions (right panel). Both spectra were background-corrected by subtraction of the buffer spectrum. Arrows in the near-UV region (260-280nm) denote the wavelengths at which subtle changes were observed in the spectra of the glycated Hb preparations.

Far-UV CD (Figure 5.8, left panel) showed that both glycated and un-glycated Hb shared a high similarity in secondary structure, indicating that the α-helix strands (denoted by the peak at 180-200nm and the trough at 200-240nm) were largely unaffected by the glycation process. *In vitro* glycation of Hb therefore did not result in the unfolding of the protein, a finding contrary to the work of Sen et al (2005) (as discussed above). However, in the near-UV region (Figure 5.8, right panel), there were subtle differences between the glycated and un-glycated Hb spectra; namely, the peak intensity between 260 and 280nm was increased in the glycated Hb sample. In addition, a change, albeit small, was seen in the shoulder at 270nm in the un-glycated Hb sample, which was less prominent than in the glycated Hb. Taken together, these spectra indicated that whilst secondary structure was unaffected, *in vitro* glycation appeared to alter the spatial disposition of the aromatic amino acids

e.g., the orientation of the phenylalanine (260-270nm) and/or tryptophan (275-285nm region) residues.

5.3.5 Quantification of iron release from glycated and un-glycated Hb during exposure to a continuous flux of H_2O_2

Hb glycated *in vitro* with either glucose or fructose is more prone to H_2O_2-mediated degradation than is un-glycated Hb, resulting in increased iron release (Sen et al., 2005; Bose & Chakraborti, 2008). Thus, it is likely that haem from any glycated Hb exposed to H_2O_2 as a result of interactions with *S. gordonii* may lose its iron more readily. To test this possibility, glycated and un-glycated Hb (200µM tetramer basis; prepared as above) was incubated with 50mM glucose and 0.01µM GOX; concentrations at which generated a continuous flux of H_2O_2 equivalent to that produced by a 1.00 OD_{600} suspension of *S. gordonii* cells in NaCl-Tris buffer, pH 7.5, at 37°C for 24 hours. Fe(III)iron release from the Hb was monitored using the ferrozine assay to yield a magenta coloured complex with λ_{max} at 562nm having an extinction coefficient of $28mM^{-1}\ cm^{-1}$ (Ceriotti & Ceriotti, 1980). The experiment was repeated using the three separate preparations of both glycated and un-glycated Hb (Figure 5.9).

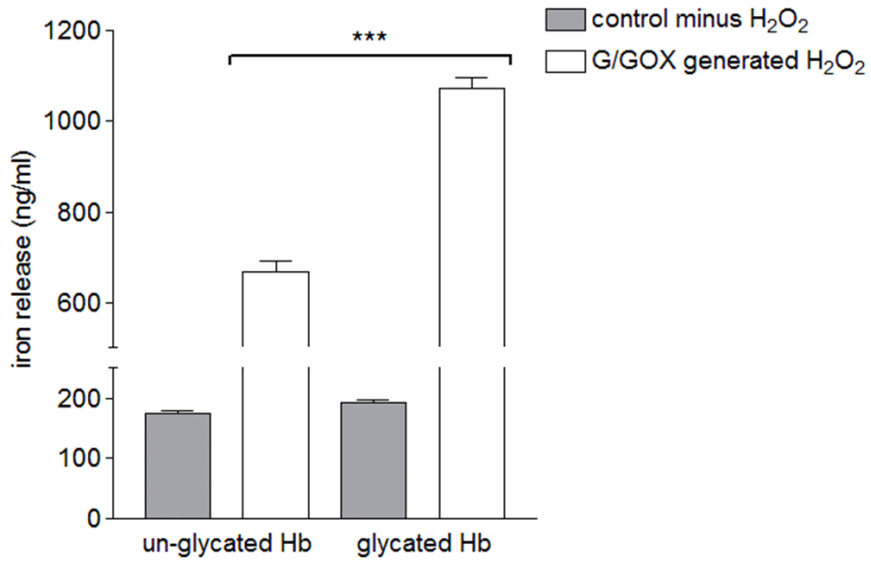

Figure 5.9 – Quantification of Fe(III) iron release from glycated and un-glycated Hb following exposure to a continuous flux of H_2O_2. Glycated and un-glycated Hb

(200µM with respect to tetramer) were exposed to a continuous flux of H_2O_2 generated by 50mM glucose and 0.01µM GOX for 24 hours at 37°C. Control Hb samples were incubated in the same buffer minus glucose and GOX addition. Fe(III) iron was quantified using the colorimetric ferrozine assay. Bars show mean ± SEM of assays on three separate Hb preparations; *** $p < 0.001$; unpaired t test.

Figure 5.9 shows that more Fe(III)iron was liberated from glycated Hb than un-glycated Hb (1074.4 ± 23.1ng/ml vs 667.3 ± 24.5ng/ml, respectively) during exposure to a continuous flux of H_2O_2. It is noteworthy that although these levels of iron release were relatively small, they are in line with other work on iron release during exposure of glycated and un-glycated Hb to H_2O_2 (Bose & Chakraborti, 2008). It should also be noted that both glycated and un-glycated Hb preparations showed the presence of free iron in the absence of exposure to H_2O_2, which is also in accordance with previous observations (Panter, 1994). However, following exposure to H_2O_2 at concentrations equivalent to that produced by a 1.00 OD_{600} suspension of *S. gordonii* cells, there was approximately a 1.6-fold increase in iron released from glycated Hb than from un-glycated Hb.

Interestingly, no free iron was detected when the above experiment was repeated where the H_2O_2 was produced by *S. gordonii* cells. For this, glycated and un-glycated Hb was incubated with *S. gordonii* cell suspensions (1.00 OD_{600}) in BHI broth for 24 hours at 37°C. As it has been shown that streptococci species produce siderophores; small compounds capable of scavenging free iron (Ge & Sun, 2014), it is possible that *S. gordonii* may have acquired the additional iron released from the Hb. Therefore, the G/GOX enzymatic reaction was an appropriate model system to mimic the production of H_2O_2 generated in a continuous flux by *S. gordonii* cell suspensions.

5.4 Discussion and conclusions

Poor glycaemic control in diabetics results in high circulating levels of glycated Hb and this correlates with PD severity which is characterised by an increased risk of alveolar bone loss and enhanced gingival tissue bleeding (Taylor et al., 1998; Sanchez-Dominquez et al., 2015; Ervasti et al., 1985; Bandyopadhyay et al., 2010).

Importantly, clinical studies have also shown that numbers of *P. gingivalis* isolated from subgingival plaque were increased in diabetic individuals with high levels of circulating glycated Hb (Makiura et al., 2008), although the reasons for this increased prevalence of *P. gingivalis* is not fully understood. As there must be sufficient concentrations of haem to support the growth of *P. gingivalis* in the plaque environment, it could be that haem availability is enhanced in diabetic individuals and this may contribute to an increase in colonisation and numbers of *P. gingivalis*. In line with this possibility, here it was investigated whether the HmuY haemophore of *P. gingivalis* could acquire haem more readily from glycated Hb than from un-glycated Hb.

Multiple sites of glycation resulting from *in vitro* non-enzymatic glycation of Hb were detected by mass spectrometry. Specifically, a total of 8 lysine residues were identified as being glycated in the α-chain, whilst 10 were identified in the β-chain. Lysine residues of Hb are commonly glycated *in vivo* (Lee et al., 2011) and have also been observed following *in vitro* glycation (Ito et al., 2011), not least because of the 4-carbon side-chain which increases exposure of the side chain -NH_2 group to the external environment (Figure 5.10; Ansari et al., 2011; Ito et al., 2011). It is worth noting that the glycated lysine residues identified in this study largely correlated with those described in previous publications for Hb glycated both *in vitro* and *in vivo* (Table 5.1). It was postulated that variations in glycation profiles between studies likely arise through differences in experimental design of the *in vitro* glycation procedure. The concentrations of both glucose and Hb, the *in vitro* glycation period and protein conformation (e.g., whether the Hb is in the form of tetramer, dimer or individual α-/β-chains) all affect the glycation profile (Zhang et al., 2001).

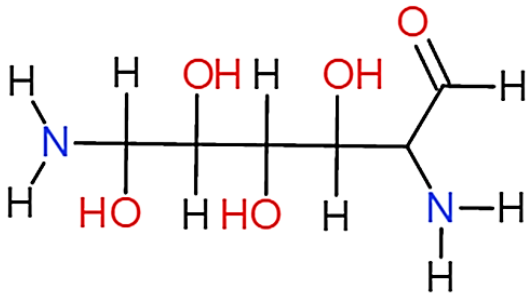

Figure 5.10 – The structure of lysine

Of the glycated lysine Hb residues identified here by mass spectrometry, the majority were seen to be located on the surface of the Hb (Figure 5.5). This is logical as these residues would be exposed to the external micro-environment and are thus potentially more vulnerable to glycation. It is noteworthy that all the glycated lysine residues identified in human Hb have been shown to be surface located (Ito et al., 2011). However, there is evidence to suggest that glycation may also occur on residues that lie within the haem pocket, notably, Lys-61(α) and Lys-66(β) (Iwamoto et al., 2001; Wang et al., 2014). These residues were also identified as being glycated in this study, and are located on the E helix of the α- and β- chains, which contain the histidine residues (His-58 and His-63, respectively) involved in oxygen binding to the haem iron. As these lysine residues cooperate with the histidine in oxygen binding, it is likely that glycation at these sites may also reduce oxygen affinity (Friess et al., 2003; Rosa et al., 1969). Indeed, others have shown that glycated oxyHb and oxymyoglobin both have an increased propensity to auto-oxidise to their met-forms (Sen et al., 2005; Roy et al, 2004).

The haem-globin linkage is weakened in both glycated Hb and myoglobin, which increases the rate of haem transfer to serum albumin (Roy et al, 2004; Sen et al., 2005). As HmuY extracts Fe(III)haem more readily from metHb (Smalley et al., 2011) due to the 10^8-fold decrease in globin-haem affinity in the oxidised Hb species (Hargrove et al., 1996), the weakened haem-globin linkage in glycated Hb may account for the observed increase in haem pick up by the haemophore from glycated Hb (Figure 5.7). However, there is no literature describing the effect of glycation of a lysine residue in the haem pocket that interferes with the function of

the proximal histidines (His-87 in α-chain or His-92 in β-chain), which could theoretically weaken the haem-globin linkage. As the work of Sen et al (2005) did not elaborate on the cause of the weakened haem-globin linkage in glycated Hb, it is difficult to assign a specific mechanism by which glycation may affect the stability of the haem within the Hb.

Near- and far-UV CD was used here to compare any structural differences between glycated and un-glycated Hb. Sen et al (2005) concluded that non-enzymatic Hb glycation resulted in a decrease in negative ellipticity in the far-UV region that is associated with a reduction in the α-helix content of the protein. However, here it was shown that upon glycation, glycated Hb possessed an almost identical secondary structure to that of un-glycated Hb. The conflicting observations in CD analysis of the glycated Hb secondary structure between this work and that of Sen et al (2005) could be explained by the duration of Hb glycation. It has been shown that the extent of far-UV CD spectroscopical changes in glycated Hb are related to the duration of glycation; the longer the glycation period, the greater the level of unfolding of the α-helices (Bakhti et al., 2007). Sen et al (2005) purified glycated Hb from erythrocytes of patients with diabetes, thus it was difficult to draw exact comparisons between the glycated Hb preparations used in their work and those used in this study. Indeed, it has been shown that glycation of Hb *in vivo* occurs slowly during the lifespan of an erythrocyte (~120 days) (Bunn et al., 1976), which may result in the formation of cross-linked Hb derivatives such as AGEs (Turk et al., 1998). Interestingly, it has been shown that AGEs have a different CD spectral profile than glycated Hb with simple modified peptide(s) (known as an Amadori arrangement) (Iram et al., 2013). Therefore, as the 7-day Hb *in vitro* glycation period used in this work resulted in the formation of glycated Hb with a simple sugar addition, and no AGE formation, this may explain why no obvious differences were observed in far-UV CD between the glycated and un-glycated Hb preparations used in this study.

Here, near-UV CD analysis of glycated and un-glycated Hb indicated subtle structural differences attributable to changes in the spatial disposition of the aromatic amino acids. Specifically, the increase in peak intensity of the glycated Hb

sample between 260nm and 280nm suggested that the phenylalanine (260-270nm) and/or tryptophan (275-285nm) residues were affected following the glycation process. As only lysine residues were identified as being glycated in the Hb preparation (section 5.3.1), it is likely that glycation at a lysine residue altered the optical properties of a neighbouring phenylalanine and/or tryptophan residue(s). Indeed, others have shown that the structural conformations of tryptophan moieties are altered during Hb glycation (Sen et al., 2005; Bose & Chakraborti, 2008). In light of the mass spectrometry and CD data, it is possible to tentatively suggest that a glycation of the Lys-90(α) and Lys-95(β) residues, which are located on the same F8 helix-loop as the proximal histidines (His-87(α) and His-92(β), respectively), may weaken the stability of the haem-globin linkage; the His(F8)-haem iron covalent bond, which, in myoglobin, is important in controlling Fe(III)haem dissociation (Hargrove et al., 1996).

A bi-directional link exists between increased circulating free iron and diabetic complications including renal disease (Fernandez-Real et al., 2002). Glycated Hb is also more prone to H_2O_2-mediated damage (Kar & Chakraborti, 1999; Sen et al., 2005; Bose & Chakraborti, 2008) in which the Hb and haem structures are broken down, resulting in the release of iron (Halliwell & Gutteridge, 1990). It was found here that more iron was released from glycated Hb than un-glycated Hb when subject to a continuous flux of H_2O_2 generated by the G/GOX enzymatic reaction. However, there was no significant difference in the amount of iron released in the glycated and un-glycated Hb preparations when incubated with 1.00 OD_{600} *S. gordonii* cell suspensions. This was a puzzling observation as the concentrations of G/GOX used generated a similar flux of H_2O_2 to that of the cells. The fate of any iron released under these conditions is not known but it is possible that the iron may have been taken up by the cells as it is known that streptococci species produce siderophores which scavenge free iron from the immediate environment before delivery to the cell for uptake. If this were the case, H_2O_2-mediated degradation of glycated Hb might advantage streptococci which have a growth requirement for iron (Ge & Sun, 2014) and may provide a mechanism to explain the increased

numbers of oral streptococci in supragingival plaque in diabetic individuals with severe PD (Kampoo et al., 2014).

In summary, the results in this chapter have demonstrated that Fe(III)haem was more readily extracted by HmuY from glycated Hb compared to un-glycated Hb. This was likely due to the weakening of the haem-globin linkage (His(F8)-haem iron covalent bond) arising from a glycated lysine residue(s) in the haem pocket. Thus, as glycated Hb provides a more accessible haem source than un-glycated Hb, this may offer an explanation as to why *P. gingivalis* numbers are increased in subgingival plaque of diabetic individuals (Makiura et al., 2008) who have elevated serum and GCF levels of glycated Hb. Iron was also liberated more freely from glycated Hb than its un-glycated counterpart when exposed to a continuous flux of H_2O_2, and this may also aid colonisation and growth of H_2O_2-producing oral streptococci species including *S. gordonii* in the plaque of diabetic patients, as well as advantaging *P. gingivalis*.

Chapter 6 General Discussion

6.1 Background to the project; the importance of metHb formation and haem availability in the virulence of *P. gingivalis*

Periodontitis (PD) is an inflammatory disease of the gums and surrounding tissue of the teeth, arising from the accumulation of bacteria in dental plaque (Loesche & Grossman, 2001). The dental plaque community comprises of over 700 species or phylotypes of microorganisms (Aas et al., 2005), including approximately 280 bacterial species which have been cultivated and formally identified (Dewhirst et al., 2010). Of these bacterial species, *P. gingivalis* is widely acknowledged as a "keystone pathogen" associated in the development of PD (Hajishengallis, 2015). *P. gingivalis* possesses an absolute growth requirement for haem (Marsh et al., 1994). However, in the host, free haem is highly toxic and its concentration is restricted through the sequestering actions of haem-carrying proteins albumin and haemopexin, or complexed with Hb. Thus, through the synergistic activity of Arg- and Lys- specific gingipains, in conjunction with the actions of haemophores such as HmuY and HusA, *P. gingivalis* must facilitate the extraction of haem from these host haem-proteins including Hb (Smalley et al., 2007; 2008; 2011; Gao et al., 2010; Olzcak & Smalley, 2016).

P. gingivalis and neighbouring colonisers of dental plaque are likely exposed to Hb, following haemolysis of erythrocytes, which may gain access to the diseased periodontal pocket/gingival sulcus as a result of PD-associated tissue micro-ulceration. Periodontal tissues are perfused with oxygenated Hb, where oxygen saturation levels of Hb as high as 80% have been measured (Hanioka et al., 1989; 2005). Acquisition of haem directly from oxyHb by *P. gingivalis* is difficult since oxyHb is refractory to the protease activity of *P. gingivalis* (Smalley et al., 2007; 2008). It was discovered that acquisition of haem from oxyHb by *P. gingivalis* requires its prior oxidation to metHb by the action of Arg-specific gingipains, before further globin degradation by the Lys-specific gingipains which enhances haem release (Smalley et al., 2008). The oxidation of the haem iron from Fe(II) in oxyHb to Fe(III) in metHb results in a 10^8-fold reduction in haem-globin affinity (Hargrove et al., 1996).

The gingipains of *P. gingivalis* also play an essential role in the development of the cell surface black pigmentation associated with growth of the bacterium on blood agar. This phenomenon arises by the accumulation of μ-oxo bishaem (dimers) on the surface of the cell following breakdown of Hb and release of haem; a process mediated by the sequential actions of RgpA and Kgp, as revealed through examination of the pigmentation behaviour of gingipain-deficient strains of *P. gingivalis* and the effects of isolated gingipains on Hb individually (Smalley et al., 2004; 2007; 2008). This emphasised the importance of the Arg-specific gingipain in mediating the critical step of oxidation of oxyHb to metHb (Smalley et al., 2004; 2007; 2008).

Recent evidence from Smalley and colleagues suggests that *P. gingivalis* may utilise the virulence properties of neighbouring microorganisms to aid in the process of oxyHb oxidation and haem capture (Byrne et al., 2013; Benedyk et al., 2015). *P. intermedia*, a co-aggregating black-pigmenting anaerobe belonging to the "Orange" consortium of oral species, produces interpain A (InpA), a cysteine protease that behaves in a similar manner to RgpA in facilitating the oxidation of oxyHb to metHb (Byrne et al., 2010). Haem acquisition by the *P. gingivalis* HmuY haemophore was found to be increased from metHb formed by InpA compared to auto-oxidised metHb (Byrne et al., 2013). In addition, pyocyanin, a blue phenazine redox compound produced by *P. aeruginosa*, was also capable of mediating oxyHb oxidation to metHb (Benedyk et al., 2015). This was a significant observation as *P. aeruginosa* and *P. gingivalis* have been found to co-colonise the lungs of individuals with cystic fibrosis (CF) (Rogers et al., 2004; Tunney et al., 2008). Pyocyanin vastly increased the rate of metHb formation and subsequent haem acquisition by HmuY, and upregulated *P. gingivalis* gingipain activity *in vivo* (Benedyk et al., 2015). Furthermore, when mice were challenged with pyocyanin and *P. gingivalis* they displayed enhanced mortality and morbidity compared to those administered *P. gingivalis* alone (Benedyk et al., 2015). It was concluded that pyocyanin, by promoting haem availability through metHb formation and increasing gingipain production, contributed to enhanced disease severity associated with *P. gingivalis*-*P. aeruginosa* co-infection in the CF lung.

6.2 *S. gordonii* enhances haem availability to the HmuY haemophore of *P. gingivalis*

S. gordonii cells mediated the formation of metHb when grown on horse blood agar, or in suspension with oxyHb. *S. gordonii* is classified as a viridans streptococci due to its ability to mediate α-haemolysis, a phenomenon, manifest as a yellow-green discolouration surrounding colonies on blood agar. Barnard & Stinson (1996) identified H_2O_2 as the "α-haemolytic agent" produced by *S. gordonii*. They primarily identified and purified the α-haemolytic agent from growth cultures of *S. gordonii*, and suggested that the α-haemolytic effect was accompanied by oxidation of the Hb Fe(II)haem iron species. However, the present study has extended their work in identifying metHb as the Hb species present in zones of α-haemolysis mediated by *S. gordonii*.

Clinically, periodontal pockets display a range of O_2 partial pressures, with moderate and deep pockets associated with PD having an average pO_2 between 11.6 and 15.0mmHg, with O_2 consisting of approximately 1-2% of the total atmospheric gases in the deep pockets (Loesche et al., 1983; Mettraux et al., 1984). In this context, it was found (Chapter 3) that *S. gordonii* displayed α-haemolysis which was accompanied by metHb formation under micro-aerobic and anaerobic environments, as well as aerobically. This is of significance since it demonstrates that if coaggregated, *S. gordonii* could provide *P. gingivalis* with a vital source of haem in environments which may not be conducive to growth (e.g., in aerobic environments in dental plaque) and production of Arg- and Lys- specific gingipains (which are otherwise needed for oxyHb oxidation and haem release).

To date, HmuY is the best characterised haemophore of *P. gingivalis* (Olzcak et al., 2005; Smalley & Olzcak, 2015). This 23kDa protein is both surface located and secreted by *P. gingivalis*, and is essential for scavenging any free haem in solution, that complexed as metHb, or bound by albumin and haemopexin (Smalley & Olzcak, 2016). Thus, the haemophore provides an ideal model system to probe haem acquisition by *P. gingivalis* from these haem-containing species, including Hb (Smalley et al., 2011; Byrne et al., 2013; Benedyk et al., 2015). It was found here

that HmuY could readily extract haem from the metHb formed by *S. gordonii* cells as a result of exposure to H_2O_2. This indicated that the haem in the Hb species remained stable during exposure of oxyHb to H_2O_2 (generated via G/GOX or *S. gordonii* cells), an important observation as Hb is prone to H_2O_2-mediated oxidative damage, resulting in haem and Hb protein degradation (Nagababu & Rifkind, 2000).

The HmuY-Fe(III)haem complex also remained stable to H_2O_2 at concentrations produced by the *S. gordonii* cells (Chapter 4). This was of particular significance since the apo-form of HmuY will likely be exposed to H_2O_2 *in vivo* following co-aggregation of *P. gingivalis* with *S. gordonii*. The haemophore is released by *P. gingivalis* in response to external haem concentrations in the immediate environment; the *hmu* operon which encodes for HmuY being up-regulated in haem-limited environments (Lewis et al., 2006; Olzcak et al., 2005). Thus, the haemophore will be subject to, and must remain resistant to, an array of environmental conditions in dental plaque to allow sufficient delivery of haem to the cell. The findings here add to recent observations that the haemophore is resistant to gingipain and InpA protease activity as well as chemical and thermal degradation (Wojtowicz et al., 2009; Byrne et al., 2013).

It was also shown that HmuY could wrest Fe(III)haem at an increased rate from metHb generated by *S. gordonii* cell suspensions than from auto-oxidised metHb. CD analysis indicated that this was likely due to subtle changes in the structure of metHb generated by exposure to H_2O_2. Specifically, near-UV CD analysis of the metHb structures suggested that the spatial disposition of the aromatic amino acid side-chains were altered following exposure to H_2O_2. H_2O_2 can oxidise tyrosine residues in the haem pocket during oxyHb oxidation (Giulivi & Davies, 1993), which is known to result in the rotation of a tyrosine phenol ring around the C^{β} bond in a tyrosyl radical and an alteration to the Hb structure (Svistunenko et al., 2002). This may account for the increased haem pick up by HmuY, especially if the conformational change was affecting the haem iron-Hb covalent linkage. However, assay for this biochemical change was beyond the scope of this study although others have used Electron Paramagnetic Resonance spectroscopy, a highly sensitive technique to detect such tyrosine radicals in Hb (Svistunenko et al., 2002).

6.3 Glycated Hb provides an enhanced source of haem to the HmuY haemophore of *P. gingivalis*

In addition to the primary objectives which were to identify a potential role for *S. gordonii* in haem acquisition by *P. gingivalis*, this work investigated the relative rates of HmuY-Fe(III)haem complex formation from glycated Hb compared to un-glycated Hb. A strong positive correlation exists between poorly controlled glycaemia in diabetes and PD; the work of Taylor et al (1998) and Sanchez-Dominquez et al (2015) showing that type II diabetic individuals with moderately to high HbA_{1c} levels (>6.5-9% of total Hb levels) correlated with an increased risk of alveolar bone loss and PD severity. Furthermore, aggravated gingival tissue bleeding in severe PD is clinically seen in individuals with poorly controlled diabetes (Ervasti et al., 1985; Bandyopadhyay et al., 2010). However, the mechanistic pathways that link PD and diabetes are not fully understood. It has been suggested that an altered immune response in diabetics, possibly arising through the increased blood content of the inflammatory AGEs, may contribute to the development of PD (Ohlrich et al., 2010). These AGEs have been found in higher number in the gingival tissue of diabetic individuals (Schmidt et al., 1996). Thus, aggravated gingival tissue bleeding, and elevated levels of AGEs including glycated Hb in the tissue, may provide an increased source of blood, Hb, and thus haem, to *P. gingivalis* and other black pigmenting bacteria which have been found in higher numbers in the subgingival plaque of diabetic individuals (Makiura et al., 2008).

Here it was demonstrated that HmuY could acquire haem more readily from glycated Hb than un-glycated Hb. An explanation for this increased rate of haem pick up was provided by near-UV CD analysis which showed subtle alterations in the spatial disposition of the tryptophan and/or phenylalanine side-chains. Mass spectrometry of *in vitro* glycated Hb purified by PBA affinity resin indicated that all glycation sites were located on lysine residues. A total of 8 and 10 glycated lysine sites were detected in α- and β- chains, with two lysine residues located on the same F8 helix-loop as the proximal histidines (His-87(α) and His-92(β), respectively); Lys-90(α) and Lys-95(β). It could be postulated that a glycation at these sites in the

haem pocket, may disrupt the optical properties of neighbouring tryptophan and/or phenylalanine residues, but most importantly may weaken the haem-globin linkage. This suggestion is in line with the work of Sen et al (2005) and Roy et al (2004) who found that the glycation of myoglobin and Hb resulted in the disruption of the haem-globin linkage, as judged by increased haem transfer to serum albumin. A similar mechanism may be in place between the glycated Hb and HmuY, and explain the increased rate of haem transfer from the glycated protein to the haemophore.

Interestingly, it has also previously been shown that glycated oxyHb has an increased tendency to auto-oxidise (Sen et al., 2005); the reason for this may reside in the distortion of the haem pocket geometry following glycation of the protein, facilitating an enhanced oxidative nucleophile attack by OH^- or H_2O on the Fe(II)haem iron (Springer et al., 1989). Here, *in vitro* glycated Hb comprised approximately 92% in the met-form compared to 95% metHb in the control. The increased rate of oxidation of glycated Hb (Sen et al., 2005) may provide a slightly greater advantage to *P. gingivalis* in acquiring haem via HmuY from glycated Hb in diabetics.

A further potentially important feature of glycated Hb is its increased propensity for oxidative damage. Glycated Hb is more prone to destruction by H_2O_2 than un-glycated Hb, resulting in a degradation of the haem molecule, and loss of iron (Sen et al., 2005). This may advantage species of streptococci which produce siderophores to scavenge free iron (Ge & Sun, 2014). An enhanced source of iron may promote growth and survival of such species in the host, in an otherwise iron-depleted environment, where at physiological pH, Fe(III) iron is insoluble in aqueous solution with the majority sequestered in Hb (76 %) (Weinberg, 1984; 1993). Interestingly, numbers of oral streptococci are elevated in supragingival plaque of diabetic individuals (Kampoo et al., 2014), and gingival tissue bleeding (exacerbated in diabetics; Ervasti et al., 1985; Bandyopadhyay et al., 2010) potentially exposes *S. gordonii* and other viridans streptococci to glycated Hb in the periodontal pocket. The finding that iron was released more readily from glycated Hb than un-glycated Hb during exposure to a continuous flux of H_2O_2 (specifically at concentrations produced by *S. gordonii* cell suspensions) may feature as a means of enhancing

streptococcal growth and survival. There is also evidence to suggest that *P. gingivalis* may possess an absolute requirement for iron; *P. gingivalis* is unable to grow in media without iron supplementation (Kesavalu et al., 2003). Furthermore, *P. gingivalis* cells grown in iron-depleted media displayed reduced virulence traits in a murine model of *P. gingivalis*-induced PD (Kesavalu et al., 2003). If this is the case, iron release from glycated Hb may also aid growth and virulence of *P. gingivalis*.

6.4 Final remarks

This study has been successful in identifying a mechanism by which *S. gordonii* could increase haem availability and potentially aid *P. gingivalis* in haem acquisition *in vivo*. Through the production of H_2O_2, *S. gordonii* can mediate the formation of metHb, a substrate that can be readily utilised by the HmuY haemophore of *P. gingivalis*. This has expanded on recent observations that *P. gingivalis* may utilise other species to increase haem availability (Byrne et al., 2013; Benedyk et al., 2015). In addition, this work found that glycated Hb is more susceptible than un-glycated Hb to haem extraction by HmuY. As *P. gingivalis*, a "keystone pathogen" involved in the development of PD, displays an essential growth requirement for haem, it is of utmost importance to reduce the availability of this vital co-factor to the organism, thereby to attenuate its growth and virulence. It is becoming clear that *P. gingivalis* may be able to make use of other mechanisms/factors through which haem availability might be guaranteed. Thus, any future experimental work needs to be focused upon the identification of the mechanisms and potential roles of other oral bacterial species in contributing to an available "haem pool" and in aiding haem acquisition by *P. gingivalis*. This knowledge may inform progress in the development of new therapeutic measures that could minimise the pathogenicity of *P. gingivalis* through restricting the availability of haem to the organism.

References

(1) Aas, J. A., Paster, B. J., Stokes, L. N., Olsen, I., & Dewhirst, F. E. (2005). Defining the normal bacterial flora of the oral cavity. J Clin Microbiol, 43(11), 5721-5732.

(2) Abbass, M. M., Korany, N. S., Salama, A. H., Dmytryk, J. J., & Safiejko-Mroczka, B. (2012). The relationship between receptor for advanced glycation end products expression and the severity of periodontal disease in the gingiva of diabetic and non diabetic periodontitis patients. Arch Oral Biol, 57(10), 1342-1354.

(3) Aduse-Opoku, J., Davies, N. N., Gallagher, A., Hashim, A., Evans, H. E., Rangarajan, M., . . . Curtis, M. A. (2000). Generation of lys-gingipain protease activity in *Porphyromonas gingivalis* W50 is independent of Arg-gingipain protease activities. Microbiology, 146 (Pt 8), 1933-1940.

(4) Aduse-Opoku, J., Slaney, J. M., Rangarajan, M., Muir, J., Young, K. A., & Curtis, M. A. (1997). The Tla protein of *Porphyromonas gingivalis* W50: a homolog of the RI protease precursor (PrpRI) is an outer membrane receptor required for growth on low levels of hemin. J Bacteriol, 179(15), 4778-4788.

(5) Amano, A., Tamagawa, H., Shizukuishi, S., & Tsunemitsu, A. (1986). Superoxide dismutase, catalase and peroxidases in oral anaerobic bacteria. J Osaka Univ Dent Sch, 26, 187-192.

(6) American Diabetes Association. (2010). Diagnosis and Classification of Diabetes Mellitus. In (Vol. 33, pp. 62–69): Diabetes Care.

(7) Andrewes, FW, & Horder, TJ. (1906). A study of the streptococci pathogenic for man. In (Vol. 168, pp. 708-713): The Lancet.

(8) Ansari, N. A., Moinuddin, & Ali, R. (2011). Glycated lysine residues: a marker for non-enzymatic protein glycation in age-related diseases. Dis Markers, 30(6), 317-324.

(9) Ansari, N. A., & Dash, D. (2013). Amadori glycated proteins: role in production of autoantibodies in diabetes mellitus and effect of inhibitors on non-enzymatic glycation. Aging Dis, 4(1), 50-56.

(10) Antonini, E, & Brunori, M. (1971). Hemoglobin and Myoglobin in Their Reactions with Ligands (A Neuberger & E.L. Tatum Eds.). Amsterdam, Netherlands: North Holland Publishing Company.

(11) Aronson, D. (2008). Hyperglycemia and the pathobiology of diabetic complications. Adv Cardiol, 45, 1-16.

(12) Ascenzi, P., Bocedi, A., Visca, P., Altruda, F., Tolosano, E., Beringhelli, T., & Fasano, M. (2005). Hemoglobin and heme scavenging. IUBMB Life, 57(11), 749-759.

(13) Asher, C., de Villiers, K. A., & Egan, T. J. (2009). Speciation of ferriprotoporphyrin IX in aqueous and mixed aqueous solution is controlled by solvent identity, pH, and salt concentration. Inorg Chem, 48(16), 7994-8003.

(14) Bakhti, M., Habibi-Rezaei, M., Moosavi-Movahedi, A. A., & Khazaei, M. R. (2007). Consequential alterations in haemoglobin structure upon glycation with fructose: prevention by acetylsalicylic acid. J Biochem, 141(6), 827-833.

(15) Balagopalakrishna, C., Manoharan, P. T., Abugo, O. O., & Rifkind, J. M. (1996). Production of superoxide from hemoglobin-bound oxygen under hypoxic conditions. Biochemistry, 35(20), 6393-6398.

(16) Bandyopadhyay, D., Marlow, N. M., Fernandes, J. K., & Leite, R. S. (2010). Periodontal disease progression and glycaemic control among Gullah African Americans with type-2 diabetes. J Clin Periodontol, 37(6), 501-509.

(17) Barnard, J. P., & Stinson, M. W. (1996). The alpha-hemolysin of *Streptococcus gordonii* is hydrogen peroxide. Infect Immun, 64(9), 3853-3857.

(18) Barnard, J. P., & Stinson, M. W. (1999). Influence of Environmental Conditions on Hydrogen Peroxide Formation by *Streptococcus gordonii*. Infect Immun, 67(12): 6558–6564.

(19) Barrick, D. (1994). Replacement of the proximal ligand of sperm whale myoglobin with free imidazole in the mutant His-93-->Gly. Biochemistry, 33(21), 6546-6554.

(20) Beaven, G. H., Chen, S. H., d' Albis, A., & Gratzer, W. B. (1974). A spectroscopic study of the haemin--human-serum-albumin system. Eur J Biochem, 41(3), 539-546.

(21) Beers, R. F., & Sizer, I. W. (1952). A spectrophotometric method for measuring the breakdown of hydrogen peroxide by catalase. J Biol Chem, 195(1), 133-140.

(22) Benedyk, M., Byrne, D. P., Glowczyk, I., Potempa, J., Olczak, M., Olczak, T., & Smalley, J. W. (2015). Pyocyanin a contributory factor in haem acquisition and virulence enhancement of *Porphyromonas gingivalis* in the lung [corrected]. PLoS One, 10(2), e0118319.

(23) Bickel, M., Cimasoni, G., & Andersen, E. (1985a). Flow and albumin content of early (pre-inflammatory) gingival crevicular fluid from human subjects. Arch Oral Biol, 30(8), 599-602.

(24) Bickel, M., & Cimasoni, G. (1985b). The pH of human crevicular fluid measured by a new microanalytical technique. J Periodontal Res, 20(1), 35-40.

(25) Bienert G., Schjoerring J, K., Jahn T, P. (2006) Membrane transport of hydrogen peroxide. Biochim Biophys Acta. 1758(8): 994-1003.

(26) Bondy-Carey, J. L., Galicia, J., Bagaitkar, J., Potempa, J. S., Potempa, B., Kinane, D. F., . . . Scott, D. A. (2013). Neutrophils alter epithelial response to *Porphyromonas gingivalis* in a gingival crevice model. Mol Oral Microbiol, 28(2), 102-113.

(27) Bose, T., & Chakraborti, A. S. (2008). Fructose-induced structural and functional modifications of hemoglobin: implication for oxidative stress in diabetes mellitus. Biochim Biophys Acta, 1780(5), 800-808.

(28) Bradshaw, D. J., Homer, K. A., Marsh, P. D., & Beighton, D. (1994). Metabolic cooperation in oral microbial communities during growth on mucin. Microbiology, 140 (Pt 12), 3407-3412.

(29) Bramanti, T. E., & Holt, S. C. (1990). Iron-regulated outer membrane proteins in the periodontopathic bacterium, *Bacteroides gingivalis*. Biochem Biophys Res Commun, 166(3), 1146-1154.

(30) Bunn, H. F., Haney, D. N., Kamin, S., Gabbay, K. H., & Gallop, P. M. (1976). The biosynthesis of human hemoglobin A1c. Slow glycosylation of hemoglobin *in vivo*. J Clin Invest, 57(6), 1652-1659.

(31) Bunn, H. F., Shapiro, R., McManus, M., Garrick, L., McDonald, M. J., Gallop, P. M., & Gabbay, K. H. (1979). Structural heterogeneity of human hemoglobin A due to nonenzymatic glycosylation. J Biol Chem, 254(10), 3892-3898.

(32) Byers, H. L., Tarelli, E., Homer, K. A., Hambley, H., & Beighton, D. (1999). Growth of viridans streptococci on human serum alpha1-acid glycoprotein. J Dent Res, 78(7), 1370-1380.

(33) Byrne, D. P., (2011). Mechanisms of haem acquisition by the black-pigmenting anaerobes, *Prevotella intermedia* and *Porphyromonas gingivalis* (Unpublished doctoral thesis). University of Liverpool, United Kingdom

(34) Byrne, D. P., Wawrzonek, K., Jaworska, A., Birss, A. J., Potempa, J., & Smalley, J. W. (2010). Role of the cysteine protease interpain A of *Prevotella intermedia* in breakdown and release of haem from haemoglobin. Biochem J, 425(1), 257-264.

(35) Byrne, D. P., Potempa, J., Olczak, T., & Smalley, J. W. (2013). Evidence of mutualism between two periodontal pathogens: co-operative haem acquisition by the HmuY haemophore of *Porphyromonas gingivalis* and the cysteine protease interpain A (InpA) of *Prevotella intermedia*. Mol Oral Microbiol, 28(3), 219-229.

(36) Caldas, R. R., Le Gall, F., Revert, K., Rault, G., Virmaux, M., Gouriou, S., Héry-Arnaud, G., Barbier, G., Boisramé, S. (2015) *Pseudomonas aeruginosa* and Periodontal Pathogens in the Oral Cavity and Lungs of Cystic Fibrosis Patients: a Case-Control Study. J. Clin Microbiol. 53(6):1898-907.

(37) Caldwell, C. C., Chen, Y., Goetzmann, H. S., Hao, Y., Borchers, M. T., Hassett, D. J., . . . Lau, G. W. (2009). *Pseudomonas aeruginosa* exotoxin pyocyanin causes cystic fibrosis airway pathogenesis. Am J Pathol, 175(6), 2473-2488.

(38) Camp, N. E. (2007). Methemoglobinemia. J Emerg Nurs, 33(2), 172-174.

(39) Ceriotti, F., & Ceriotti, G. (1980). Improved direct specific determination of serum iron and total iron-binding capacity. Clin Chem, 26(2), 327-331.

(40) Ch'ng, S. L., & Marinah, T. A. (1988). *In vitro* glycation of dried serum. Clin Chim Acta, 173(2), 165-171.

(41) Chandki, R., Banthia, P., & Banthia, R. (2011). Biofilms: A microbial home. J Indian Soc Periodontol, 15(2), 111-114.

(42) Chapple, I. L. (2014) Time to take periodontitis seriously. BMJ 348: g2645.

(43) Chung, W. O., Demuth, D. R., & Lamont, R. J. (2000). Identification of a *Porphyromonas gingivalis* receptor for the *Streptococcus gordonii* SspB protein. Infect Immun, 68(12), 6758-6762.

(44) Cintra, L. T., Samuel, R. O., Facundo, A. C., Prieto, A. K., Sumida, D. H., Bomfim, S. R., . . . Gomes-Filho, J. E. (2014). Relationships between oral infections and blood glucose concentrations or HbA1c levels in normal and diabetic rats. Int Endod J, 47(3), 228-237.

(45) Cooper, C. E., Schaer, D. J., Buehler, P. W., Wilson, M. T., Reeder, B. J., Silkstone, G., . . . Alayash, A. I. (2013). Haptoglobin binding stabilizes hemoglobin ferryl iron and the globin radical on tyrosine β145. Antioxid Redox Signal, 18(17), 2264-2273.

(46) Curtis, M. A., Kuramitsu, H. K., Lantz, M., Macrina, F. L., Nakayama, K., Potempa, J., . . . Aduse-Opoku, J. (1999). Molecular genetics and nomenclature of proteases of *Porphyromonas gingivalis*. J Periodontal Res, 34(8), 464-472.

(47) Dalziel, K., & O'Brien, J. R. (1957). Side reactions in the deoxygenation of dilute oxyhaemoglobin solutions by sodium dithionite. Biochem J, 67(1), 119-124.

(48) Darveau, R. P., Hajishengallis, G., & Curtis, M. A. (2012). *Porphyromonas gingivalis* as a potential community activist for disease. J Dent Res, 91(9), 816-820.

(49) Dashper, S. G., Ang, C. S., Veith, P. D., Mitchell, H. L., Lo, A. W., Seers, C. A., . . . Reynolds, E. C. (2009). Response of *Porphyromonas gingivalis* to heme limitation in continuous culture. J Bacteriol, 191(3), 1044-1055.

(50) Dashper, S. G., Hendtlass, A., Slakeski, N., Jackson, C., Cross, K. J., Brownfield, L., . . . Reynolds, E. C. (2000). Characterization of a novel outer membrane hemin-binding protein of *Porphyromonas gingivalis*. J Bacteriol, 182(22), 6456-6462.

(51)de Villiers, K. A., Kaschula, C. H., Egan, T. J., & Marques, H. M. (2007). Speciation and structure of ferriprotoporphyrin IX in aqueous solution: spectroscopic and diffusion measurements demonstrate dimerization, but not mu-oxo dimer formation. J Biol Inorg Chem, 12(1), 101-117.

(52) DeCarlo, A. A., Paramaesvaran, M., Yun, P. L., Collyer, C., & Hunter, N. (1999). Porphyrin-mediated binding to hemoglobin by the HA2 domain of cysteine proteinases (gingipains) and hemagglutinins from the periodontal pathogen *Porphyromonas gingivalis*. J Bacteriol, 181(12), 3784-3791.

(53) Delpierrre, G., Vertommen, D., Communi, D., Rider, M. H., & Van Schaftingen, E. (2004). Identification of fructosamine residues deglycated by fructosamine-3-kinase in human hemoglobin. J Biol Chem, 279(26), 27613-27620.

(54) Dewhirst, F. E., Chen, T., Izard, J., Paster, B. J., Tanner, A. C., Yu, W. H., . . . Wade, W. G. (2010). The human oral microbiome. J Bacteriol, 192(19), 5002-5017.

(55) Eggert, F. M., Drewell, L., Bigelow, J. A., Speck, J. E., & Goldner, M. (1991). The pH of gingival crevices and periodontal pockets in children, teenagers and adults. Arch Oral Biol, 36(3), 233-238.

(56) Ervasti, T., Knuuttila, M., Pohjamo, L., & Haukipuro, K. (1985). Relation between control of diabetes and gingival bleeding. J Periodontol, 56(3), 154-157.

(57) Falkler, W. A., Clayman, E. B., & Shaefer, D. F. (1983). Haemolysis of human erythrocytes by the *Fusobacterium nucleatum* associated with periodontal disease. Arch Oral Biol, 28(8), 735-739.

(58) Fernandez-Real, J. M., López-Bermejo, A., & Ricart, W. (2002). Cross-talk between iron metabolism and diabetes. Diabetes, 51(8), 2348-2354.

(59) Ficara, A. J., Levin, M. P., Grower, M. F., & Kramer, G. D. (1975). A comparison of the glucose and protein content of gingival fluid from diabetics and nondiabetics. J Periodontal Res, 10(3), 171-175.

(60) Flemming, H. C., & Wingender, J. (2010). The biofilm matrix. Nat Rev Microbiol, 8(9), 623-633.

(61) Fluckiger, R., & Winterhalter, K. H. (1976). *In vitro* synthesis of hemoglobin AIc. FEBS Lett, 71(2), 356-360.

(62) Fouad, A., Barry, J., Russo, J., Radolf, J., & Zhu, Q. (2002a). Periapical lesion progression with controlled microbial inoculation in a type I diabetic mouse model. J Endod, 28(1), 8-16.

(63) Fouad, A. F., Barry, J., Caimano, M., Clawson, M., Zhu, Q., Carver, R., . . . Radolf, J. D. (2002b). PCR-based identification of bacteria associated with endodontic infections. J Clin Microbiol, 40(9), 3223-3231.

(64) Fouad, A. F., & Burleson, J. (2003). The effect of diabetes mellitus on endodontic treatment outcome: data from an electronic patient record. J Am Dent Assoc, 134(1), 43-51; quiz 117-118.

(65) Fouad, A. F., Kum, K. Y., Clawson, M. L., Barry, J., Abenoja, C., Zhu, Q., . . . Radolf, J. D. (2003). Molecular characterization of the presence of *Eubacterium* spp and *Streptococcus* spp in endodontic infections. Oral Microbiol Immunol, 18(4), 249-255.

(66) Friess, U., Beck, A., Kohne, E., Lehmann, R., Koch, S., Haring, H. U., . . . Schleicher, E. (2003). Novel hemoglobin variant [beta66(E10) Lys-->Asn], with decreased oxygen affinity, causes falsely low hemoglobin A1c values by HPLC. Clin Chem, 49(8), 1412-1415.

(67) Gao, J. L., Nguyen, K. A., & Hunter, N. (2010). Characterization of a hemophore-like protein from *Porphyromonas gingivalis*. J Biol Chem, 285(51), 40028-40038.

(68) Ge, R., & Sun, X. (2014). Iron acquisition and regulation systems in Streptococcus species. Metallomics, 6(5), 996-1003.

(69) Giulivi, C., & Davies, K. J. (1990). A novel antioxidant role for hemoglobin. The comproportionation of ferrylhemoglobin with oxyhemoglobin. J Biol Chem, 265(32), 19453-19460.

(70) Giulivi, C., & Davies, K. J. (1993). Dityrosine and tyrosine oxidation products are endogenous markers for the selective proteolysis of oxidatively modified red blood cell hemoglobin by (the 19 S) proteasome. J Biol Chem, 268(12), 8752-8759.

(71) Giulivi, C., & Davies, K. J. (1994). Hydrogen peroxide-mediated ferrylhemoglobin generation *in vitro* and in red blood cells. Methods Enzymol, 231, 490-496.

(72) Goldin, A., Beckman, J. A., Schmidt, A. M., & Creager, M. A. (2006). Advanced glycation end products: sparking the development of diabetic vascular injury. Circulation, 114(6), 597-605.

(73) Goodson, J. M. (2003). Gingival crevice fluid flow. Periodontol 2000, 31, 43-54.

(74) Griffiths, G. S. (2003). Formation, collection and significance of gingival crevice fluid. Periodontol 2000, 31, 32-42.

(75) Grossi, S. G., & Genco, R. J. (1998). Periodontal disease and diabetes mellitus: a two-way relationship. Ann Periodontol, 3(1), 51-61.

(76) Gutteridge, J. M. (1986). Iron promoters of the Fenton reaction and lipid peroxidation can be released from haemoglobin by peroxides. FEBS Lett, 201(2), 291-295.

(77) Hajishengallis, G. (2014) The inflammophilic character of the periodontitis-associated microbiota. Mol Oral Microbiol. 29(6):248-57.

(78) Hajishengallis, G. (2015). Periodontitis: from microbial immune subversion to systemic inflammation. Nat Rev Immunol, 15(1), 30-44.

(79) Hale, J. P., Winlove, C. P., & Petrov, P. G. (2011). Effect of hydroperoxides on red blood cell membrane mechanical properties. Biophys J, 101(8), 1921-1929.

(80) Halliwell, B., Gutteridge, J. M. (1990) Role of free radicals and catalytic metal ions in human disease: an overview. Methods Enzymol.186:1-85.

(81) Hanioka, T., Matsuse, R., Shigemoto, Y., Ojima, M., & Shizukuishi, S. (2005). Relationship between periodontal disease status and combination of biochemical assays of gingival crevicular fluid. J Periodontal Res, 40(4), 331-338.

(82) Hanioka, T., Shizukuishi, S., Tsunemitsu, A., Joh, S., Sugiyama, K., & Sato, N. (1989). Haemoglobin concentration and oxygen saturation in dog gingiva with experimentally induced periodontitis. Arch Oral Biol, 34(8), 657-663.

(83) Hargrove, M. S., Barrick, D. & Olson, J. S (1996). The association rate constant for haem binding to globin is independent of protein structure. Biochemistry. 35, 11293 – 11299.

(84) Hashioka, K., Yamasaki, M., Nakane, A., Horiba, N., & Nakamura, H. (1992). The relationship between clinical symptoms and anaerobic bacteria from infected root canals. J Endod, 18(11), 558-561.

(85) Hendtlass, A., Dashper, S. G., & Reynolds, E. C. (2000). Identification of an antigenic protein Pga30 from *Porphyromonas gingivalis* W50. Oral Microbiol Immunol, 15(6), 383-387.

(86) Herold, S., & Rehmann, F. J. (2003). Kinetics of the reactions of nitrogen monoxide and nitrite with ferryl hemoglobin. Free Radic Biol Med, 34(5), 531-545.

(87) Hintao, J., Teanpaisan, R., Chongsuvivatwong, V., Dahlen, G., & Rattarasarn, C. (2007). Root surface and coronal caries in adults with type 2 diabetes mellitus. Community Dent Oral Epidemiol, 35(4), 302-309.

(88) Hiratsuka, K., Hayakawa, M., Kiyama-Kishikawa, M., Sasaki, Y., Hirai, T., & Abiko, Y. (2008). Role of the hemin-binding protein 35 (HBP35) of *Porphyromonas gingivalis* in coaggregation. Microb Pathog, 44(4), 320-328.

(89) Hiratsuka, K., Kiyama-Kishikawa, M., & Abiko, Y. (2010). Hemin-binding protein 35 (HBP35) plays an important role in bacteria-mammalian cells interactions in *Porphyromonas gingivalis*. Microb Pathog, 48(3-4), 116-123.

(90) Homer, K. A., & Beighton, D. (1992). Synergistic degradation of bovine serum albumin by mutans streptococci and other dental plaque bacteria. FEMS Microbiol Lett, 69(3), 259-262.

(91) Hrkal, Z., Vodrázka, Z., & Kalousek, I. (1974). Transfer of heme from ferrihemoglobin and ferrihemoglobin isolated chains to hemopexin. Eur J Biochem, 43(1), 73-78.

(92) Iram, A., Alam, T., Khan, J. M., Khan, T. A., Khan, R. H., & Naeem, A. (2013). Molten globule of hemoglobin proceeds into aggregates and advanced glycated end products. PLoS One, 8(8), e72075.

(93) Ito, S., Nakahari, T., & Yamamoto, D. (2011). The structural feature surrounding glycated lysine residues in human hemoglobin. Biomed Res, 32(3), 217-223.

(94) Iwamoto, H., Motomiya, Y., Miura, K., Morisawa, M., Yoshimura, Y., & Maruyama, I. (2001). Immunochemical assay of hemoglobin with N(epsilon)-(carboxymethyl)lysine at lysine 66 of the beta chain. Clin Chem, 47(7), 1249-1255.

(95) Jakubovics, N. S., & Kolenbrander, P. E. (2010). The road to ruin: the formation of disease-associated oral biofilms. Oral Dis, 16(8), 729-739.

(96) Jarolim, P., Lahav, M., Liu, S. C., & Palek, J. (1990). Effect of hemoglobin oxidation products on the stability of red cell membrane skeletons and the associations of skeletal proteins: correlation with a release of hemin. Blood, 76(10), 2125-2131.

(97) Jiang, Z. Y., Woollard, A. C., & Wolff, S. P. (1990). Hydrogen peroxide production during experimental protein glycation. FEBS Lett, 268(1), 69-71.

(98) Jones, P., Robson, T., & Brown, S. B. (1973). The catalase activity of ferrihaems. Biochem J, 135(2), 353-359.

(99) Kahlon, A. S., & Pathak, R. (2011). Patterns of glycemic control using glycosylated hemoglobin in diabetics. J Pharm Bioallied Sci, 3(3), 324-328.

(100) Kamaguch, A., Nakayama, K., Ohyama, T., Watanabe, T., Okamoto, M., & Baba, H. (2001). Coaggregation of *Porphyromonas gingivalis* and *Prevotella intermedia*. Microbiol Immunol, 45(9), 649-656.

(101) Kampoo, K., Teanpaisan, R., Ledder, R. G., & McBain, A. J. (2014). Oral bacterial communities in individuals with type 2 diabetes who live in southern Thailand. Appl Environ Microbiol, 80(2), 662-671.

(102) Kar, M., & Chakraborti, A. S. (1999). Release of iron from haemoglobin--a possible source of free radicals in diabetes mellitus. Indian J Exp Biol, 37(2), 190-192.

(103) Kar, M., & Chakroborti, A. S. (2001). Effect of glycosylation on iron-mediated free radical reactions of hemoglobin. Current Science. Vol. 80, pp. 770-773.

(104) Kelly, S. M., Jess, T. J., & Price, N. C. (2005). How to study proteins by circular dichroism. Biochim Biophys Acta, 1751(2), 119-139.

(105) Kelm, M., Dahmann, R., Wink, D., & Feelisch, M. (1997). The nitric oxide/superoxide assay. Insights into the biological chemistry of the NO/O_2. interaction. J Biol Chem, 272(15), 9922-9932.

(106) Kesavalu, L., Holt, S. C., & Ebersole, J. L. (2003). *In vitro* environmental regulation of *Porphyromonas gingivalis* growth and virulence. Oral Microbiol Immunol, 18(4), 226-233.

(107) Koike, M. (1989). [Biochemical investigation on periodontal tissue of abutment teeth. Analysis of proteins in gingival crevicular fluid by high performance liquid chromatography]. Nihon Hotetsu Shika Gakkai Zasshi, 33(3), 667-681.

(108) Kreth, J., Merritt, J., & Qi, F. (2009). Bacterial and host interactions of oral streptococci. DNA Cell Biol, 28(8), 397-403.

(109) Lalla, E., Lamster, I. B., Feit, M., Huang, L., & Schmidt, A. M. (1998). A murine model of accelerated periodontal disease in diabetes. J Periodontal Res, 33(7), 387-399.

(110) Lamont, R. J., El-Sabaeny, A., Park, Y., Cook, G. S., Costerton, J. W., & Demuth, D. R. (2002). Role of the *Streptococcus gordonii* SspB protein in the development of *Porphyromonas gingivalis* biofilms on streptococcal substrates. Microbiology, 148(Pt 6), 1627-1636.

(111) Lee, B. S., Jayathilaka, G. D., Huang, J. S., Vida, L. N., Honig, G. R., & Gupta, S. (2011). Analyses of *in vitro* nonenzymatic glycation of normal and variant hemoglobins by MALDI-TOF mass spectrometry. J Biomol Tech, 22(3), 90-94.

(112) Leung, K. P., & Folk, S. P. (2002). Effects of porphyrins and inorganic iron on the growth of *Prevotella intermedia*. FEMS Microbiol Lett, 209(1), 15-21.

(113) Lewis, J. P., Plata, K., Yu, F., Rosato, A., & Anaya, C. (2006). Transcriptional organization, regulation and role of the *Porphyromonas gingivalis* W83 hmu haemin-uptake locus. Microbiology, 152(Pt 11), 3367-3382.

(114) Li, D., Zhang, X., Long, Y., & Sun, X. (2006). Inactivation of Hemoglobin by Hydrogen Peroxide and Protection by a Reductant Substrate. Life Science Journal, Vol. 3, pp. 52-58.

(115) Li, H., Yang, H., Ding, Y., Aprecio, R., Zhang, W., Wang, Q., & Li, Y. (2013). Experimental periodontitis induced by *Porphyromonas gingivalis* does not alter the onset or severity of diabetes in mice. J Periodontal Res, 48(5), 582-590.

(116) Liu, X., Olczak, T., Guo, H. C., Dixon, D. W., & Genco, C. A. (2006). Identification of amino acid residues involved in heme binding and hemoprotein utilization in the *Porphyromonas gingivalis* heme receptor HmuR. Infect Immun, 74(2), 1222-1232.

(117) Liu, X., Ramsey, M. M., Chen, X., Koley, D., Whiteley, M., & Bard, A. J. (2011). Real-time mapping of a hydrogen peroxide concentration profile across a polymicrobial bacterial biofilm using scanning electrochemical microscopy. Proc Natl Acad Sci U S A, 108(7), 2668-2673.

(118) Loesche, W. J., Grossman, N. S. (2001) Periodontal disease as a specific, albeit chronic, infection: diagnosis and treatment. Clin Microbiol Rev. 2001 Oct;14(4):727-52.

(119) Loesche, W. J., Gusberti, F., Mettraux, G., Higgins, T., & Syed, S. (1983). Relationship between oxygen tension and subgingival bacterial flora in untreated human periodontal pockets. Infect Immun, 42(2), 659-667.

(120) Love, R. M., McMillan, M. D., & Jenkinson, H. F. (1997). Invasion of dentinal tubules by oral streptococci is associated with collagen recognition mediated by the antigen I/II family of polypeptides. Infect Immun, 65(12), 5157-5164.

(121) Love, R. M., McMillan, M. D., Park, Y., & Jenkinson, H. F. (2000). Coinvasion of dentinal tubules by *Porphyromonas gingivalis* and *Streptococcus gordonii* depends upon binding specificity of streptococcal antigen I/II adhesin. Infect Immun, 68(3), 1359-1365.

(122) Lunt, S. Y., & Vander Heiden, M. G. (2011). Aerobic glycolysis: meeting the metabolic requirements of cell proliferation. Annu Rev Cell Dev Biol, 27, 441-464.

(123) Maeda, K., Nagata, H., Yamamoto, Y., Tanaka, M., Tanaka, J., Minamino, N., & Shizukuishi, S. (2004). Glyceraldehyde-3-phosphate dehydrogenase of Streptococcus oralis functions as a coadhesin for *Porphyromonas gingivalis* major fimbriae. Infect Immun, 72(3), 1341-1348.

(124) Makiura, N., Ojima, M., Kou, Y., Furuta, N., Okahashi, N., Shizukuishi, S., & Amano, A. (2008). Relationship of *Porphyromonas gingivalis* with glycemic level in patients with type 2 diabetes following periodontal treatment. Oral Microbiol Immunol, 23(4), 348-351.

(125) Makris, K., & Spanou, L. (2011). Is there a relationship between mean blood glucose and glycated hemoglobin? J Diabetes Sci Technol, 5(6), 1572-1583.

(126) Marotta, P. S., Fontes, T. V., Armada, L., Lima, K. C., Rôças, I. N., & Siqueira, J. F. (2012). Type 2 diabetes mellitus and the prevalence of apical periodontitis and endodontic treatment in an adult Brazilian population. J Endod, 38(3), 297-300.

(127) Marsh, P. D. (2004). Dental plaque as a microbial biofilm. Caries Res, 38(3), 204-211.

(128) Marsh, P. D., & Devine, D. A. (2011). How is the development of dental biofilms influenced by the host? J Clin Periodontol, 38 Suppl 11, 28-35.

(129) Marsh, P. D., McDermid, A. S., McKee, A. S., & Baskerville, A. (1994). The effect of growth rate and haemin on the virulence and proteolytic activity of *Porphyromonas gingivalis* W50. Microbiology, 140 (Pt 4), 861-865.

(130) Messenger, A. J. M. & Barclay, R. (1983), Bacteria, iron and pathogenicity. Biochem. Educ., 11: 54–63.

(131) Mettraux, G. R., Gusberti, F. A., & Graf, H. (1984). Oxygen tension (pO_2) in untreated human periodontal pockets. J Periodontol, 55(9), 516-521.

(132) Middle, F. A., Bannister, A., Bellingham, A. J., & Dean, P. D. (1983). Separation of glycosylated haemoglobins using immobilized phenylboronic acid. Effect of ligand concentration, column operating conditions, and comparison with ion-exchange and isoelectric-focusing. Biochem J, 209(3), 771-779.

(133) Minetti, M., Mallozzi, C., Scorza, G., Scott, M. D., Kuypers, F. A., & Lubin, B. H. (1993). Role of oxygen and carbon radicals in hemoglobin oxidation. Arch Biochem Biophys, 302(1), 233-244.

(134) Muller-Eberhard, U. & Morgan, W.T. (1975). Porphyrin binding proteins in serum. Ann. N. Y. Acad. Sci. 244, 624-649

(135) Mukherjee, Kanai. (2010). Medical Laboratory Technology: A procedure manual for routine diagnostic tests (Vol. II): Tata McGraw Hill Education Ltd.

(136) Nagababu, E., & Rifkind, J. M. (2000). Reaction of hydrogen peroxide with ferrylhemoglobin: superoxide production and heme degradation. Biochemistry, 39(40), 12503-12511.

(137) Narayanan, L. L., & Vaishnavi, C. (2010). Endodontic microbiology. J Conserv Dent, 13(4), 233-239.

(138) Nelson, K. E., Fleischmann, R. D., DeBoy, R. T., Paulsen, I. T., Fouts, D. E., Eisen, J. A., . . . Fraser, C. M. (2003). Complete genome sequence of the oral

pathogenic Bacterium *Porphyromonas gingivalis* strain W83. J Bacteriol, 185(18), 5591-5601.

(139) Nhien, N. T., Huy, N. T., Naito, M., Oida, T., Uyen, D. T., Huang, M., . . . Kamei, K. (2010) Neutralization of toxic haem by *Porphyromonas gingivalis* haemoglobin receptor. J Biochem 147: 317–325.

(140) Noronha G. F., Nayak M., Ramya M. K., Nambiar J, & Moopilmidhunmohanan. (2015). Spectroscopic Evaluation of Enterococcus Faecalis, And Streptococcus Species in Secondary Root Canal Infection of Type-2 Diabetic Patients. Indian Journal of Applied Research. (Vol. 5, pp. 69-72)

(141) O'Brien-Simpson, N. M., Veith, P. D., Dashper, S. G., & Reynolds, E. C. (2003). *Porphyromonas gingivalis* gingipains: the molecular teeth of a microbial vampire. Curr Protein Pept Sci, 4(6), 409-426.

(142) Ohlrich, E. J., Cullinan, M. P., & Leichter, J. W. (2010). Diabetes, periodontitis, and the subgingival microbiota. J Oral Microbiol, 21;2.

(143) Olczak, T., Simpson, W., Liu, X., Genco, C.A. (2005). Iron and heme utilization in *Porphyromonas gingivalis*. FEMS Microbiol Rev. 29(1):119-44.

(144) Olczak, T., Dixon, D. W., & Genco, C. A. (2001). Binding specificity of the *Porphyromonas gingivalis* heme and hemoglobin receptor HmuR, gingipain K, and gingipain R1 for heme, porphyrins, and metalloporphyrins. J Bacteriol, 183(19), 5599-5608.

(145) Olczak, T., Sroka, A., Potempa, J., & Olczak, M. (2008). *Porphyromonas gingivalis* HmuY and HmuR: further characterization of a novel mechanism of heme utilization. Arch Microbiol, 189(3), 197-210.

(146) Olczak, T., Wójtowicz, H., Ciuraszkiewicz, J., Olczak M. (2010) Species specificity, surface exposure, protein expression, immunogenicity, and participation in biofilm formation of *Porphyromonas gingivalis* HmuY BMC Microbiol. 4; 10:134.

(147) Olson, J. S., Mathews, A. J., Rohlfs, R. J., Springer, B. A., Egeberg, K. D., Sligar, S. G., . . . Nagai, K. (1988). The role of the distal histidine in myoglobin and haemoglobin. Nature, 336(6196), 265-266.

(148) Pandey, A. V., Joshi, S. K., Tekwani, B. L., & Chauhan, V. S. (1999). A colorimetric assay for heme in biological samples using 96-well plates. Anal Biochem, 268(1), 159-161.

(149) Panter, S. S. (1994). Release of iron from hemoglobin. Methods Enzymol, 231, 502-514.

(150) Paramaesvaran, M., Nguyen, K. A., Caldon, E., McDonald, J. A., Najdi, S., Gonzaga, G., . . . Collyer, C. A. (2003). Porphyrin-mediated cell surface heme capture from hemoglobin by *Porphyromonas gingivalis*. J Bacteriol, 185(8), 2528-2537.

(151) Percy, M. J., McFerran, N. V., & Lappin, T. R. (2005). Disorders of oxidised haemoglobin. Blood Rev, 19(2), 61-68.

(152) Perutz, M. F. (1990). Mechanisms regulating the reactions of human hemoglobin with oxygen and carbon monoxide. Annu Rev Physiol, 52, 1-25.

(153) Perutz, M. F., Wilkinson, A. J., Paoli, M., & Dodson, G. G. (1998). The stereochemical mechanism of the cooperative effects in hemoglobin revisited. Annu Rev Biophys Biomol Struct, 27, 1-34.

(154) Petersen, P. E., Bourgeois, D., Ogawa, H., Estupinan-Day, S. & Ndiaye, C. (2005) The global burden of oral diseases and risks to oral health. Bull World Health Organ 83: 661–669.

(155) Pietri, R., Román-Morales, E., & López-Garriga, J. (2011). Hydrogen sulfide and hemeproteins: knowledge and mysteries. Antioxid Redox Signal, 15(2), 393-404.

(156) Pike, R., McGraw, W., Potempa, J., & Travis, J. (1994). Lysine- and arginine-specific proteinases from *Porphyromonas gingivalis*. Isolation, characterization, and evidence for the existence of complexes with hemagglutinins. J Biol Chem, 269(1), 406-411.

(157) Potempa, J., Sroka, A., Imamura, T., & Travis, J. (2003). Gingipains, the major cysteine proteinases and virulence factors of *Porphyromonas gingivalis*: structure, function and assembly of multidomain protein complexes. Curr Protein Pept Sci, 4(6), 397-407.

(158) Pratt-Terpstra, I. H., Weerkamp, A. H., & Busscher, H. J. (1989). The effects of pellicle formation on streptococcal adhesion to human enamel and artificial substrata with various surface free-energies. J Dent Res, 68(3), 463-467.

(159) Quintero, A. J., Prada, P., Inostroza, C. M., Chaparro, A. Sanz, A. F., Ramírez, V. L., & Morales, H. C. (2011). Presence of *Porphyromonas gingivalis*, *Tannerella forsythia*, *Treponema denticola* and *Aggregatibacter actinomycetemcomitans* in the subgingival biofilm of diabetic mellitus 2 patients: a cross sectional study. Revista Clínica de Periodoncia, Implantología y Rehabilitación Oral. (Vol. 4, pp. 54-58).

(160) Rachmilewitz, E. A., & Harari, E. (1972). Intermediate hemichrome formation after oxidation of three unstable hemoglobins (Freiburg, Riverdale-Bronx and Köln). Hamatol Bluttransfus, 10, 241-250.

(161) Rechetzki, K. F., Henneberg, R., da Silva, P. H., & do Nascimento, A. J. (2012). Reference values for methemoglobin concentrations in children. Rev Bras Hematol Hemoter, 34(1), 14-16. doi:10.5581/1516-8484.20120007

(162) Reeder, B. J., Grey, M., Silaghi-Dumitrescu, R. L., Svistunenko, D. A., Bülow, L., Cooper, C. E., & Wilson, M. T. (2008). Tyrosine residues as redox cofactors in human hemoglobin: implications for engineering nontoxic blood substitutes. J Biol Chem, 283(45), 30780-30787.

(163) Rifkind, J. M., Abugo, O., Levy, A., & Heim, J. (1994). Detection, formation, and relevance of hemichromes and hemochromes. Methods Enzymol, 231, 449-480.

(164) Rifkind, J. M., & Nagababu, E. (2013). Hemoglobin redox reactions and red blood cell aging. Antioxid Redox Signal, 18(17), 2274-2283.

(165) Rogers, G. B., Carroll, M. P., Serisier, D. J., Hockey, P. M., Jones, G., & Bruce, K. D. (2004). characterization of bacterial community diversity in cystic fibrosis lung infections by use of 16s ribosomal DNA terminal restriction fragment length polymorphism profiling. J Clin Microbiol, 42(11), 5176-5183.

(166) Romero-Espejel, M. E., González-López, M. A., & Olivares-Trejo, J.e J. (2013). *Streptococcus pneumoniae* requires iron for its viability and expresses two membrane proteins that bind haemoglobin and haem. Metallomics, 5(4), 384-389.

(167) Roper, J. M., Raux, E., Brindley, A. A., Schubert, H. L., Gharbia, S. E., Shah, H. N., & Warren, M. J. (2000). The enigma of cobalamin (Vitamin B12) biosynthesis in *Porphyromonas gingivalis*. Identification and characterization of a functional corrin pathway. J Biol Chem, 275(51), 40316-40323.

(168) Rosa, J., Labie, D., Wajcman, H., Boigne, J. M., Cabannes, R., Bierme, R., & Ruffie, J. (1969). Haemoglobin I toulouse: beta-66 (E 10) lys glu: a new abnormal haemoglobin with a mutation localized on the E 10 porphyrin surrounding zone. Nature, 223(5202), 190-191.

(169) Roy, A., Sen, S., & Chakraborti, A. S. (2004). *In vitro* nonenzymatic glycation enhances the role of myoglobin as a source of oxidative stress. Free Radic Res, 38(2), 139-146.

(170) Ryan, C. S., & Kleinberg, I. (1995). Bacteria in human mouths involved in the production and utilization of hydrogen peroxide. Arch Oral Biol, 40(8), 753-763.

(171) Ryter, S. W., & Tyrrell, R. M. (2000). The heme synthesis and degradation pathways: role in oxidant sensitivity. Heme oxygenase has both pro- and antioxidant properties. Free Radic Biol Med, 28(2), 289-309.

(172) Salehi, N., Moosavi-Movahedi, A. A., Fotouhi, L., Yousefinejad, S., Shourian, M., Hosseinzadeh, R., . . . Habibi-Rezaei, M. (2014). Heme degradation upon production of endogenous hydrogen peroxide via interaction of hemoglobin with sodium dodecyl sulfate. J Photochem Photobiol B, 133, 11-17.

(173) Schifferle, R. E., Shostad, S. A., Bayers-Thering, M. T., Dyer, D. W., & Neiders, M. E. (1996). Effect of protoporphyrin IX limitation on *Porphyromonas gingivalis*. J Endod, 22(7), 352-355.

(174) Schlienger, J. L., Anceau, A., Chabrier, G., North, M. L., & Stephan, F. (1982). Effect of diabetic control on the level of circulating thyroid hormones. Diabetologia, 22(6), 486-488.

(175) Schmidt, A. M., Weidman, E., Lalla, E., Yan, S. D., Hori, O., Cao, R., . . . Lamster, I. B. (1996). Advanced glycation end products (AGEs) induce oxidant stress in the gingiva: a potential mechanism underlying accelerated periodontal disease associated with diabetes. J Periodontal Res, 31(7), 508-515.

(176) Selvin, E., Steffes, M. W., Zhu, H., Matsushita, K., Wagenknecht, L., Pankow, J., . . . Brancati, F. L. (2010). Glycated hemoglobin, diabetes, and cardiovascular risk in nondiabetic adults. N Engl J Med, 362(9), 800-811.

(177) Sen, S., Kar, M., Roy, A., & Chakraborti, A. S. (2005). Effect of nonenzymatic glycation on functional and structural properties of hemoglobin. Biophys Chem, 113(3), 289-298.

(178) Shapiro, R., McManus, M. J., Zalut, C., & Bunn, H. F. (1980). Sites of nonenzymatic glycosylation of human hemoglobin A. J Biol Chem, 255(7), 3120-3127.

(179) Shibata, Y., Hiratsuka, K., Hayakawa, M., Shiroza, T., Takiguchi, H., Nagatsuka, Y., & Abiko, Y. (2003). A 35-kDa co-aggregation factor is a hemin binding protein in *Porphyromonas gingivalis*. Biochem Biophys Res Commun, 300(2), 351-356.

(180) Shikama, K. (1985). Nature of the FeO_2 bonding in myoglobin: an overview from physical to clinical biochemistry. Experientia, 41(6), 701-706.

(181) Shikama, K. (1990). Autoxidation of oxymyoglobin: a meeting point of the stabilization and the activation of molecular oxygen. Biol Rev Camb Philos Soc, 65(4), 517-527.

(182) Shikama, K. (1998). The Molecular Mechanism of Autoxidation for Myoglobin and Hemoglobin: A Venerable Puzzle. Chem Rev, 98(4), 1357-1374.

(183) Shilov, I. V., Seymour, S. L., Patel, A. A., Loboda, A., Tang, W. H., Keating, S. P., . . . Schaeffer, D. A. (2007). The Paragon Algorithm, a next generation search

engine that uses sequence temperature values and feature probabilities to identify peptides from tandem mass spectra. Mol Cell Proteomics, 6(9), 1638-1655.

(184) Shizukuishi, S., Tazaki, K., Inoshita, E., Kataoka, K., Hanioka, T., & Amano, A. (1995). Effect of concentration of compounds containing iron on the growth of *Porphyromonas gingivalis*. FEMS Microbiol Lett, 131(3), 313-317.

(185) Silva, G., Jeney, V., Chora, A., Larsen, R., Balla, J., & Soares, M. P. (2009). Oxidized hemoglobin is an endogenous proinflammatory agonist that targets vascular endothelial cells. J Biol Chem, 284(43), 29582-29595.

(186) Simpson, W., Olczak, T., & Genco, C. A. (2000). Characterization and expression of HmuR, a TonB-dependent hemoglobin receptor of *Porphyromonas gingivalis*. J Bacteriol, 182(20), 5737-5748.

(187) Smalley, J. W., Birss, A. J., McKee, A. S., & Marsh, P. D. (1996). Haemin binding as a factor in the virulence of *Porphyromonas gingivalis*. FEMS Microbiol Lett, 141(1), 65-70.

(188) Smalley, J. W., Birss, A. J., McKee, A. S., & Marsh, P. D. (1998). Hemin regulation of hemoglobin binding by *Porphyromonas gingivalis*. Curr Microbiol, 36(2), 102-106.

(189) Smalley, J. W., Birss, A. J., & Silver, J. (2000). The periodontal pathogen *Porphyromonas gingivalis* harnesses the chemistry of the mu-oxo bishaem of iron protoporphyrin IX to protect against hydrogen peroxide. FEMS Microbiol Lett, 183(1), 159-164.

(190) Smalley, J. W., Birss, A. J., Szmigielski, B., & Potempa, J. (2006). The HA2 haemagglutinin domain of the lysine-specific gingipain (Kgp) of *Porphyromonas gingivalis* promotes micro-oxo bishaem formation from monomeric iron(III) protoporphyrin IX. Microbiology, 152(Pt 6), 1839-1845.

(191) Smalley, J. W., Birss, A. J., Szmigielski, B., & Potempa, J. (2007). Sequential action of R- and K-specific gingipains of *Porphyromonas gingivalis* in the generation of the haem-containing pigment from oxyhaemoglobin. Arch Biochem Biophys, 465(1), 44-49.

(192) Smalley, J. W., Birss, A. J., Szmigielski, B., & Potempa, J. (2008). Mechanism of methaemoglobin breakdown by the lysine-specific gingipain of the periodontal pathogen *Porphyromonas gingivalis*. Biol Chem, 389(9), 1235-1238.

(193) Smalley, J. W., Birss, A. J., Withnall, R., & Silver, J. (2002). Interactions of *Porphyromonas gingivalis* with oxyhaemoglobin and deoxyhaemoglobin. Biochem J, 362(Pt 1), 239-245.

(194) Smalley, J. W., Byrne, D. P., Birss, A. J., Wojtowicz, H., Sroka, A., Potempa, J., & Olczak, T. (2011). HmuY haemophore and gingipain proteases constitute a unique syntrophic system of haem acquisition by *Porphyromonas gingivalis*. PLoS One, 6(2), e17182.

(195) Smalley, J. W., Dwarakanath, D., Rhodes, J. M., & Hart, C. A. (1994). Mucin-sulphatase activity of some oral streptococci. Caries Res, 28(6), 416-420.

(196) Smalley, J. W., & Olczak, T. (2015). Haem acquisition mechanisms of *Porphyromonas gingivalis* - strategies used in polymicrobial community in a haem-limited host environment. Mol Oral Microbiol.

(197) Smalley, J. W., Silver, J., Marsh, P. J., & Birss, A. J. (1998). The periodontopathogen *Porphyromonas gingivalis* binds iron protoporphyrin IX in the mu-oxo dimeric form: an oxidative buffer and possible pathogenic mechanism. Biochem J, 331 (Pt 3), 681-685.

(198) Smalley, J. W., Thomas, M. F., Birss, A. J., Withnall, R., & Silver, J. (2004). A combination of both arginine- and lysine-specific gingipain activity of *Porphyromonas gingivalis* is necessary for the generation of the micro-oxo bishaem-containing pigment from haemoglobin. Biochem J, 379(Pt 3), 833-840.

(199) Smith, A., & McCulloh, R. J. (2015). Hemopexin and haptoglobin: allies against heme toxicity from hemoglobin not contenders. Front Physiol, 6, 187.

(200) Snyder, L. M., Fortier, N. L., Trainor, J., Jacobs, J., Leb, L., Lubin, B., . . . Mohandas, N. (1985). Effect of hydrogen peroxide exposure on normal human erythrocyte deformability, morphology, surface characteristics, and spectrin-hemoglobin cross-linking. J Clin Invest, 76(5), 1971-1977.

(201) Socransky, S. S., & Haffajee, A. D. (1991). Microbial mechanisms in the pathogenesis of destructive periodontal diseases: a critical assessment. J Periodontal Res, 26(3 Pt 2), 195-212.

(202) Socransky, S. S., & Haffajee, A. D. (2005). Periodontal microbial ecology. Periodontol 2000, 38, 135-187.

(203) Springer, B. A., Egeberg, K. D., Sligar, S. G., Rohlfs, R. J., Mathews, A. J., & Olson, J. S. (1989). Discrimination between oxygen and carbon monoxide and inhibition of autooxidation by myoglobin. Site-directed mutagenesis of the distal histidine. J Biol Chem, 264(6), 3057-3060.

(204) Springsteen, P, & Wang, B. (2002). A detailed examination of boronic acid–diol complexation. Tetrahedron; Vol. 58, pp. 5291-5300.

(205) Stewart, P. S. (2003). Diffusion in biofilms. J Bacteriol, 185(5), 1485-1491.

(206) Stinson, M. W., Safulko, K., & Levine, M. J. (1991). Adherence of *Porphyromonas (Bacteroides) gingivalis* to *Streptococcus sanguis in vitro*. Infect Immun, 59(1), 102-108.

(207) Sugawara, Y., Matsuoka, A., Kaino, A., & Shikama, K. (1995). Role of globin moiety in the autoxidation reaction of oxymyoglobin: effect of 8 M urea. Biophys J, 69(2), 583-592.

(208) Sundqvist, G., Johansson, E., & Sjögren, U. (1989). Prevalence of black-pigmented bacteroides species in root canal infections. J Endod, 15(1), 13-19.

(209) Svistunenko, D. A. (2005). Reaction of haem containing proteins and enzymes with hydroperoxides: the radical view. Biochim Biophys Acta, 1707(1), 127-155.

(210) Svistunenko, D. A., Dunne, J., Fryer, M., Nicholls, P., Reeder, B. J., Wilson, M. T., . . . Cooper, C. E. (2002). Comparative study of tyrosine radicals in hemoglobin and myoglobins treated with hydrogen peroxide. Biophys J, 83(5), 2845-2855.

(211) Sztiller, M., Puchala, M., Kowalczyk, A., & Bartosz, G. (2006). The influence of ferrylhemoglobin and methemoglobin on the human erythrocyte membrane. Redox Rep, 11(6), 263-271.

(212) Sánchez-Domínguez, B., López-López, J., Jané-Salas, E., Castellanos-Cosano, L., Velasco-Ortega, E., & Segura-Egea, J. J. (2015). Glycated hemoglobin levels and prevalence of apical periodontitis in type 2 diabetic patients. J Endod, 41(5), 601-606.

(213) Tanaka, M., Hanioka, T., Takaya, K., & Shizukuishi, S. (1998). Association of oxygen tension in human periodontal pockets with gingival inflammation. J Periodontol, 69(10), 1127-1130.

(214) Taylor, G. W., Burt, B. A., Becker, M. P., Genco, R. J., Shlossman, M., Knowler, W. C., & Pettitt, D. J. (1998). Non-insulin dependent diabetes mellitus and alveolar bone loss progression over 2 years. J Periodontol, 69(1), 76-83.

(215) Tew, J. G., Marshall, D. R., Burmeister, J. A., & Ranney, R. R. (1985). Relationship between gingival crevicular fluid and serum antibody titers in young adults with generalized and localized periodontitis. Infect Immun, 49(3), 487-493.

(216) Thurnheer, T., Belibasakis, G. N., & Bostanci, N. (2014). Colonisation of gingival epithelia by subgingival biofilms *in vitro*: role of "red complex" bacteria. Arch Oral Biol, 59(9), 977-986.

(217) Tsuruga, M., Matsuoka, A., Hachimori, A., Sugawara, Y., & Shikama, K. (1998). The molecular mechanism of autoxidation for human oxyhemoglobin. Tilting

of the distal histidine causes nonequivalent oxidation in the beta chain. J Biol Chem, 273(15), 8607-8615.

(218) Tsuruga, M., & Shikama, K. (1997). Biphasic nature in the autoxidation reaction of human oxyhemoglobin. Biochim Biophys Acta, 1337(1), 96-104.

(219) Tunney, M. M., Field, T. R., Moriarty, T. F., Patrick, S., Doering, G., Muhlebach, M. S., . . . Elborn, J. S. (2008). Detection of anaerobic bacteria in high numbers in sputum from patients with cystic fibrosis. Am J Respir Crit Care Med, 177(9), 995-1001.

(220) Turk, Z., Mesić, R., & Benko, B. (1998). Comparison of advanced glycation endproducts on haemoglobin (Hb-AGE) and haemoglobin A_{1c} for the assessment of diabetic control. Clin Chim Acta, 277(2), 159-170.

(221) Verderame, R. A., Cobb, C. M., Killoy, W. J., & Drisko, C. L. (1989). Scanning electron microscopic examination of pocket wall epithelium and associated plaque in localized juvenile periodontitis. J Clin Periodontol, 16(4), 234-241.

(222) Wandersman, C., & Delepelaire, P. (2012). Haemophore functions revisited. Mol Microbiol, 85(4), 618-631.

(223) Wang, S. H., Wang, T. F., Wu, C. H., & Chen, S. H. (2014). In-depth comparative characterization of hemoglobin glycation in normal and diabetic bloods by LC-MSMS. J Am Soc Mass Spectrom, 25(5), 758-766.

(224) Wautier, J. L., & Schmidt, A. M. (2004). Protein glycation: a firm link to endothelial cell dysfunction. Circ Res, 95(3), 233-238.

(225) Weinberg, E. D. (1984). Iron withholding: a defense against infection and neoplasia. Physiol Rev, 64(1), 65-102.

(226) Weinberg, E. D. (1993). The development of awareness of iron-withholding defense. Perspect Biol Med, 36(2), 215-221.

(227) Whittaker, C. J., Klier, C. M., & Kolenbrander, P. E. (1996). Mechanisms of adhesion by oral bacteria. Annu Rev Microbiol, 50, 513-552.

(228) Wickström, C., Herzberg, M. C., Beighton, D., & Svensäter, G. (2009). Proteolytic degradation of human salivary MUC5B by dental biofilms. Microbiology, 155(Pt 9), 2866-2872.

(229) Wilson, R., Pitt, T., Taylor, G., Watson, D., MacDermot, J., Sykes, D., . . . Cole, P. (1987). Pyocyanin and 1-hydroxyphenazine produced by *Pseudomonas aeruginosa* inhibit the beating of human respiratory cilia *in vitro*. J Clin Invest, 79(1), 221-229.

(230) Winterbourn, C. C. (1985). Free-radical production and oxidative reactions of hemoglobin. Environ Health Perspect, 64, 321-330.

(231) Winterbourn, C. C. (1990). Oxidative reactions of hemoglobin. Methods Enzymol, 186, 265-272.

(232) Winterbourn, C. C., McGrath, B. M., & Carrell, R. W. (1976). Reactions involving superoxide and normal and unstable haemoglobins. Biochem J, 155(3), 493-502.

(233) Wright, R. O., Lewander, W. J., & Woolf, A. D. (1999). Methemoglobinemia: etiology, pharmacology, and clinical management. Ann Emerg Med, 34(5), 646-656.

(234) Wójtowicz, H., Guevara, T., Tallant, C., Olczak, M., Sroka, A., Potempa, J., . . . Gomis-Rüth, F. X. (2009). Unique structure and stability of HmuY, a novel heme-binding protein of *Porphyromonas gingivalis*. PLoS Pathog, 5(5), e1000419.

(235) Ximénez-Fyvie, L. A., Haffajee, A. D., & Socransky, S. S. (2000). Microbial composition of supra- and subgingival plaque in subjects with adult periodontitis. J Clin Periodontol, 27(10), 722-732.

(236) Yang, F., & Phillips, G. N. (1996). Crystal structures of CO-, deoxy- and met-myoglobins at various pH values. J Mol Biol, 256(4), 762-774.

(237) Zhang, X., Medzihradszky, K. F., Cunningham, J., Lee, P. D., Rognerud, C. L., Ou, C. N., . . . Witkowska, H. E. (2001). Characterization of glycated hemoglobin in diabetic patients: usefulness of electrospray mass spectrometry in monitoring the extent and distribution of glycation. J Chromatogr B Biomed Sci Appl, 759(1), 1-15.

(238) Zhang, Y., Samson, F. E., Nelson, S. R., & Pazdernik, T. L. (1996). Nitric oxide detection with intracerebral microdialysis: important considerations in the application of the hemoglobin-trapping technique. J Neurosci Methods, 68(2), 165-173.